VAMAS

Technical Working Area 3
CERAMICS

Fracture Toughness of Advanced Ceramics by the Surface Crack in Flexure (SCF) Method: A VAMAS Round Robin

June 1994
VAMAS Report 17
ISSN 1016-2186

Versailles Project on Advanced Materials and Standards
Canada, CEC, Germany, France, Italy, Japan, UK, USA

VAMAS
Technical Working Area 3

Fracture Toughness of Advanced Ceramics by the Surface Crack in Flexure (SCF) Method: A VAMAS Round Robin

by

George D. Quinn
National Institute of Standards and Technology (NIST)
Gaithersburg, MD 20899, USA

Jakob J. Kübler
Swiss Federal Laboratories for Materials Testing and Research (EMPA)
Dübendorf, Switzerland

Robert J. Gettings
National Institute of Standards and Technology
Gaithersburg, MD 20899, USA

June 1994

VAMAS Report No. 17
ISSN 1016-2186

SUMMARY

Fracture toughness was measured by the surface crack in flexure method (also known as the controlled surface flaw method) on three monolithic advanced ceramics. These were hot-pressed silicon nitride, hot-isostatic pressed silicon nitride, and yttria-stabilized tetragonal zirconia polycrystal (Y-TZP). These materials have different degrees of difficulty in the application of this test method. Most labs had little problem with the hot-pressed silicon nitride and obtained very consistent results. The fracture toughness for 107 specimens was 4.6 ± 0.4 MPa·$\sqrt{m}$ (mean, standard deviation). Reasonably consistent results were obtained for the hipped silicon nitride. The fracture toughness for 105 specimens was 5.0 ± 0.6 MPa·$\sqrt{m}$. There was fair agreement for the Y-TZP. For the labs whose results were accepted, the fracture toughness results were: 4.4 ± 0.4 MPa·$\sqrt{m}$.

The calculated toughness depends upon the stress at fracture and the precrack size and shape. The stress can be measured very accurately and precisely. Since toughness depends upon the square root of crack size, the uncertainty in the size measurement is diminished in the calculated results. Indeed, the round robin showed that the method was surprisingly robust with respect to the crack size measurements. Some fractographic experience or skill is a prerequisite for assurance of correct results, however.

KEY WORDS Fracture toughness, advanced ceramics, advanced technical ceramics, precrack, silicon nitride, zirconia, fractography, flexure, controlled surface flaw, surface crack.

CONTENTS

Summary i

Contents ii

Introduction 1

Materials 9

Experimental Procedure 14

Results
- General 21
- Hot-Pressed Silicon Nitride 24
- Hot-Isostatic Pressed Silicon Nitride 29
- Yttria-Stabilized Tetragonal Zirconia 33

Discussion 42

Conclusions 54

Acknowledgements 56

References 57

Appendices

A1 Instructions for the Round Robin
A2 Fractographic Procedures Used by the Participants
A3 Individual Fracture Toughness Outcomes
A4 Influence of the Uncertainty of the Precrack Size Measurements Upon the Calculated Fracture Toughness
A5 Notes on the Stress Intensity Shape Factor, Y

INTRODUCTION

The Versailles Advanced Materials and Standards (VAMAS) project is an international collaboration for prestandardization research. The round robin exercise reported here is the sixth project undertaken by Technical Working Area (TWA) #3, Ceramics. There is considerable worldwide interest in standardizing and improving test procedures for the determination of fracture toughness of advanced ceramics. This is the third fracture toughness round robin that TWA #3 has organized. One earlier project was coordinated by the Japan Fine Ceramic Center (JFCC) and featured the Single-Edge Precracked Beam (SEPB), Indentation Fracture (IF), and Indentation Strength (IS) methods [1-5]. The second project was also coordinated by JFCC and featured high-temperature testing with Chevron Notch (CNB), Single-Edge V-Notched (SEVNB), and SEPB methods [6,7].

The present round robin uses a different technique, the surface crack in flexure method (SCF), also known as the controlled surface flaw (CSF) method. This round robin, jointly organized by the National Institute of Standards and Technology (NIST), and the Swiss Federal Laboratories for Materials Testing and Research (EMPA), commenced in November 1992 and concluded in September 1993. Twenty-four laboratories agreed to participate, and the twenty listed in Table 1 completed their testing.[1]

The surface crack method follows conventional practice to measure fracture toughness: a specimen is precracked, the specimen is fractured, the precrack size is measured, and the toughness is computed from a stress intensity formula for a well-defined crack geometry. A hardness machine with a Knoop indenter is used to create a flaw in a common flexure specimen. In brittle materials, the indenter not only forms the impression, but also a semicircular or semielliptical crack under the surface (Figures 1 and 2). The novel aspect of the method (relative to metals toughness testing) is that the precrack is very small, on the order of size of the **real** flaws in a ceramic, and fractographic techniques are needed to see and measure the precrack. Flexure stress can be measured quite accurately and precisely, but like any fracture toughness test, some care and skill is involved in obtaining and measuring the precrack. The precrack can be modelled by a semicircle or semiellipse for which there is extensive literature and, in recent years, a convergence of solutions for the stress intensity factors.

---

[1] The labs in Table 1 are listed in a different order than the numbering sequence in the results section.

TABLE 1
Participating Laboratories

Denmark	
RISO	Riso National Laboratory - Roskilde Dr. C. P. Debel
Germany	
DLR	German Aerospace Research Establishment - Cologne Dr. Jurgen Göring
BAM	German Federal Institute for Materials Research - Berlin Dr. Christian Ullner
KfK	Nuclear Research Center - Karlsruhe Prof. Dietrich Munz, Dr. Theo Fett
FhG	Fraunhofer Institute for Mechanics of Materials - Freiburg, Dr. Thomas Hollstein, Dr. Eckhard Gehrke
Italy	
IRTEC	National Research Council Institute for Ceramics Technology - Faenza Dr. Goffredo de Portu
Centro Ceramico	Center of Research and Testing of the Ceramic Industry - Bologna Dr. Leonardo Esposito, Dr. Antonella Tucci
Netherlands	
ECN	Netherlands Energy Research Foundation - Petten Dr. B. J. de Smet and Mr. P. W. Bach
CTK	Center for Technical Ceramics - Eindhoven Dr. Leonardus Dortmans
France	
ENSMP	Centre of Materials, Pierre-Marie Fourt - Evry Dr. M. Boussuge
USA	
Alfred	Alfred University - New York Prof. James Varner
NASA-Lewis	National Aeronautics and Space Administration - Cleveland Mr. Jonathan Salem
NIST	National Institute of Standards and Technology - Gaithersburg Mr. George Quinn, Mr. Robert Gettings
Switzerland	
EMPA	Swiss Federal Laboratories for Materials Testing and Research - Dübendorf Mr. Jakob Kübler, Mr. Roland Bächtold
Belgium	
VITO	Flemish Institute for Technological Research - Mol Dr. W. Vandermeulen
CRIBC	Belgian Ceramic Research Center - Mons Dr. Veronique Lardot, Dr. P. Descamps
Sweden	
RIT	Royal Institute of Technology - Stockholm Dr. David Rowcliffe
United Kingdom	
NPL	National Physical Laboratory - Teddington Dr. Roger Morrell
Morgan	Morgan Materials Technology, Ltd. - Stourport-on-Severn Mr. Reginald Stannard
T&N	T&N Technology, Ltd. - Cawston Dr. Robert Wordsworth, Dr. Carol Pindar

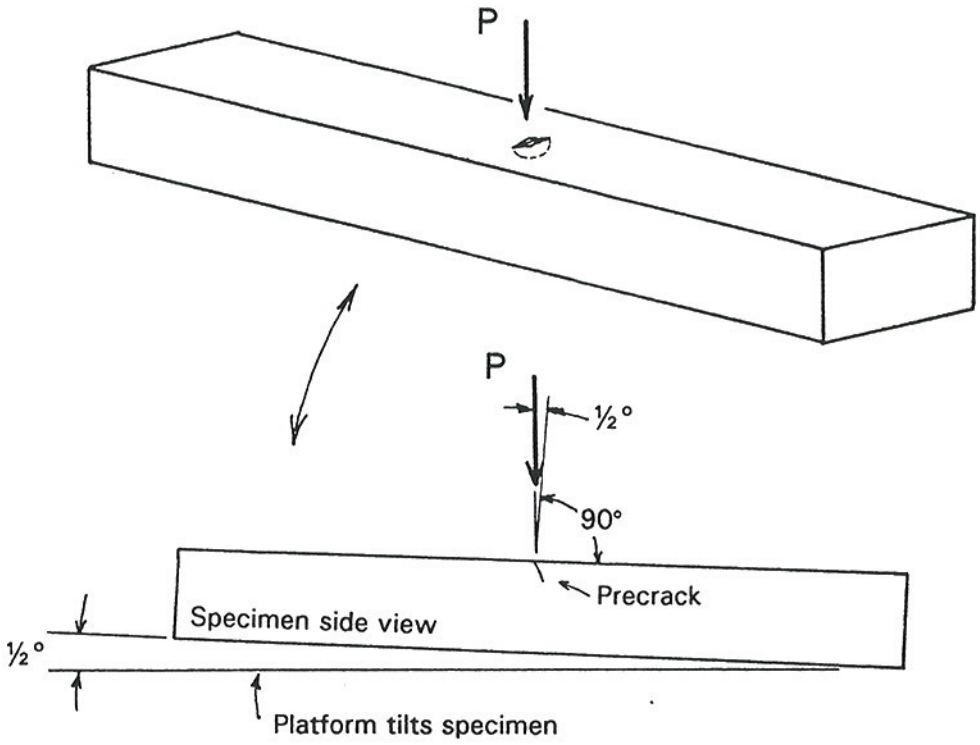

Figure 1. Flexure specimen with a surface crack induced by Knoop indentation. The specimen is tilted slightly so that the precrack is slightly off-perpendicular to the surface.

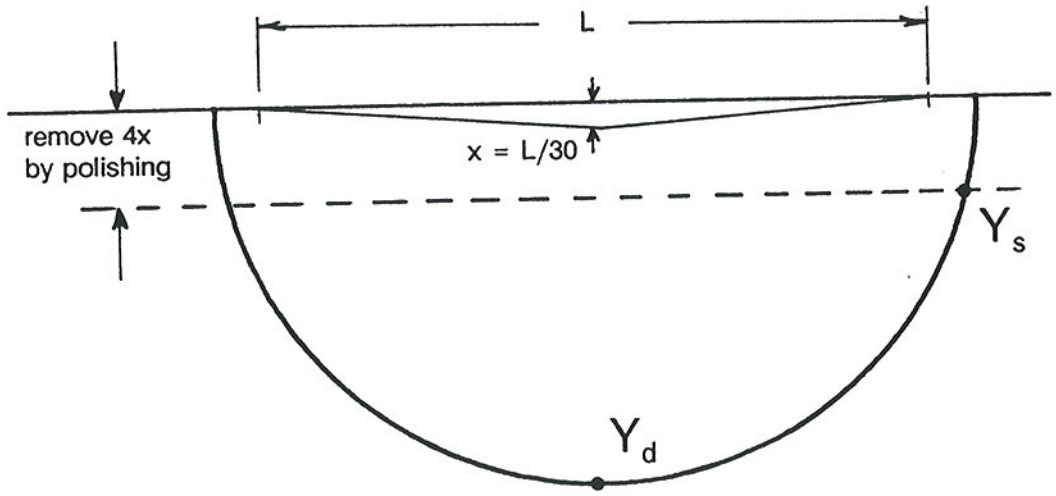

Figure 2. Schematic of the precrack formed under a Knoop indent. The indent and the residual stress zones underneath are removed by polishing away 4 times the depth of the impression (X). A nearly semielliptical precrack is formed, which may have a maximum stress intensity shape factor, Y, at the surface, Y_s, or at the depth, Y_d.

This method was developed in the early 1970's as an alternative to classic fracture mechanics tests using large saw-cut precracks. Kenny [8] made a row of Knoop indentations across the face of cemented tungsten carbide specimens to create a single-edge cracked beam specimen. Kinsman et al. [9] carried the method further by applying only one indentation, but from a Vickers indenter. Petrovic et al. [10-12] then made the critical observation that residual stresses underneath the indentation were influencing the fracture toughness and demonstrated that annealing or polishing were effective means to eliminate the residual stresses. They used the Knoop indenter to make the precrack since only one primary median crack was formed. In addition, it was later noted that lateral cracks were less of an interference to Knoop induced precracks than for Vickers precracks. Knoop precracks are larger than those produced by Vickers indenters at the same load [13,14].

The Knoop precrack is often a semicircle with a diameter approximately equal to the length of the Knoop hardness impression as shown in Figure 2. Although both polishing and annealing can be used to remove the residual stresses, polishing is preferred since annealing has a risk of crack blunting or healing. The amount to polish away has been empirically determined to be about 3-4X the depth of the Knoop impression [10-13,15,16]. This amount is very easy to determine and the polishing can be easily done by hand. The Knoop indentation load can be varied to create larger or smaller precracks as needed. Strength testing is conducted using any one of the standard flexure test methods. These are capable of measuring the fracture stress with an accuracy and precision within 1-3%. The precrack size is then measured on the fracture surface. The uncertainty in the fracture toughness results due to uncertainty in the precrack size measurements is less well-known.

Through the years, many investigators have utilized the Knoop surface crack method for fracture toughness evaluation [10-12, 16-30]. (Many groups have also used Knoop induced surface cracks for crack growth studies [31-42].) The method has been used successfully and given credible results on: hot-pressed, sintered, hipped and reaction-bonded silicon nitrides; hot-pressed, sintered and reaction-bonded silicon carbides; tungsten carbide; titanium carbide; magnesium aluminate spinel; glasses; glass ceramics; and sintered and hot-pressed aluminas. In the instances where different investigators or laboratories have tried the same material, precrack size measurements have often been very consistent (e.g., References 28 and 33 which compared sizes to earlier work of Petrovic et al. [10].)

The method is very similar to the new ASTM standard practice for metals: E 740-88, "Standard Practice for Fracture Testing with Surface-Crack Tension Specimens"[43]. Semielliptical surface cracks are introduced by machining and fatigue precracking into metallic specimens which are loaded to fracture as illustrated in Figure 3. Standard E 740-88 states "A number of different types of

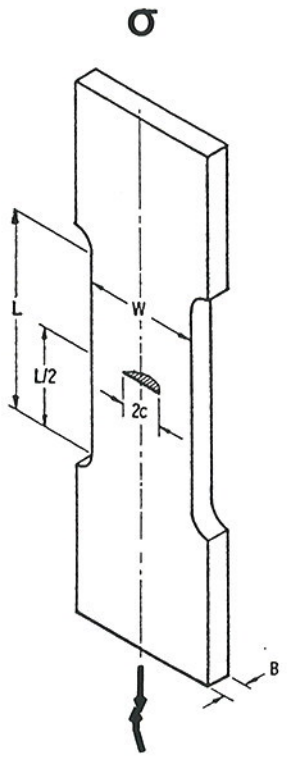

Figure 3. Schematic of the surface crack in tension specimen used in ASTM standard E 740-88.

fracture specimens have been developed to date. Of these, the Surface-Crack Tension specimen is one of the most representative of structures with defects that actually occur in service." Appendix A3 of E 740-88 also notes that the user must be cautious if stable crack extension occurs during the test, and the convention is to compute a nominal fracture toughness based on original crack dimensions and maximum load. (Crack mouth opening displacement techniques are recommended to enable a qualitative assessment of whether stable crack growth occurs.) The procedures in the VAMAS round-robin for ceramics are conceptually the same as those in E 740-88. Indeed, the same stress intensity shape factors are used. We therefore propose changing the name of this method from "controlled flaw" or "controlled surface flaw" to "surface crack in flexure" (SCF) method in order to bring it into harmony with the fracture mechanics conventions and literature.

In general, the SCF method is regarded as producing credible results for fracture toughness which often agree with data produced by other rigorously-conducted fracture mechanics procedures. For example, Ghosh et al. [21] obtained superb surface crack results

that concurred with chevron notch and double torsion data. The Japan Fine Ceramics Association conducted intensive studies of fracture toughness methods from 1984 through 1988 which led to the establishment in 1990 of the Japanese Industrial Standard, JIS R 1607, "Testing Methods for Fracture Toughness of High Performance Ceramics" [44]. In the preliminary phase of this work, excellent results were obtained with the Knoop surface crack method for silicon carbide [45,46]. The results from four of five participating labs agreed with SEPB results, whereas chevron notch, indentation strength and indentation fracture data did not. Surface crack results for an alumina were, again dismissing one lab's results, very consistent but about 15% lower than SEPB data. This may have been a consequence of R-curve behavior (crack extension resistance varies with crack length). No success with the surface crack method was obtained on a partially stabilized zirconia, for which SEPB data gave about 6.5 MPa·$\sqrt{m}$, since no median crack formed under the Knoop impression [46]. The method was held apparently in good regard and was the last candidate method to be dropped in the "weeding-out" process that led to creation of JIS R 1607. The difficulty in detecting the precracks and the fact the method did not work for zirconia were the primary reasons [45,46]. The present round robin will reexamine the suitability of this method for zirconia.

Evans [47] recently summarized the state of indentation microflaw testing: "Many of the indentation methods are only approximate and do not provide the quality of fracture resistance data needed to rigorously relate toughness to microstructure. The surface flaw methods, introduced first by Petrovic and Jacobson, seem to be the most precise, provided that residual stresses are eliminated by polishing out the plastic zone."

The surface crack method will not work on all materials. For it to be successful, the following criteria must be met:

1. The material must be hard and brittle.
2. It must be possible to detect the precracks.
3. The precracks should be larger than the naturally occurring flaws in the material.
4. The precrack size should be some multiple of the grain size in order to assure that what is measured is a polycrystalline fracture toughness (rather than a single crystal fracture toughness), if so desired.

Difficulties arise if the material is too coarse-grained, porous or tough. With soft or porous materials, no crack will form under the indentation. Materials with too high a fracture toughness will form very small precracks that will be removed when the indentation is polished away. In some materials (such as the hipped silicon nitride in this round robin), the precracks may not be flat, but may be irregular, due to the precrack following density or microstructural variations. The precrack may be made up by several

separate segments. Several new experimental techniques were developed in this round robin to enhance the detectability of the precracks.

As noted above, one of the materials for which this method has not worked in the past has been zirconia. Usually, shallow median or Palmqvist precracks form under the Knoop indentation, but they tend to be removed during the subsequent polishing steps. For this round robin a new, modified surface crack procedure was developed which has some potential.

In addition to the above limitations, there can be interferences from:

1. R-curve behavior (increasing crack resistance with crack extension.)
2. Environmentally-assisted crack growth (most often from water in liquid or gaseous form.)

These interferences will affect all fracture toughness methods. R-curve phenomena have received considerable attention in recent years. This round robin project was not designed to be a fundamental materials science study to explore all aspects of crack-microstructure interactions. Instead, it is intended to be an evaluation of the accuracy, precision, consistency, practicality, and technical veracity of the surface crack method. The materials chosen for this study vary from a hot-pressed silicon nitride where no R-curve or environmentally-assisted crack growth behavior was expected, to a zirconia with potentially complicated R-curve behavior.

The surface crack method has the virtue that it can measure the fracture toughness at the size scale of real flaws. Large crack specimens may not give relevant fracture toughness values. In principle, the precrack size and rate of loading could be varied in order to study a variety of topics, such as R-curve behavior.

This round robin was intended to evaluate suitability of the surface crack method for three advanced ceramics. Two silicon nitrides were included with different degrees of difficulty in detecting the precrack. The hot-pressed silicon nitride is easier to measure, either with an ordinary optical microscope at 300-400X, or with a scanning electron microscope. This material is very similar to the hot-pressed silicon nitride that Petrovic et al. [10-12] used in their early study. The hot-isostatic pressed silicon nitride was more difficult and is typical of many sintered or hipped ceramics. The zirconia was included as a special challenge.

Almost seven hundred specimens were distributed to twenty four laboratories. The objectives of this round-robin were:

1. Determine whether participants can use the SCF method on three

advanced ceramics of varying difficulty.
2. Determine whether precracks can be measured with consistency.
3. Determine the accuracy and precision of the method.
4. Evaluate the practicality of the method.
5. Discover what new techniques, suggestions, and ideas the participants may have had.

MATERIALS

Three materials were used in the round robin: a hot-pressed silicon nitride, Norton grade NC-132[2,3]; a hot-isostatic pressed (hipped) silicon nitride, a variety of ESK grade EKasin-D[4]; and a sintered and post-hipped, yttria-stabilized tetragonal zirconia (TZP). General property characterization data is included in Table 2.

Table 2
Properties of the three materials in the round robin.

Material	ρ	σ_0	m	E	ν	HK2	G.S.
NC-132 Si_3N_4+	3.23	741	12.5	320	0.27	14.7	<2*
Hipped Si_3N_4#	3.18	859	13.6	315	0.27	14.4	0.85
Y-TZP Zirconia#	6.03	774	13.9	211	0.31	10.4	0.45

ρ	Density (g/cm³)
σ_0	Characteristic Strength of Specimen, 4 Point (MPa); DIN 51-110, Part 3, Ref. 48; ASTM C 1239-93, Ref. 49.
m	Weibull 2 Parameter Modulus, Maximum Likelihood; DIN 51-110, Part 3, Ref. 48; ASTM C 1239-93, Ref. 49.
E	Elastic Modulus, Sonic or Resonance, (GPa)
ν	Poisson's Ratio
HK2	Hardness, Knoop, 19.8 N (2 kgf), (GPa)
G.S.	Grain Size, Mean Intercept Length, (micrometers)
*	Equiaxed grains 0.1 to 1.0 micrometers; elongated grains 0.5 to 2.0 micrometers; aspect ratios est. 1:2 to 1:6; from Ref. 50)
+	All data except hardness and grain size from Reference 51.
#	All data except hardness from Reference 52.

a. *Hot-pressed Silicon Nitride, NC-132*
All specimens in this round robin were cut from a single plate nominally 155 x 155 x 25 mm in size that was produced in 1974 by uniaxial hot pressing. This material was pressed with a sintering aid of about 1 weight percent MgO which combines with residual SiO_2 on the starting powder surface. The material was fully dense with a density of 3.23 g/cm³ measured both by a water displacement and

---

2 Certain commercial equipment, instruments, or materials are identified in this report to specify adequately the experimental procedure. Such identification does not imply recommendation or endorsement by the National Institute of Standards and Technology or the Swiss Federal Laboratories for Materials Testing and Research, nor does it imply that the materials or equipment identified are necessarily the best for the purpose.

3 St. Gobain/Norton, Worcester, MA.

4 Elektroschmeltzwerk Kempten Gmbh, Kempten, Germany. The designation Ekasin-D was usually applied to hot-pressed material. The same material and additive was used in this study, except that the material was hipped.

geometric means. It has a uniform, fine β silicon nitride grain structure as illustrated in Figure 4. Occasional tungsten related inclusions are present in this material from the ball milling process. Additional details are in References [34, 50, 51, 53]. The specimen size was 3 x 4 x 47.6 mm. Unfortunately, most chamfers were too large and were not within specifications. This caused a reduction of the "moment of inertia" of the cross section, and thus the formula for stress (which assumes a rectangular shape) was an underestimate of the true stress [54]. The maximum error was estimated to be 1.9%, but since the chamfers were not uniform from specimen to specimen, no attempt was made to correct the stress. The most probable error for a specimen was 1% or less. All 240 specimens for this round robin were cut with the same orientation, with the 3 x 47.6 mm faces parallel to the billet top and bottom flat surfaces. Two surfaces were ground with a 900 grit (8 micrometer) grinding wheel in order to provide a flat, uniform, and near polish-quality surface for the Knoop indentation.

NC-132 HPSN was used for many years in many mechanical property studies due to its good properties and uniformity. Indeed, much of the early work by Petrovic and associates featured this material or its immediate commercial predecessor, HS-130, [10-12] and it has been widely used in crack growth studies (e.g., References 31, 33-35). Precrack detection is relatively easy in this material.

b. *Hot-Isostatic Pressed Silicon Nitride*
This material was fabricated in the form of four 50 mm diameter cylinders, 100 mm long, that were cold-isostatic pressed, then hot-isostatic pressed at 1760°C for 1 hour at 2000 bar. Computed x-ray tomography profiles showed that the material was very uniform. The sintering aid was 1.5 wt % magnesia. Density was 3.18 g/cm^3. Figure 5 shows the microstructure which had an average grain size of 0.85 micrometers when measured by the mean linear intercept method of ENV 623-3, "Testing of Monolithic Advanced Technical Ceramics, Part 3, Determination of Grain Size" [55].

Flexural strength was determined in accordance with prEN 843-1, Mechanical Properties at Room Temperature, Determination of Flexural Strength" [56].[5] The characteristic strength of the specimen was 859 MPa with a Weibull modulus of 14. The distribution appeared bimodal, however. These estimates were obtained by a maximum likelihood analysis in accordance with DIN 51-110, Part 3, "Testing of Advanced Technical Ceramics: Determination of the Weibull-Parameters" [48].[6] Additional infor-

---

[5] This practice is consistent with ASTM standard C 1161-90 [57], and MIL STD 1942(A) [58].

[6] This practice is consistent with ASTM Standard C 1239-93, Standard Practice for Reporting Uniaxial Strength Data and Estimating Weibull Distribution Parameters for Advanced Ceramics" [49] for the case where strength is

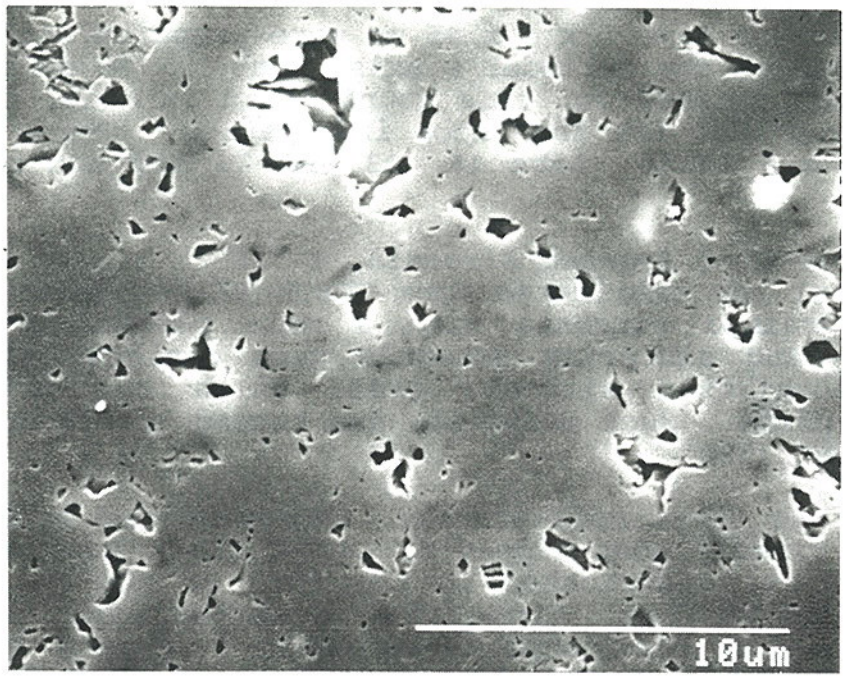

Figure 4. Microstructure of the NC-132 hot-pressed silicon nitride. The etching procedure has removed some of the boundary phase and metallic inclusions.

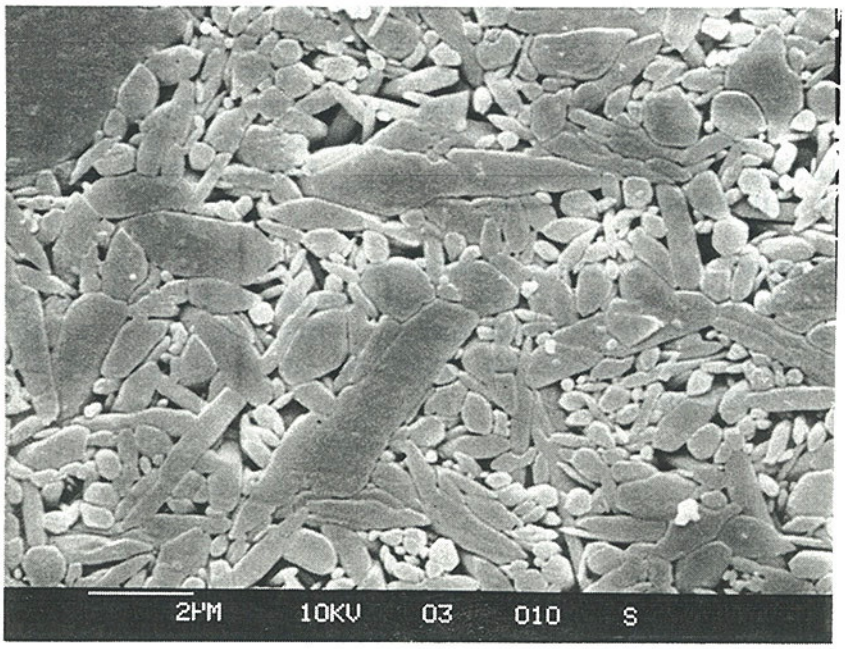

Figure 5. Microstructure of the hipped silicon nitride. Etching has removed the boundary phase.

mation is available in [52].

220 specimens of size 3 x 4 x 45 mm were prepared with their long axis parallel to the cylinder's axis. One 3 x 45 mm face of each specimen was polished for this round robin in order to provide a flat and even face for the Knoop indentation. These were enough for twenty one labs. Labs 16, 23 and 24 did not receive this material.

c. *Hot-Isostatic Pressed Zirconia, Y-TZP*
This material was fabricated from TOSOH TZ-3Y powder[7] which is a very fine-grained zirconia with 3 mole percent yttria. The composition and sintering schedule were designed to produce a partially-stabilized zirconia (PSZ) which has primarily the tetragonal phase. Such materials are termed "tetragonal zirconia polycrystals" (TZP).

The powder was first cold-pressed, then sintered at 1510°C for 2 hours, and finally post-hipped at 1450°C for 1 hour at 1100 bar. The material was fabricated in the form of two 50 mm diameter cylinders, 200 mm long. Computed x-ray tomography indicated that there was negligible density variation. Figure 6 shows the microstructure which had an average grain size (ENV 623-3 [55]) of 0.45 micrometers. X-ray diffraction on a ground surface revealed mostly tetragonal and/or cubic phase. EMPA detected a small amount of monoclinic zirconia on one specimen. Centro Ceramico detected no monoclinic phase on other bars, either in the as-received state or after machine grinding/polishing with 180-800 grit SiC papers to remove the indentation. NIST detected a slight (~5%) amount of monoclinic phase on a specimen after 180 and 240 grit SiC paper polishing to remove the indentation. The Y-TZP density was 6.03 g/cm^3. Flexure strength testing at room temperature (prEN 843-1 [56]) gave a characteristic strength of the specimen of 859 MPa with a Weibull modulus of 13.6. Additional details on this material are in Reference 52.

240 flexure specimens were prepared with size 3 x 4 x 45 mm and distributed to all labs. All specimens were cut with their long axis parallel to the cylinder axis. One narrow 3 x 45 mm face was polished on each specimen to provide a suitable surface for the indentation precrack.

---

[7] Toyo Soda Manufacturing Co., LTD, Tokyo, Japan.

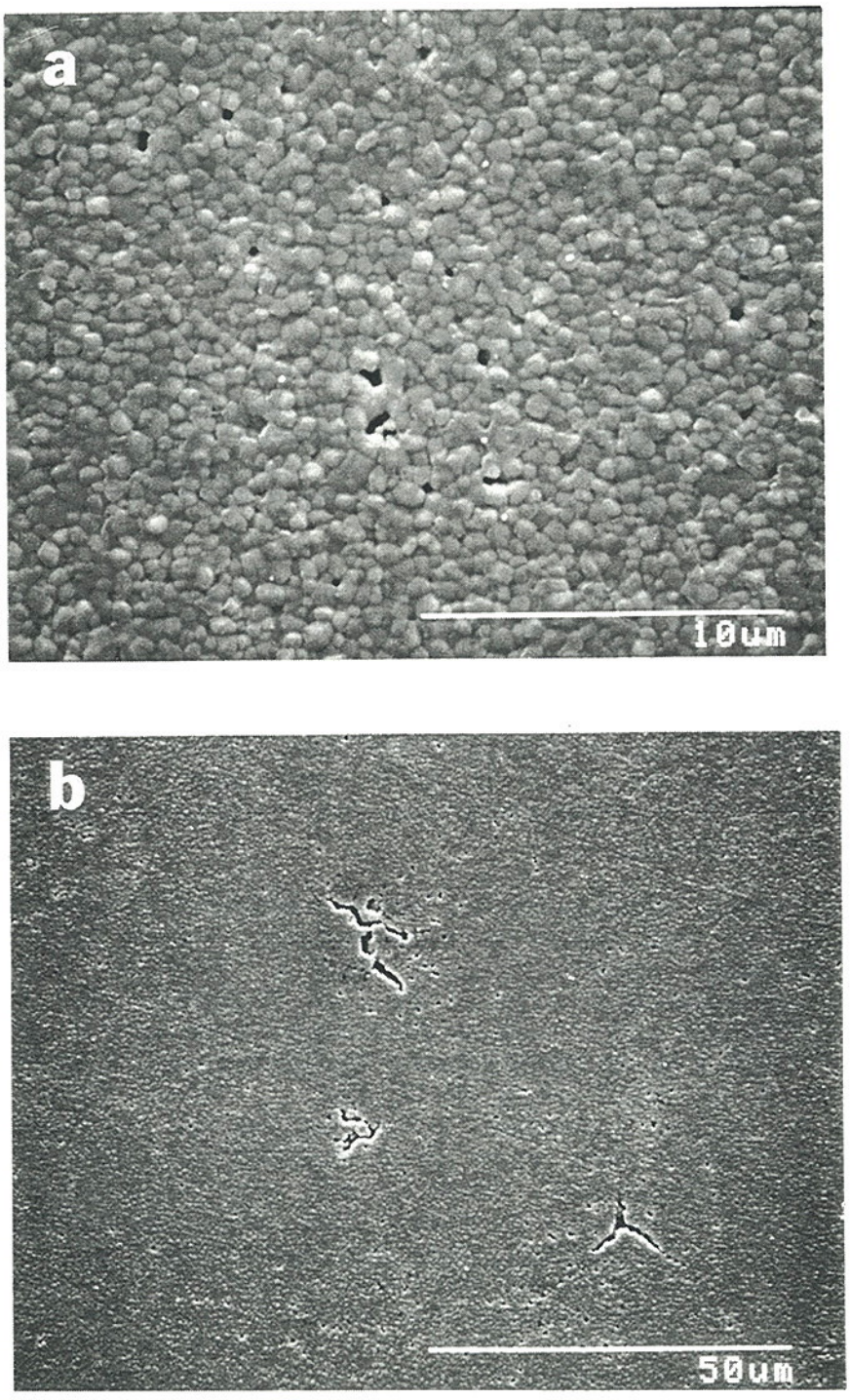

Figure 6. Microstructure of the yttria-stabilized tetragonal zirconia (Y-TZP). (a) shows the usual structure; (b) shows an area with three sintering defects.

EXPERIMENTAL PROCEDURE

General
The detailed instructions that were furnished to all participating labs are included as Appendix I to this report. Only a summary of the procedure is presented here with some clarifying discussion.

Each laboratory received ten specimens of each of the three materials, with the exception of labs 16, 23, and 24 which received no hipped silicon nitride due to a specimen shortage. Part 1, testing the hot-pressed NC-132 silicon nitride, was mandatory. Laboratories could then do either Part 2, the hipped silicon nitride; or Part 3, the zirconia; or both.

The instructions stated that only five of the hot-pressed NC-132 silicon nitride and the zirconia specimens were to be tested. (The remaining five were spares for supplemental testing such as trying different loading rates, specimen orientations, or test methods altogether.) Participants who tried the hipped silicon nitride were instructed to test all ten specimens since the precracks were more difficult to find.

The flexure specimens were furnished with one or two faces already polished to provide a smooth surface for a uniform indentation.

Precracking - silicon nitride specimens
The hot-pressed and hot-isostatic pressed silicon nitride specimens were precracked with a Knoop indenter using ordinary hardness equipment. Loads of 24.5 N (2.5 kgf) and 49 N (5 kgf) were specified for the hot-pressed and hot-isostatic pressed silicon nitrides, respectively.

Most participants were able to make hardness impressions at the prescribed loads, but there were exceptions. Some laboratories did not have hardness machines that had a 24.5 N (2.5 kgf) load capability, and instead used a 29.7 N (3 kgf) load for the hot-pressed silicon nitride. This procedure was quite satisfactory. A number of labs had microhardness machines which were limited to a maximum load of only 19.8 N (2 kgf). These labs resorted to installing a Knoop indenter onto universal testing machines. Unfortunately, there was *very high scatter* in the size of their impressions and precracks. Nearly all the participants who used this process had indentation sizes that were substantially larger than those created by conventional hardness machines. High loading rates, inertia, and vibration probably caused these problems. Such procedures are not recommended for careful hardness work, but were probably satisfactory for this round robin since it was only intended to create a precrack whose size would be measured later.

Some of the labs reported difficulty with removal of the indentation and the residual stress field. Either the material removal rates were too slow, or there were problems in controlling

the amount of material removed.

The most difficult part of the project, contributing the most to the data scatter, was precrack detection and characterization. In general, the indentation load must be sufficiently large to create a dominant precrack (compared to natural flaws), but not so large as to cause a heavily damaged or distorted precrack. To enhance the detectability of the precracks, it was prescribed that the specimens be intentionally misaligned with a slight "tilt" of ½° as shown in Figure 1 and in Appendix 1. The tilt led to precracks forming at angles from 0 to 2-3° off perpendicular. This greatly enhanced the visibility of the precracks on the fracture surfaces. A larger specimen tilt angle of 2° was tried at NIST prior to the start of the round robin, but was unsuccessful because precracks tended to form at 5° or more of perpendicular. This was felt to be excessive, especially since the stress intensity shape factor, Y (see below), might be affected as discussed in Appendix 5. The simplest procedure to aid in precracking with the ½° tilt was to make a small plate with suitably-sized grooves to hold 3 and 4 mm wide specimens. The plate could be put in the indentation machine with a shim under one end of the plate to tilt one end of the specimen up by ½°. Such a plate allows many specimens to be indented with good alignment in a short period of time.

Indents were to be placed in the middle (both width and lengthwise) of the polished **wide** (4 x 47.6 mm) face for the hot-pressed silicon nitride, and into the polished **narrow** (3 x 45 mm) face for the hot-isostatic pressed silicon nitride and zirconia specimens. The wide face down orientation is customarily used for strength testing, whereas the narrow face down is often used in fracture mechanics testing (e.g. CN or SEPB methods). The intent in the present round robin was to try both ways and determine if one method was preferable.

It is essential in this method to remove the residual stresses associated with the impression. The residual stress and damage zones were removed by polishing. Petrovic and associates [10-12] empirically determined that 3 times the depth of the Knoop impression (X) is adequate, and recommended 4X to be on the safe side. Precise indentation length measurements are not necessary. More recent testing has confirmed the 3X removal criterion [15,16]. Srinivasan and Seshadri [27] suggested that only 1X was necessary for a sintered silicon carbide. The depth of an impression is approximately 1/30 of the long diagonal measurement, which can be measured with a common hardness testing machine. For the present round robin, it was requested that the participants remove 4.3 to 4.5 times the impression depth in order to ensure that the maximum stress intensity shape factor (Y) was at the deepest part of the precrack periphery as discussed below.

Precracking - zirconia
Similar Knoop indentation procedures with the zirconia were not

successful, even with loads up to 490 N (50 kgf). Median precracks might have formed, but were apparently so small that they were removed during the subsequent polishing steps. Therefore, an innovative method involving a 149 N (15 kgf) Vickers indentation **with both a ½° tilt and a 3° cant** was specified as illustrated in Figure 8. The Vickers indenter created only Palmqvist type precracks emanating from the corners of the impression. The 3° cant caused one of these cracks to be significantly larger than the other. Upon subsequent polishing (2.5X the impression depth[8]) to remove the impression and the residual stress zone underneath, the smaller Palmqvist crack was removed, but the larger crack left enough of a precrack such that it could function as a surface crack. In fact, it was not symmetrical, but was typically kidney-shaped. Other investigators have reported similar shapes, and that median half-penny cracks usually do not form under Vickers indenters in Y-TZP at loads up to 490 N (50 kgf) [45, 59-62].

The duration of load contact was important for the zirconia. Preliminary experiments at EMPA indicated that 30-45 seconds was necessary. Specimens did not fracture from precracks if the indentation time was only 8 seconds. Lab 24 reported that, contrary to the instructions, 294 N and 392 N loads were used for their precracking.

Specimen polishing
The instructions specified that 4.3-4.5X (where X is the indention depth) was to be removed from the Knoop impressions, and 2.5X for the canted Vickers indentation. A common perception is that this is a difficult time-consuming step. It should not be.

A simple procedure using dry silicon carbide abrasive paper was suggested by NIST, although other procedures were permitted (provided that undue damage was not created). The procedure is similar to that recommended by Petrovic and colleagues [11]. NIST recommended that participants use an ordinary metallographic polishing machine with a 200 mm (8") disk of 70 micrometer (180 grit) silicon carbide paper. A small holder with double edge adhesive tape would be handy to hold the specimen onto the rotating paper, although the specimens could be held with the fingers with medium pressure. Polishing should be done dry to a depth close to the final size, then a final polish done with a 40-50 micrometer (240 grit) or finer disk of silicon carbide, also dry. About one sheet or disk of paper of each grit was needed per specimen since the paper wears out rapidly. These steps required only 5-10

---

[8] This was empirically determined to be suitable in a series of preliminary experiments at EMPA in which different amounts of material were removed for a range of indentation loads.

minutes per specimen.[9] Other procedures were allowed and produced acceptable results. For example, EMPA used diamond abrasive blocks (hones)[10]. Other procedures are surely possible.

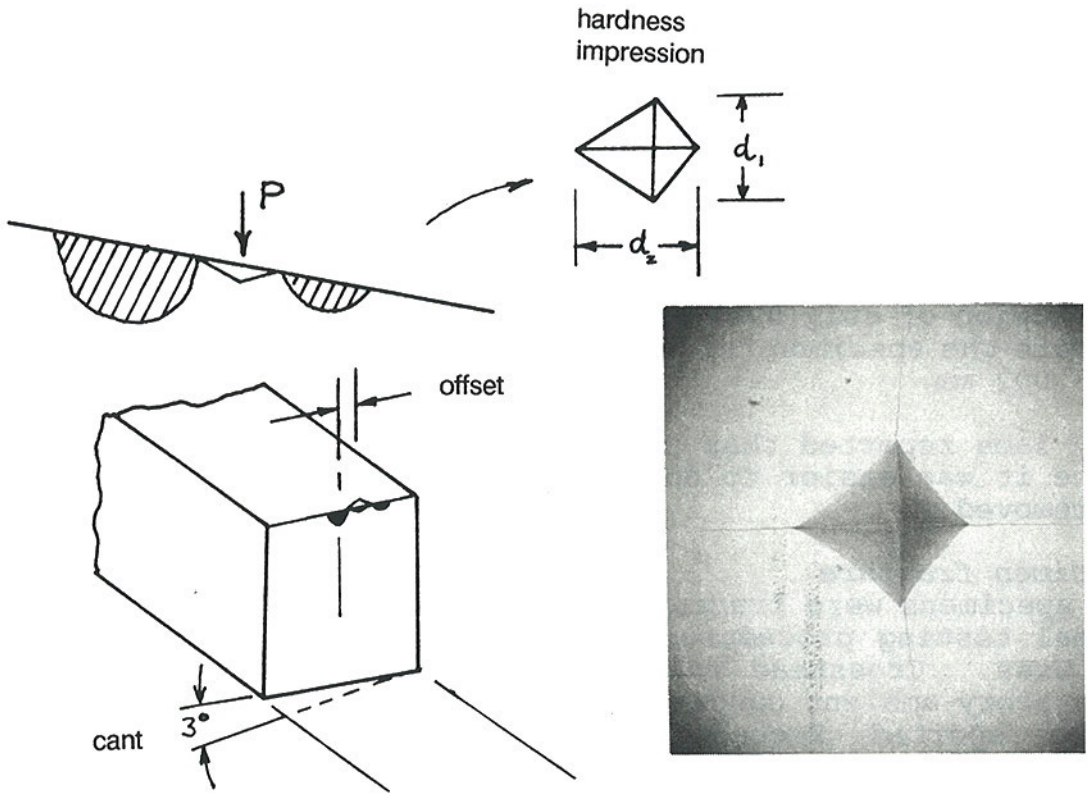

Figure 7. A new procedure with a tilted and canted Vickers indenter was used to create precracks in the zirconia. The cant causes one Palmqvist crack to be larger than the other. The insert shows a 149 N (15 kgf) indentation.

---

[9] The organizers of this round robin, the authors of this report, can attest personally to the success of this procedure. The burnt finger tips of one participant are the proof.

[10] 3M Diamond Whetstones. Diamond impregnated aluminum blocks of size 50 x 150 mm. N70 (70 micrometers, about 200 grit) was used for coarse, and N40 (about 40 micrometer, 280 grit) was used for fine polishing for the last 10 micrometers. This was done wet with an eraser as a simple hand holder.

One of the surprising outcomes of the exercise was that a number of the laboratories had difficulty with the polishing. Some indicated that they had no success with the recommended procedure. Several reported that removal rates were too slow. They may have tried to use one abrasive sheet for too long, or they may have tried polishing with a wet abrasive sheet. Several labs resorted to machining by diamond wheel grinding.

The Knoop indentations in the hot-pressed silicon nitride, NC-132, were about 150 micrometers long (for 2.5 kgf) and for the hot-isostatic pressed material, 225 micrometers long (5 kgf). Thus, about 22 and 32 micrometers of material should have been polished away from the two materials, respectively. It was not critical to polish the exact amount away, since the residual stresses should be eliminated by anything over 3X the indentation depth. One lab complained that it was not possible to remove the correct amount of material since it was extremely difficult to measure such small dimensions. Presumably they were using a hand micrometer with a resolution of only 0.01 mm, whereas most participants were able to measure the specimen thickness with micrometers with Vernier scales to 0.002 mm.

Many labs reported that polishing the narrow face was much easier since it was easier to hold the specimen and less material had to be removed.

Specimen fracture
All specimens were fractured in four point flexure fixtures, using normal testing procedures. Every laboratory utilized 20 x 40 mm fixtures. Crosshead rate was specified as 0.5 mm/min. Normal laboratory ambient conditions were used, but relative humidity had to be reported. Procedures were consistent with ASTM Standard C 1161-90 [57], MIL STD 1942A [58], and European prEN 843, Part 1 [56]. These standards are very similar [63] and require the load rollers be free to rotate to eliminate friction error.

The hot-pressed silicon nitride was tested with the precracked 4 mm wide face resting on the fixture rollers, whereas the hipped silicon nitride and zirconia were tested with the precracked 3 mm wide face in tension as shown in Appendix 1.

Precrack measurement
The fracture surface of each specimen was examined with a microscope to verify that the specimen fractured from the precrack, and if so, to measure the precrack dimensions. Participants were allowed to use either an optical or a scanning electron microscope. Both were used in some instances.

There can be problems in detecting and measuring the precrack size. Some fractographic experience is needed. In general, different techniques are needed for different materials to measure the precrack sizes. The instructions, Appendix 1, gave a number of

techniques to make this easier. To assist the participants in interpretation, example precrack photos (both SEM and optical) of the NC-132 were furnished with the instructions.

It proved to be very beneficial that the dependence of the computed toughness was on the square root of crack depth. Uncertainty in measurement of crack depth was diminished in the calculation of fracture toughness. This is in sharp contrast to other methods where an uncertainty in crack size measurement is magnified. This will be discussed in more detail below.

Calculation of fracture toughness
Fracture toughness was computed from the simple formula:

$$K_{Ic} = Y \sigma \sqrt{a} \qquad (1)$$

where: Y is the stress intensity shape factor
σ is the flexure strength of the specimen (MPa)
a is the crack depth (m)

The stress intensity shape factors, Y, for semicircular and semielliptical surface cracks in bending are from the empirical equation developed by Newman and Raju [64]. The equation was prepared for surface cracks with $a/c \leq 1.0$. It was anticipated that most participants in the present round robin would find precracks that fit this criterion, but there were some instances where the a/c ratio was slightly larger than 1.0. The Newman-Raju formula is acceptable in these instances, but as Fett discusses in Reference [65], correction terms are appropriate for a/c ratios much higher than 1.0.

The Newman-Raju formula for Y is very popular and widely accepted. It is estimated that it is accurate to within a few percent [64,65]. The new ASTM standard practice, E 740-88 "Fracture Testing with Surface Crack Tension Specimens" [43] uses it for metallic materials. For this round robin, the formulas were used as expressed in the ASTM standard, since they simplify the computation process.[11] A floppy computer disk with the Newman-Raju formula was supplied as part of the kit sent to all participants. There is only a need to compute Y at the surface, Y_s, and at the deepest part of the crack, Y_d, and not over the entire crack periphery. The *maximum* Y factor is used in equation 1, since it is expected that the critical fracture toughness, K_{Ic}, is reached at that point. The cracks are also small relative to the specimen width, and the term dealing with this factor was deleted.

---

[11] The Newman-Raju formulas are generalized, and apply to all angles along the crack front. The maximum values will always be either at the surface or the deepest point. The ASTM E-740 formulas and those used in this round robin are simplified in that they only solve for the Y factors at the two latter positions.

The crack shape after the removal of the residual damage zone may actually be a section of a circle, but comparisons of the geometries indicate that the ellipse is an excellent approximation, provided that fracture begins at the deepest part of the precrack. This is discussed more fully in Appendix 5.

There is some concern that the stress intensity factors may not be correct at the intersection of the precrack with the specimen surface [37, 66, 67]. There are also complications arising from local perturbations of the crack front, uncertainties about the ellipse approximation to the section of a circle or section of an ellipse, and possible interactions with surface damage. Therefore, the amount of material to be removed after indentation was increased from the conventional 4X recommended by Petrovic et al. [10-12] to 4.3-4.5X in order to make the precracks more elliptical in shape. This forces the maximum Y factor to be at the deepest part of the precrack.[12]

Finally, there is some question of whether the precrack tilt will alter the stress intensity factors, possibly by introducing Mode II loading to the crack. Appendix 5 presents information indicating that for tilt angles less than 5°, the influence is negligible.

---

[12] For a semicircle, the maximum Y factor is at the surface. As the shape becomes elliptical, the maximum Y increases at the deepest point, and becomes dominant for shallower ellipses with a/c ratios less than about 0.8.

RESULTS

General
None of the labs reported difficulty with the flexure strength measurements. One lab noted that their specimens impacted on the fixture after fracture, and that some fracture surfaces were lost. Difficulties in indentation and polishing steps have been noted above.

The results reported by all labs for the three materials are summarized in Table 3. The number of specimens for each set is shown in parenthesis. (Laboratories 6, 7, 14 and 16 dropped out of the round robin.) Labs used either optical or scanning electron microscopy (SEM), and sometimes both for precrack characterization. The data has been distinguished in each case in this report. In Table 3, the SEM results are in bold typeface and the optical values in normal typeface. Some labs sent results based on several different sets of photos (e.g. photos from one microscope at one magnification, and a set of different measurements taken with a different microscope, or photos interpreted by a different observer). In such instances, the round robin organizers either chose the data set with the highest magnifications and which showed the precracks the best, or the organizers contacted the individual labs and asked them to chose which set of data was the best for their own lab. In a few instances, labs reported individual specimen outcomes as "bad" or "unreliable." These were not used.

Appendix 2 lists information regarding the fractographic procedures used by the participating laboratories, as well as many example photos. All laboratories were instructed to furnish one photo of a well-defined ("good") precrack, as well as one photo of a ill-defined ("poor") precrack, for each material that they tested. The precrack outline had to be marked by the participating lab. Some labs sent marked photos of every specimen. Other labs ignored the instructions and sent no photos, or photos that were not marked. If no photos were sent, the data has been labelled in Table 3 and in the following figures with a question mark "**?**".

A grand average fracture toughness was computed for each material as discussed in Appendix 3. This required some consideration as to how to incorporate both the SEM and optical measurement. In addition, some consideration went into the deletion of several data sets. Sets not included in the grand average are included in Table 3 and in the figures, but are marked with an "**x**". Deletion of a data set was rarely done, and *only if there was evidence that the precracks had been seriously misidentified.* This was the case if fracture mirrors or hackle lines were marked in the photos. In no

Table 3

Fracture toughness results for the round robin. Each block shows a lab's mean result, the standard deviation, both in (MPa·√m), and the number of specimens tested (in parentheses). The bold values are **SEM** measurements. Otherwise, values are from optical precrack measurements.

Laboratory	NC 132 Si_3N_4	Hipped Si_3N_4	Y-TZP Zirconia
1	4.32 ± 0.12 (5)?	4.81 ± 0.34 (4)?	---
2	**4.45 ± 0.32 (5)**	**5.20 ± 0.34 (10)**	**4.42 ± 0.27 (4)+**
3	5.05 ± 0.31 (7)?	5.04 ± 0.44 (9)?	---
4	**4.64 ± 0.30 (7)**	**5.17 (1)**	**4.33 ± 0.14 (2)**
5	**4.64 ± 0.21 (7)**	**5.08 ± 0.38 (9)**	**4.90 ± 0.98 (4)+x**
6*	---	---	---
7*	---	---	---
8	**4.32 ± 0.38 (5)**	**4.73 ± 0.43 (7)**	**4.79 ± 0.41 (5)+x**
9	4.69 ± 0.19 (6)	4.50 ± 0.39 (9)	5.90 ± 0.29 (5)x
10	**4.58 ± 0.23 (3)**	**3.90 ± 0.88 (5)**	**3.55 ± 0.44 (4)**
11	**4.42 ± 0.07 (3)**	**4.59 ± 0.17 (5)**	---
12	**4.63 ± 0.32 (5)**	**4.95 ± 0.60 (9)**	---
13	**4.56 ± 0.19 (5)**	**4.74 ± 0.22 (7)**	---
14*	---	---	---
15	**4.35 ± 0.29 (5)** 4.21 ± 0.08 (5)	**5.01 ± 0.31 (6)**	**4.52 ± 0.27 (5)** 4.49 ± 0.21 (8)
16*	---	not sent	---
17	4.36 ± 0.05 (4)	5.23 ± 0.02 (3)	4.68 ± 0.20 (5)
18	**4.03 ± 0.15 (2)** 4.44 ± 0.18 (5)	---	---
19	**4.16 ± 0.28 (6)** 4.29 ± 0.19 (6)	---	---
20	**4.72 ± 0.13 (6)**	**5.15 ± 0.24 (8)**	**4.20 ± 0.40 (5)**
21	**4.74 ± 0.34 (3)+** 5.66 ± 0.65 (5)	**5.64 ± 0.71 (8)** 5.70 ± 0.33 (7)	---
22	**4.65 ± 0.19 (4)+** 4.67 ± 0.23 (3)+	**4.88 ± 0.66 (3)+** 5.25 ± 1.25 (4)+x	**4.13 ± 0.20 (2)+** 4.63 ± 0.40 (4)+
23	**4.10 (1)**	not sent	**4.64 (1)**
24	**4.66 ± 0.32 (10)**	not sent	**4.87 ± 0.80 (9)x**
Grand Avg.	**4.59 ± 0.37 (107)**	**4.95 ± 0.55 (105)**	**4.36 ± 0.44 (33)**

\+ Data revised
? Data not verified by photo
* Withdrew from round robin
x Data not used in grand total

instance did the organizers discount individual specimen results (unless the data point was labelled "bad," "unreliable," or "do not use.") Either the whole data set was included in the computation of the grand average, or it was not. The organizers did request clarification of some results, (e.g, typographical errors, or unmarked photos). In several instances, the organizers discerned problems with data sets and requested a laboratory to reexamine the data. If the data was corrected in a substantive manner, it is marked with a "+" symbol in Table 3 and the following figures.

Histograms of all accepted results for the three materials are shown also in Appendix 3.

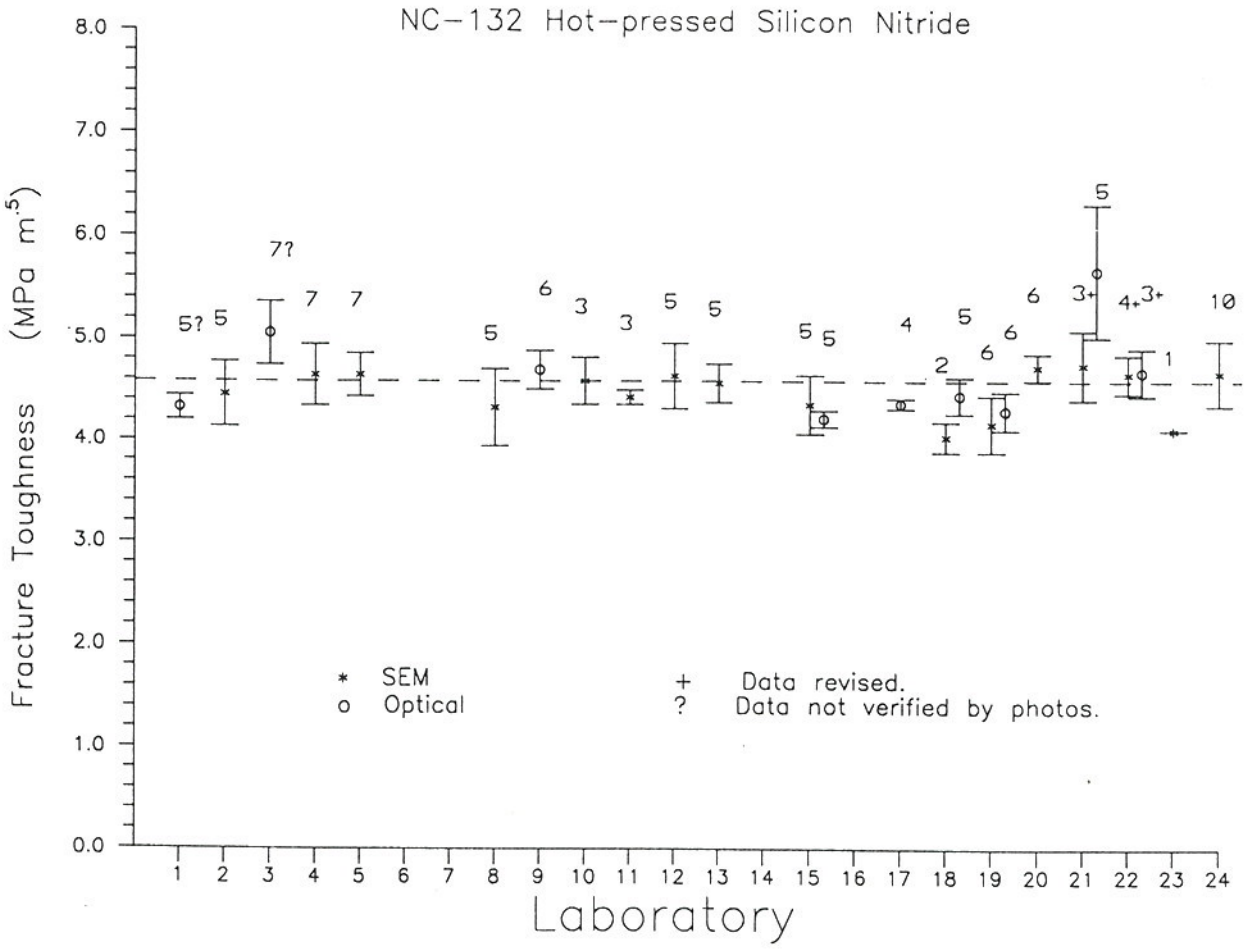

Figure 8. Master results graph for the NC-132 hot-pressed silicon nitride showing the individual lab results and standard deviations. Each data set is labelled by the number of specimens in the sample. The dashed line is the grand, population average.

NC-132, Hot-Pressed Silicon Nitride

Figure 8 and Table 3 show the results for NC-132, which had a grand average fracture toughness of 4.59 MPa·$\sqrt{m}$ and a combined standard uncertainty (i.e., estimated standard deviation) of 0.37 MPa·$\sqrt{m}$. This result was based on the outcomes of 107 specimens. (A histogram of all accepted outcomes in Appendix 3 shows the results have a bell-shaped distribution.) All twenty labs that participated had at least one successful outcome. Some labs had 100% success rates: every specimen tested yielded a result.

No data was discounted for this material. Two labs had to revise their results: lab 22 because the fracture mirror was initially marked as the precrack, and lab 21 for SEM readings wherein hackle had been initially marked. Labs 1 and 3 sent no photos, and indicated that precrack measurements were made on a microscope and not from photos.

The grand average was within the scatter bands (mean plus or minus one standard deviation) of the individual laboratories in most instances (15/20).

An alternate way of evaluating the consistency of the labs' results is to apply the central limit theorem for the variation of sample means about a population mean. The *sample means* should be distributed about the *population mean,* x, (all fracture toughness values) with a standard deviation of SD_x/n, where SD_x is the standard deviation of the population of fracture toughness values.[13] Thus, for a sample set of 5 specimens, the sample means should be distributed about the grand average with a standard deviation of $0.37/\sqrt{5} = 0.165$ MPa·$\sqrt{m}$. The more specimens in a sample, the closer the sample mean should be to the population mean. Since the labs used different numbers of specimens, their possible deviations from the population mean will vary. Twelve of nineteen (63%) labs' averages fell within one standard deviation of the mean, which is as expected (68%) for the normal distribution.[14] Sixteen of the nineteen (84%) labs had means within two standard deviations of the mean, which is somewhat less than the expected 95%.

---

13 If the mean, x, and standard deviation of the population SD_x of all fracture toughness values is known, then a given sample set of n specimens will have a sample average toughness. This sample average can, in principle, have any value in the range of toughnesses, but the value will tend to cluster about the mean of the population. The distribution of the mean values of random samples of size n from an arbitrary population approaches a normal distribution with the same mean as the population mean, and with a standard deviation of $SD_x/\sqrt{n}$.

14 The lab with only one outcome was not included. In instances where a lab had both an optical and SEM set, each data set was counted as half a data set for the lab count.

Figure 9 shows some NC-132 precracks as detected by NIST with the SEM[15]. For a 24.5 N (2.5 kgf) indentation with the proper amount of material removal, the precracks should have had a depth, a, of 35-55 micrometers. The width, 2c, should have been between 120 and 160 micrometers. Figure 10 shows additional precracks as photographed with an optical microscope[16].

Most labs used the SEM for precrack measurements. Most of these labs had little problem in finding and characterizing the precracks. Only two labs (1 and 9) had no success at all with the SEM, but they did have success with optical microscopy. Several labs used both the SEM and optical microscopy and reported interesting comparisons of the size estimates.

The testing success ratios (number of specimens with a successful outcome/total number of specimens attempted) varied considerably from lab to lab. Most labs had a high overall success rate, ranging from 50-100%. Six had 100%; four more 80% or higher; five more at 60 or 70%; two more at 50%; and two more uncertain, but at least 70%. There were only two labs with less than 50% success rates: labs 11 and 23 which both had polishing problems that caused them to remove too much material, and as a consequence, most specimens did not fail from the precrack.

Nearly all labs (17 of 20) reported that they could find the precracks without difficulty in most specimens. About 50-60% said or implied that precrack characterization was not difficult. Several labs indicated that although they could find the precrack, marking its boundary was difficult. Three labs had difficulty finding the precracks. The organizers requested two of these labs to reevaluate their assessments. Nearly all the NC-132 specimens had a maximum Y at the deepest point of the precrack. It was usually not possible to identify an exact spot on the precrack periphery as the starting point, but in some specimens, the hackle lines changed direction as they emanated from the precrack. The direction of these could be used to infer a zone of fracture initiation as indicated in Figure 11. Occasionally one specimen from a lab sample had a slightly higher value at the surface. There were two exceptions: labs 3 and 12 had maximum Y values at the surface most of the time. Lab 3 had precracks that were semicircular or even deeper than semicircles, so that the surface Y values were quite a bit higher than those in the depth. Lab 3's size estimates were not precise and were obtained from an optical microscope with no supportive photography. This may have contributed to the deviation of their results from the others. The Newman-Raju formula was used for these precracks with $a/c > 1.0$, but Lab 3 noted that formulas for deeper ellipses [65] deviated

---

15 Hitachi model S-530.

16 Zeiss model Photomicroscope III.

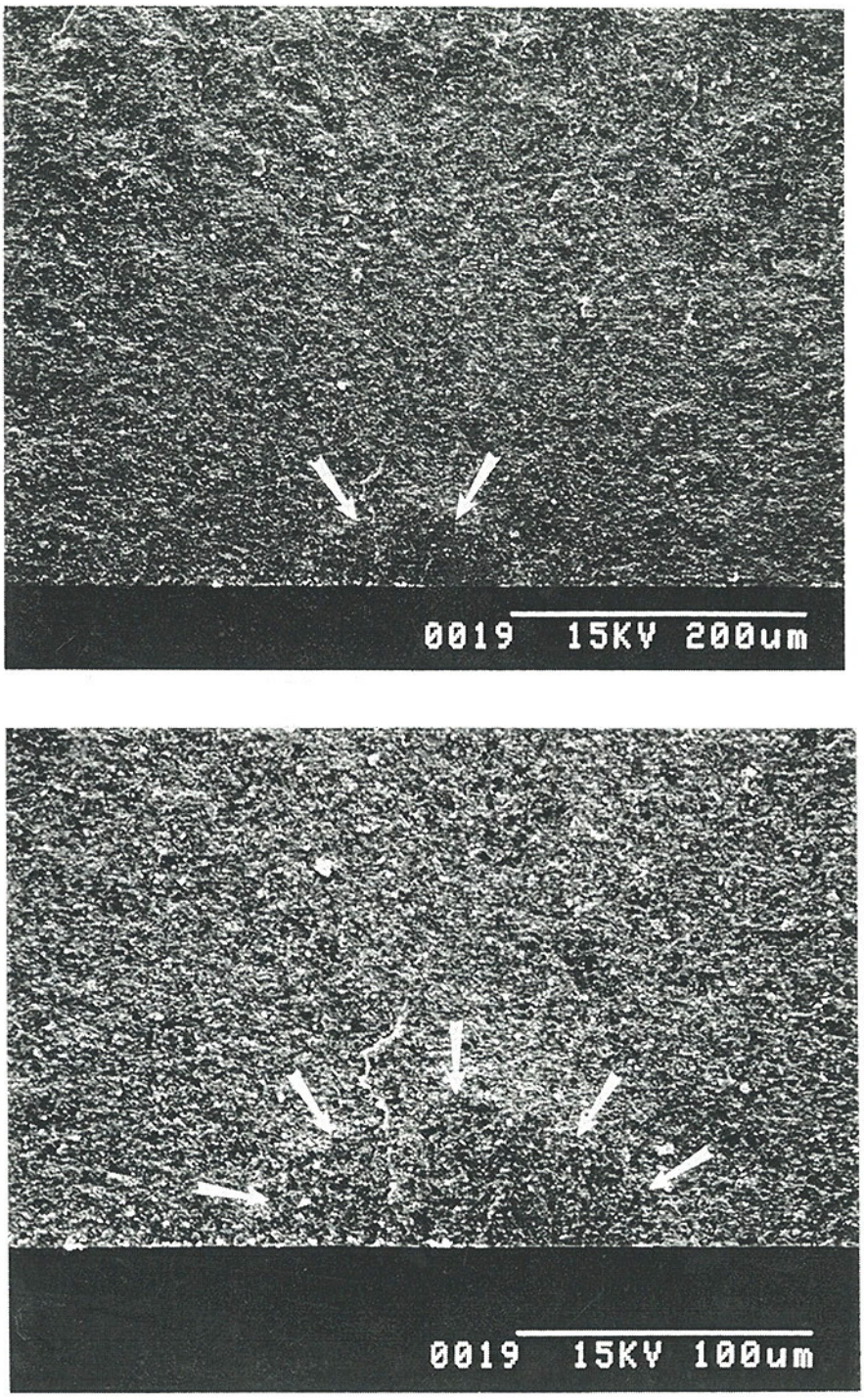

Figure 9. SEM photos of precracks in the NC-132 hot-pressed silicon nitride.

from the Newman-Raju formula by only 2%. Lab 12 had very precise readings, and the Y values at the surface were not too much different than the Y values at the deepest point. Their data is in good agreement with the grand average. Several labs noted interference of machining damage at the surface (as illustrated schematically in Appendix 1, page A1.9). A few specimens showed some evidence of a stable sub-crack pop-in at the surface, followed by general fracture from the deepest portions of the precrack as illustrated in Appendix 1.

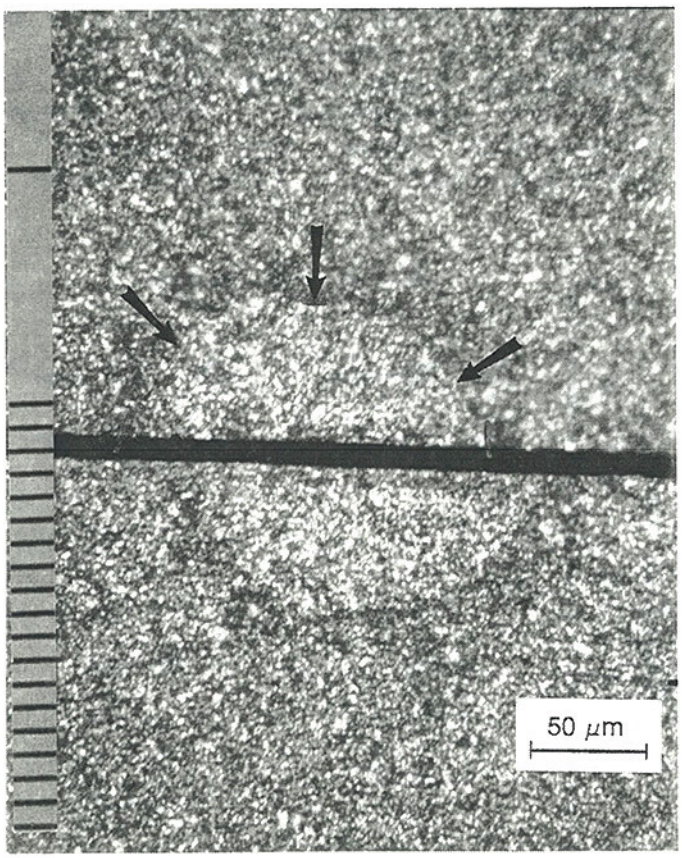

Figure 10. Optical microscope photos of precracks in the NC-132 hot-pressed silicon nitride. The two fracture halves are mounted back-to-back. The precrack is marked by arrows. It is surrounded by a small, slightly darker halo which is the region where the fracture surface changed from the initially tilted precrack to the plane of the final fast fracture.

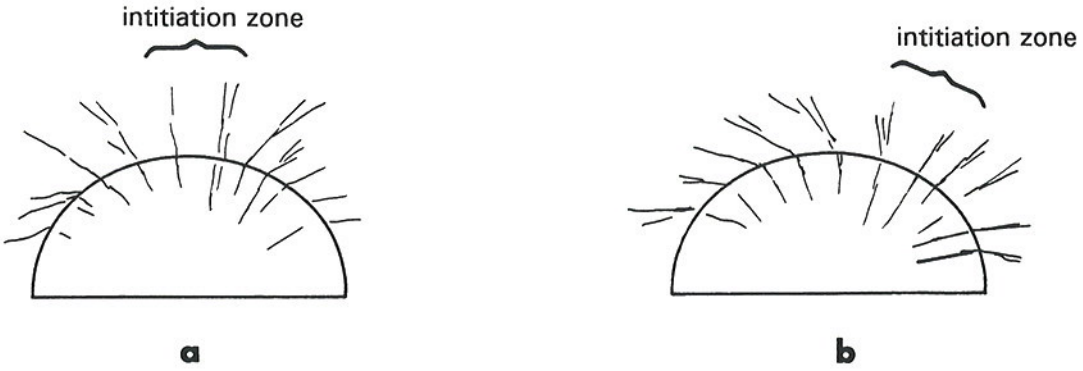

Figure 11. Schematic of the observed microhackle lines which emanated from the precracks. These often had different orientations than the microhackle lines inside the precrack and were instrumental in assessing from which part of the precrack the fracture commenced. (a) shows an example of initiation from the deepest portion of the precrack; and (b), from the side.

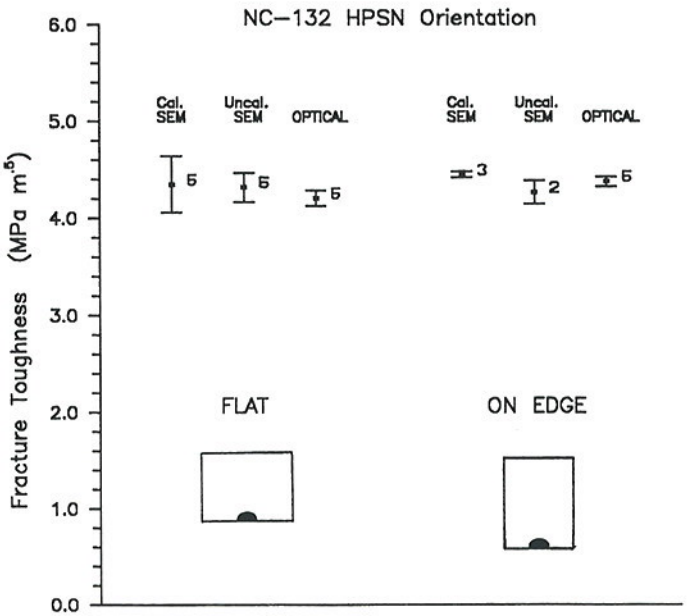

Figure 12. Fracture toughness of NC-132 silicon nitride as measured in two different orientations, both with optical and scanning electron microscopy. The uncalibrated SEM photos had precrack measurements based solely on the indicated bar marker from the SEM. The calibrated measurements used a SEM calibration standard and were more accurate.

NIST compared optical versus SEM readings on the same specimens. In addition, specimens were tested in both possible orientations (3 x 4 mm or 4 x 3 mm). The results shown in Figure 12 indicate that consistent results could be obtained either with the SEM or the optical microscope and fracture toughness did not depend upon the specimen orientation. In general, examination of all the data in Table 3 and Figure 8 suggests there is no difference in the calculated fracture toughnesses, whether measured optically or with the SEM.

The one notable exception appears to be lab 21's optical results. Two of the five optical results from this lab were very high and in the opinion of the organizers the length measurements, 2c, along the surface were excessive. This lab may have incorporated some polishing-machining damage in the precrack size, contrary to guidance in the instructions. The other three specimens gave more reasonable results. The picture qualities were less than optimal in any case.

The conclusion that the optical and SEM results are similar surprised many of the participants, since in their lab's experience, they did note some difference. This difference is probably not statistically significant, however, since the labs had small sample sizes.

Hot-Isostatic Pressed Silicon Nitride

Figure 13 and Table 3 summarize the results for this material. Of the eighteen labs which attempted this material, results were received from sixteen. The grand average fracture toughness for 105 accepted specimens was 4.95 MPa$\cdot\sqrt{m}$ with a combined standard uncertainty (i.e, standard deviation) of 0.55 MPa$\cdot\sqrt{m}$. The grand average includes all data with the exception of the optical results from lab 22, since the precracks in that instance may have been hackle lines. (Lab 22's results were redone after their initial assessment in which they erroneously identified the fracture mirror as the precrack.) No other data was revised, although three labs (1, 3 and 10) did not send photos. Two labs (18 and 19) reported that they could not see the precracks and did not report results.

Eleven of the sixteen labs had the population mean within their sample scatter band (one standard deviation).

The central limit theorem was again applied to compare individual lab means and the population mean. As before, taking into account the various number of specimens in each sample, 63% (10 of 16) of the lab means were within one standard deviation of the grand mean. Thirteen of sixteen labs (81%) were within two standard deviations, which is somewhat less than the 95% that would be expected for a normal distribution. This shortfall is not surprising since several labs experienced much greater difficulty with this material.

Figures 14 and 15 show SEM and optical photos of precracks in this material, respectively. For the 49 N (5 kgf) indentation, the precrack dimensions should have been 60-95 micrometers deep, and 210-270 micrometers wide. Precracks were much more difficult to characterize in this material. The material was intentionally chosen because of this. The precracks had features similar to the fast fracture zone, were more three dimensional in nature (not as flat as the NC-132), and appeared to be more segmented. The most reliable precrack characterization seemed to come from SEM photography with favorable viewing conditions. The best success seemed to occur with either specimen tilting or stereo SEM photography. In general, delineation of the precrack required a very close examination[17] of the microstructure to detect subtle

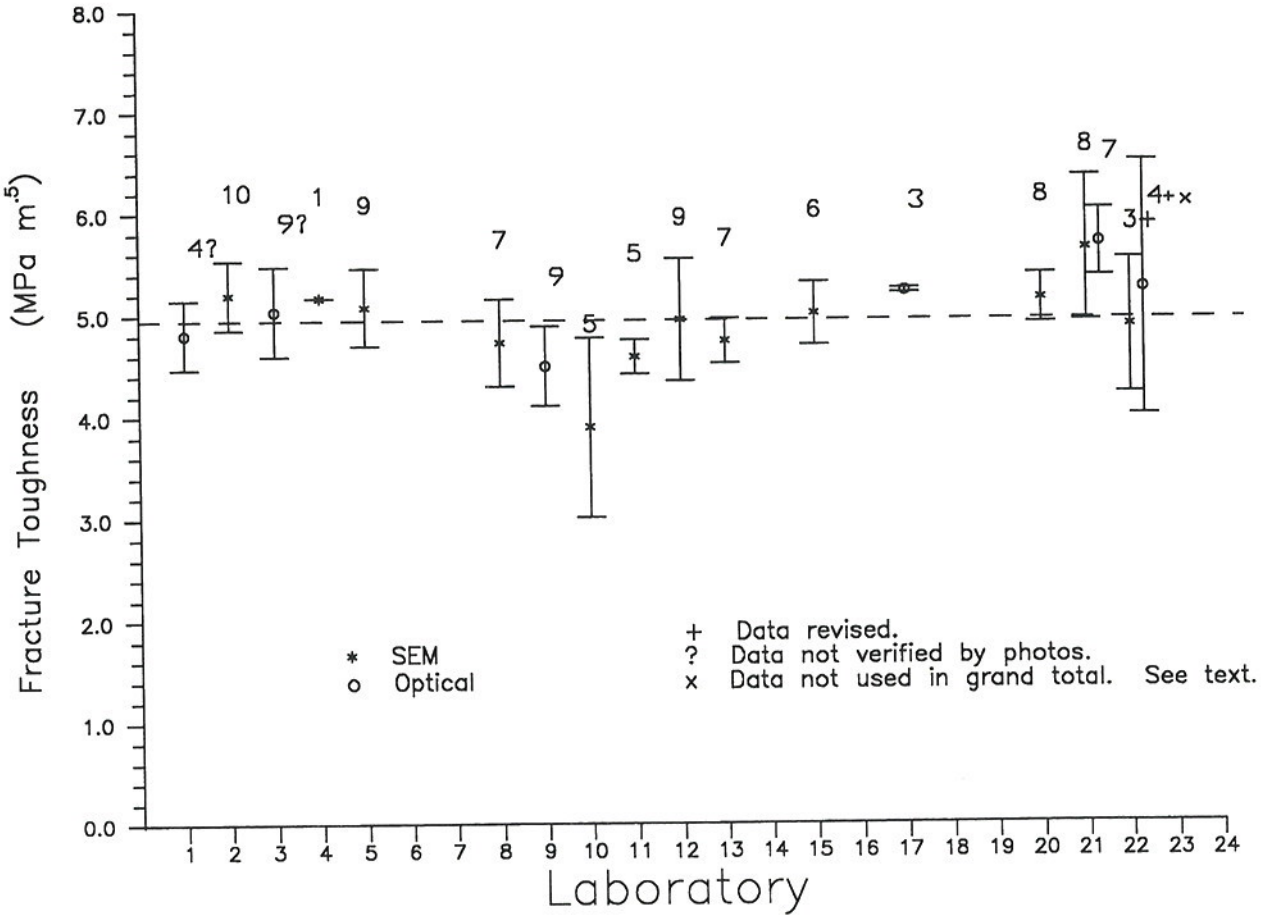

Figure 13. Master results graph for the hipped silicon nitride showing the individual lab results and standard deviations. Each data set is labelled by the number of specimens in the sample. The dashed line is the grand, population average.

---

17 Use of a hand magnifying lens in viewing the SEM photos was helpful.

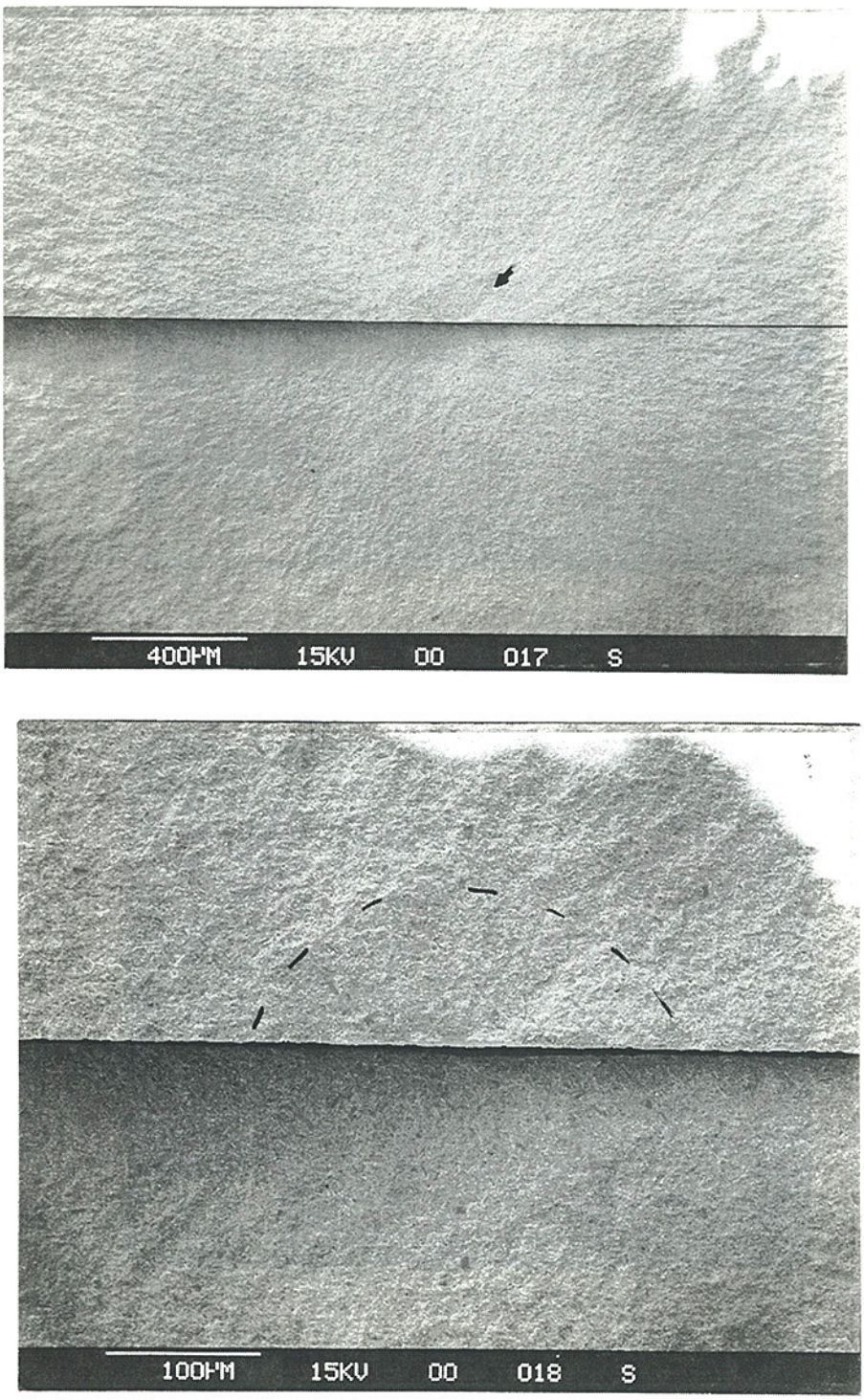

Figure 14. SEM photos of a precrack in the hipped silicon nitride. Both fracture surfaces are mounted back-to-back. The precrack is visible on the upper half, but is almost undetectable in the lower half.

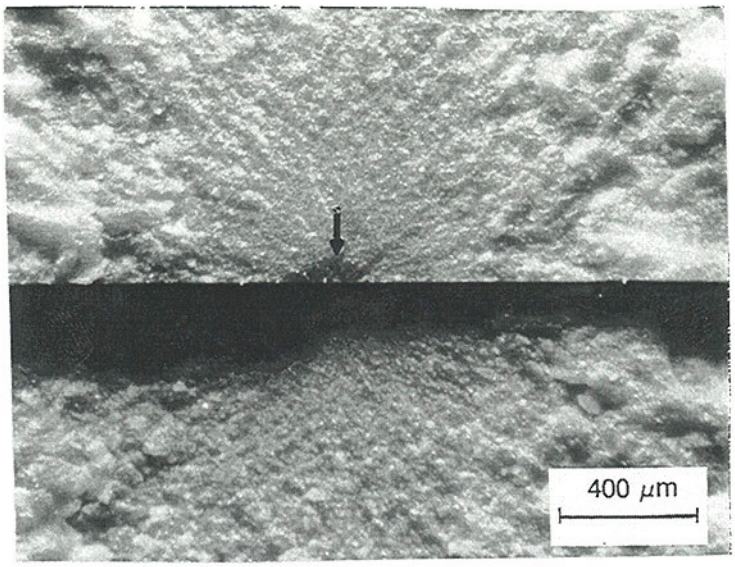

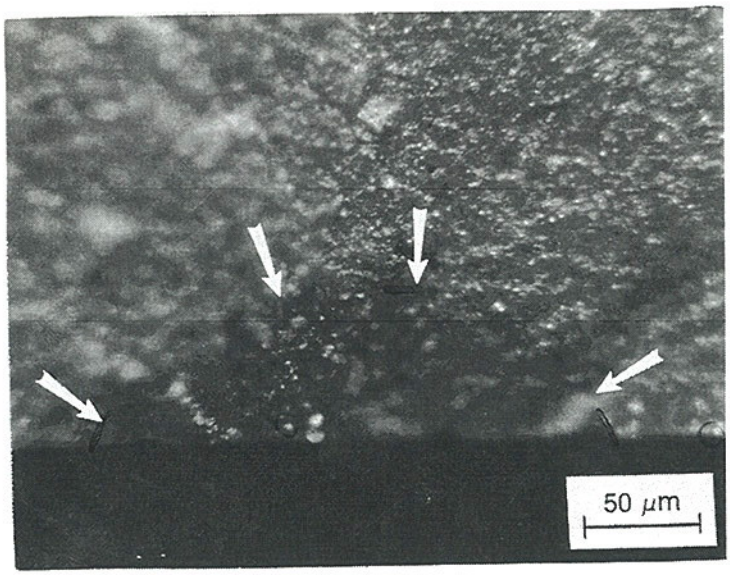

Figure 15. Optical microscope photos of precracks as detected by EMPA in the hipped silicon nitride.

boundary features, which were often not visible around the whole boundary. Stereo SEM photography was a big help in seeing the topography. The accurate delineation of the precrack by the SEM required sharp, high-quality pictures at magnifications of 250-500X. There was little or no chance of clearly seeing the precracks or their boundaries on most SEM *monitors*. Pictures were essential. Optical microscopy was sometimes successful, but usually at magnifications below 100X. Higher magnifications led to depth of field limitations.

Every laboratory reported at least some problems in identifying the precracks on their photos. Several labs produced very clear photos of the precracks but noted that they were more difficult to detect than those in the NC-132. Two labs sensed that they had photos of the precrack, but refused to make a precrack measurement since they felt it was too speculative. Several labs reported that they were furnishing estimates, but that they had little confidence in the results. One lab said that the estimates were tantamount to guesses.

Success ratios (successful outcomes/specimens tested) were much lower in this material than in the NC-132. The instructions said to test all ten specimens for this material, since it was anticipated that it would be difficult. The most common problem was in detecting the precrack as discussed above. One lab lost 5 specimens due to excessive polishing that removed most of the precrack, but then easily measured the precracks in the other 5 specimens! There appear to be three subsets: seven labs had 90-100% success rates; seven labs from 40-70%; three labs from 0-20%.

Most of the labs used the SEM to detect the precracks. Only two reported results from both the SEM and optical. Labs 1, 9, and 19 said they had no success with the SEM. Labs 21 and 22 indicated that optical microscopy was more suitable than the SEM. The data cannot be considered conclusive, but Figure 13 suggests that there is no systematic difference in the fracture toughness estimates from optical versus SEM microscopy.

Most labs (5, 9, 11-13, 15, 17, 20, and 21) had precracks with the maximum stress intensity factors usually at the deepest point. Labs 2, 3, 4, 8, 10, and lab 22 (SEM estimates) reported just the opposite. Labs 1, 21 and 22 (optical estimates) had half and half. It was difficult but not impossible to assess fractographically whether fracture initiated from the deepest portion of the precracks or from the surface. A number of examples of depth-initiated fracture were discernable in the photos sent by the participants.

Yttria-Stabilized Tetragonal Zirconia (Y-TZP)

Figure 16 and Table 3 list the results for the zirconia. This part of the project was optional, and only fourteen labs tried it. Two labs reported no success at all and four labs sent results where

the precracks were marked incorrectly. Thirty-three specimens from eight labs that sent acceptable results were used to compute the grand average of 4.36 MPa·$\sqrt{m}$ with a combined standard uncertainty (i.e., one standard deviation) of 0.44 MPa·$\sqrt{m}$.

Figure 16 illustrates (by means of the "+" symbol) that labs 2, 5, 8 and 22 revised their data. In the opinion of the organizers, lab 2 had excellent photos which showed the precrack reasonably well, but may not have marked the precrack suitably. The shape appeared more kidney-like than the ellipses drawn by lab 2. Lab 2 reestimated their precracks after reviewing the instructions. Labs 5, 8, 9, and 24 initially marked hackle lines as the precracks.

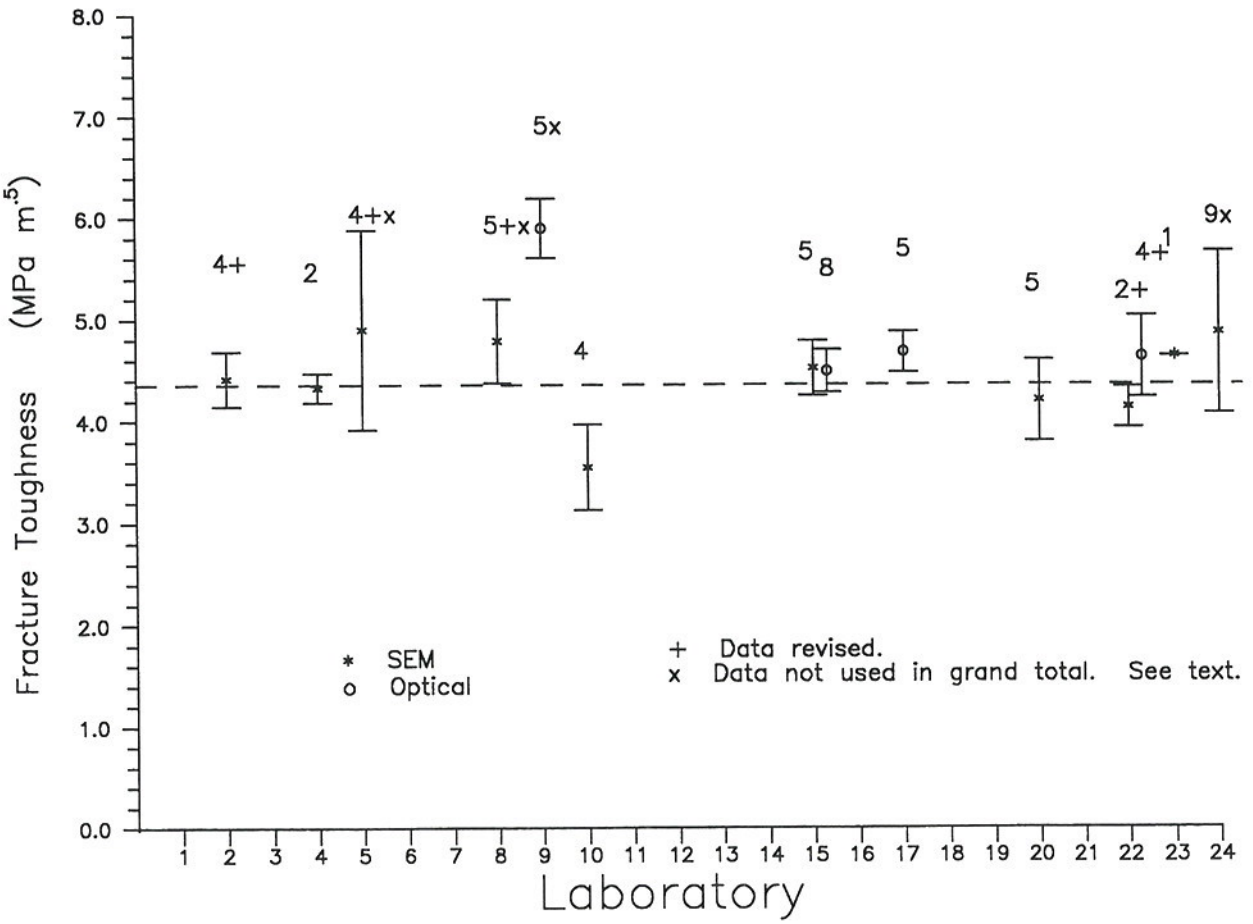

Figure 16. Master results graph for the Y-TZP zirconia showing the individual lab results and standard deviations. Each data set is labelled by the number of specimens in the sample. The dashed line is the grand, population average.

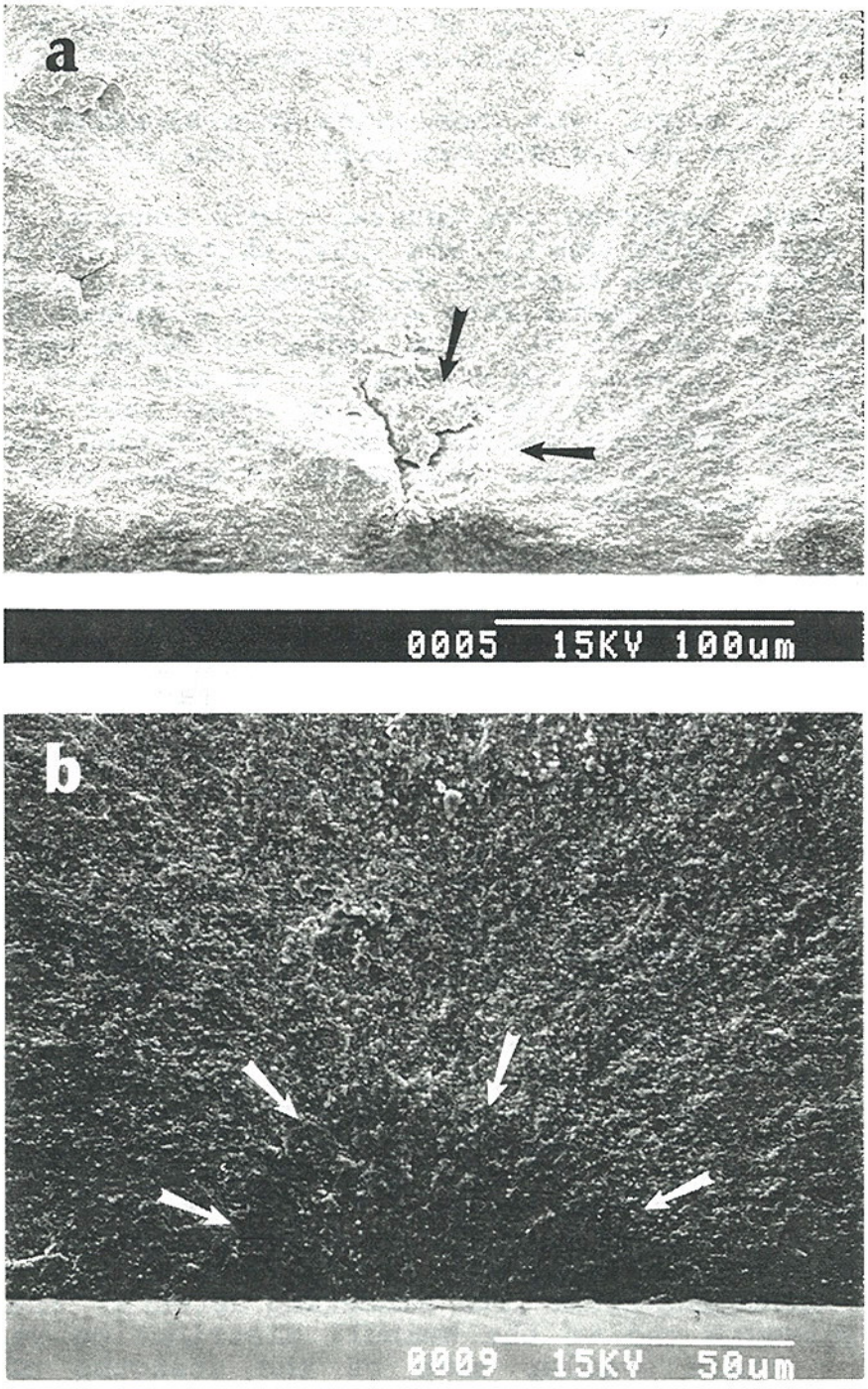

Figure 17. SEM photos of fracture origins in the Y-TZP zirconia. (a) shows a natural flaw, a sintering defect; (b) illustrates a precrack.

Lab 22 had initially marked the fracture mirror, but then found the precracks when the organizers requested a reexamination.

The organizing labs (NIST and EMPA) had precracks that were 20-40 micrometers deep. Other labs obtained precracks from 20-100 micrometers deep. Lab 24 used 294 and 392 N, (30 and 40 kgf) contrary to the instructions which specified 147 N (15 kgf).

Six of the eight labs whose data were accepted had the grand mean within their sample scatter bars (± one standard deviation).

Once again applying the central limit theorem, it was determined that only six of the 12 labs (50%) obtained lab fracture toughness means within one standard deviation of the population mean. Only 58% of the lab means were within two standard deviations. These ratios incorporate all labs including those which misinterpreted the hackle lines as the precracks. If the latter are deleted, then the ratios are much better: six of eight labs (75%) which read the precracks properly had mean toughness values within one standard deviation of the mean, and seven of eight (88%) were within two standard deviations.

Figures 17 and 18 show both SEM and optical precrack photos obtained at NIST and EMPA. Precracks should have been 20 to 40 micrometers deep, and 45 to 80 micrometers wide. Figure 19 shows that the precrack was primarily transgranular in character, whereas the subsequent fracture was intergranular. This difference is one of the key reasons the precracks were discernable. Subtle arrest marks and changes in direction of the microhackle lines at the precrack boundary were also telltale.

There was little data to compare the optical to the SEM precrack measurements for the zirconia, but lab 15 noted no difference in size estimates. Lab 22 suggested there was a difference, but since the scatter was high and the sample sizes were small (2 and 4 specimens), the evidence is not conclusive.

Success ratios varied widely for this material. The two organizing labs had little difficulty since they were familiar with the material. Lab 4 tried 10 specimens, but had the misfortune of having eight break from gross sintering defects which lowered the strength to only 260 - 360 MPa. Examples of these natural flaws are shown in Figures 6b and 17a. Lab 4 evidently received a bad batch of specimens, but they had no problem finding the precracks in the other two specimens! Other labs reported that occasionally their specimens broke from sintering defects. The strengths at the low strength end of the Weibull distribution were about 600 MPa [52]. These overlap some of the stengths of the precracked specimens. Lab 2 found the precracks reasonably easily, but they seemed to be more kidney shaped than those of other labs, causing difficulty in marking the boundaries. This material seemed to be more sensitive to the amount of material polished away: if too

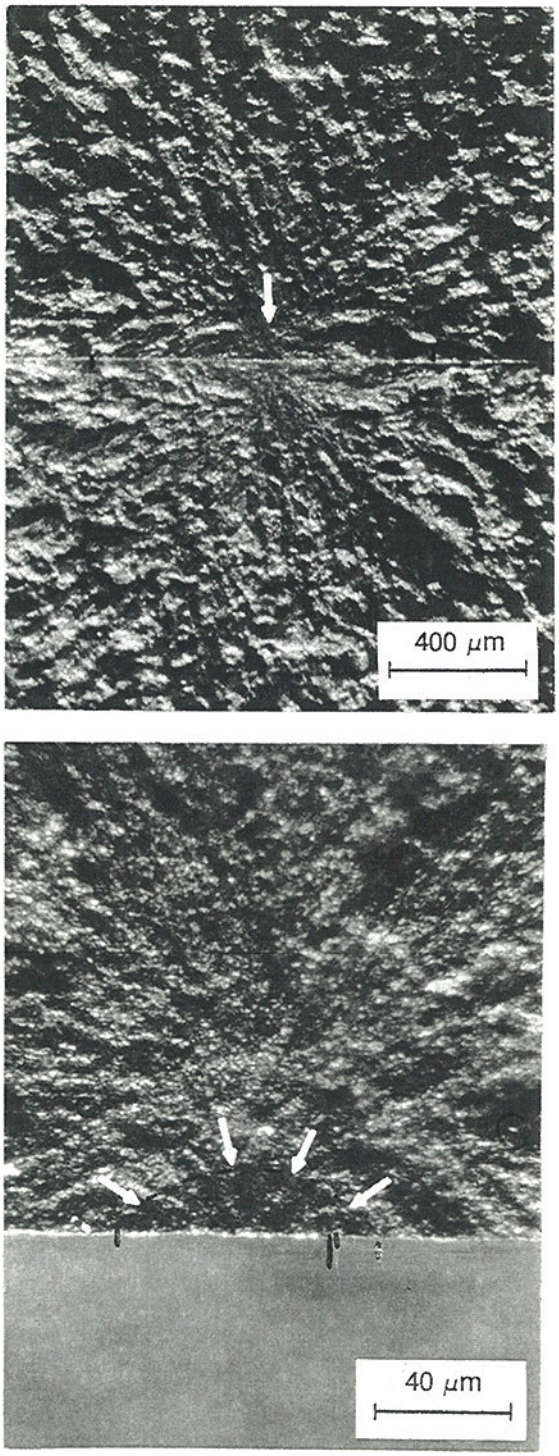

Figure 18. Optical microscope photos of precracks in the Y-TZP zirconia. A larger semiellipse around the flaw is suggestive of stable crack extension.

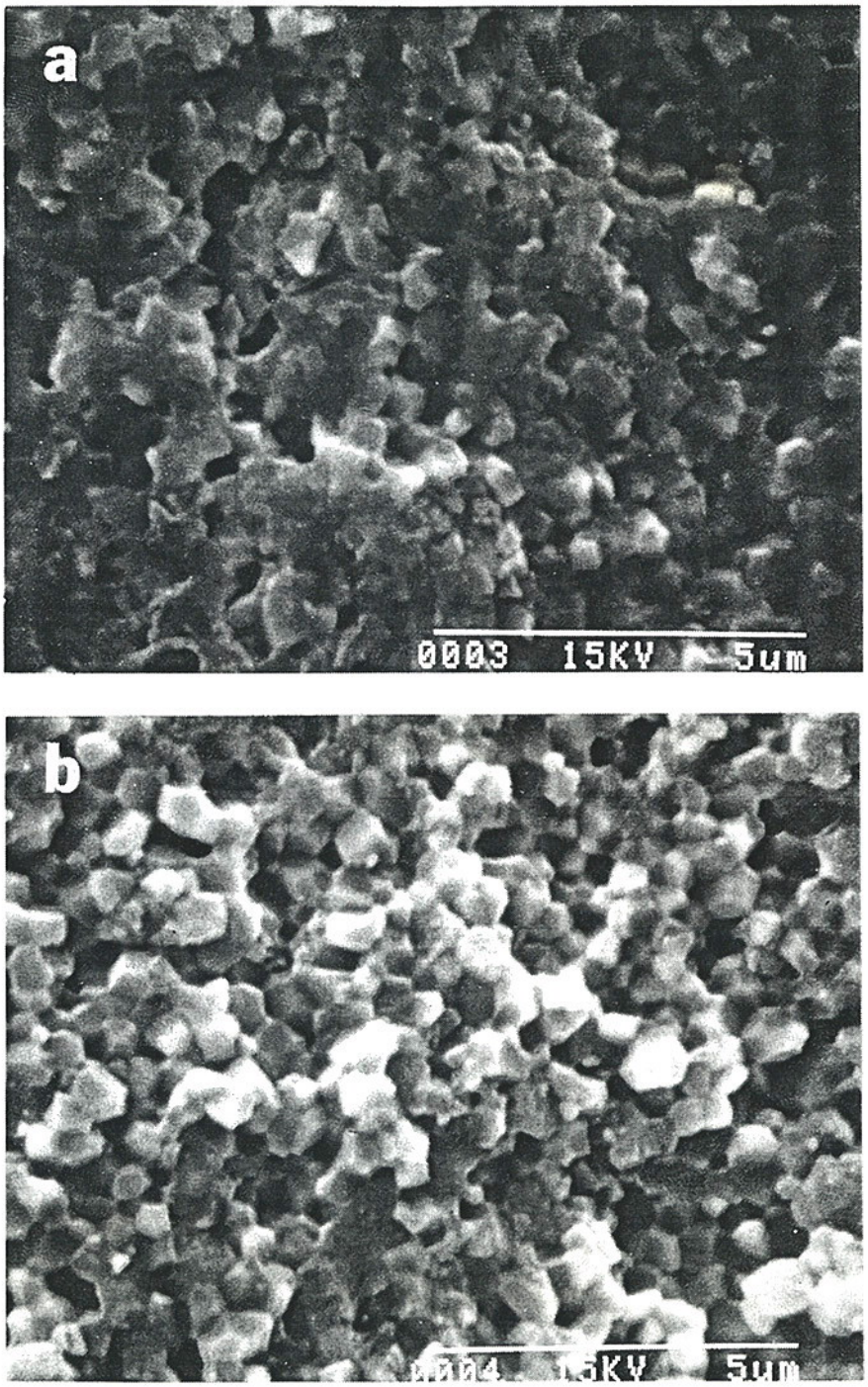

Figure 19. SEM photos illustrating (a) transgranular fracture inside the precracks, and (b) intergranular fracture outside the precrack.

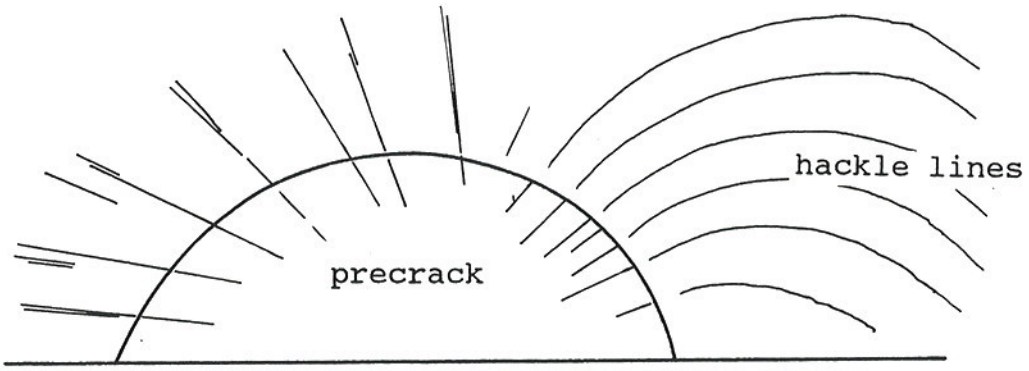

Figure 20. Schematic illustrating the unique hackle line pattern in the Y-TZP. Microhackle lines commencing inside the precrack often turned towards the initial indentation region. Several labs mistook the hackle lines as the precracks.

much was removed, the specimens broke from natural flaws.

Labs 5 and 9 marked hackle lines and missed the precracks. Lab 8 had results that were fairly consistent with the other labs, but sent one picture with hackle marked, and another picture of a different specimen with the precrack well-marked. It is not known how well the other specimens were identified. Lab 18 could not find precracks in the two specimens they tried. Lab 20 had two specimens fracture away from the precrack, but furnished superb pictures of precracks in the other three they tested. Marking the exact boundary was difficult, however. Lab 23 also had problems with specimens fracturing from natural flaws, but indicated that precrack detection was relatively easy with optical microscopy!

The vast majority of specimens for this material had maximum stress intensity factors at the surface, with the exception of lab 17, where all were at the depth. Most labs reported that <u>all</u> their maximum factors were at the surface. Some of the precracks were somewhat deeper than a semicircular shape ($a/c > 1.0$) in which case the Newman-Raju formula is not strictly appropriate. Several precracks were distinctly kidney shaped. Close examination of the fracture surfaces with the SEM failed to clarify whether fracture initiated at the surface, the depth, or along the entire crack front simultaneously. What was striking, however, was that nearly all specimens had a characteristic asymmetrical pattern of hackle emanating from the precrack as illustrated in Figure 21. The

hackle on one side of the precrack curved back sharply in the direction of the initial indentation, whereas the hackle on the other side fanned out in a conventional radial fashion.

Additional experiments were done at NIST to examine whether the removal of 2.5X after indentation was sufficient to remove the residual stress zone. If insufficient material is polished away, there will be a residual tensile stress from the indentation damage zone that will reduce the apparent measured fracture toughness. Three specimens had only 2.0X removed. All six fracture surfaces were examined both with the SEM and optical microscope. The average from the optical readings was 4.66 ± 0.43 MPa·$\sqrt{m}$ (mean, standard deviation). The average from SEM readings was 4.42 ± 0.27 MPa·$\sqrt{m}$. The precracks in these were 35 - 52 micrometers deep and most (but not all) stress intensity maximums were at the surface. These results compare to specimens with 2.5X removed that had an average of 4.49 ± 0.21 MPa·$\sqrt{m}$ for 8 optically-measured specimens, and 4.52 ± 0.27 MPa·$\sqrt{m}$ for 5 SEM-measured specimens. Thus, there is no apparent difference between the fracture toughnesses for specimens with 2.0 or 2.5X removed. Additional insight can be gained from the data of lab 10. They reported that the prescribed 149 N (15 kgf) indentation load was used, but their indentation diagonal size was only 102 micrometers. This is about 50 micrometers less than expected, which suggests the indentation diagonal size was underestimated by lab 10. Only 40 micrometers of material were reported as being polished away, which represents about 1.8X if the indents were actually formed by the prescribed 149 N (15 kgf). Thus, it is possible that lab 10 did not remove enough material to fully eliminate the residual stresses, and this may account for their low fracture toughness results.[18]

NIST performed several additional experiments to investigate whether slow crack growth or R-curve phenomena could influence the results of this round robin. Oxide ceramics such as zirconia may be susceptible to slow crack growth at room temperature due in part to a reaction of grain boundary phases with water vapor [68,69]. This might lead to rate effects during fracture testing, particularly at slower loading rates whereby the precrack could enlarge causing a reduction in fracture strength and apparent toughness. In addition, stable crack extension due to R-curve behavior could cause an increase in toughness with crack extension or precrack size. To screen for such phenomena, additional experiments were performed in a dry-nitrogen environment with a relative humidity estimated to be less than 0.25%. A simple chamber was constructed around the flexure test jig and dry nitrogen allowed to flow over the specimens for five minutes prior to testing. All specimens

---

[18] The Knoop indentation sizes reported by lab 10 for the silicon nitrides were in the correct range. The Vickers indents were approximately 50 micrometers shorter than the 150 micrometers expected for the specified load. Either the indentation size or the load must have been in error.

were dried in a vacuum oven at 100°C for 2 hours prior to testing and were transferred and stored in a desiccator prior to testing. Two loading rates were used: 0.5 mm/min and 0.025 mm/min. The faster rate led to fractures in 40-50 seconds; the slower rate, 10-15 minutes. Of ten specimens tested, three fractures from the surface crack were obtained at each rate. (Four specimens fractured from sintering defects.)

Table 4 presents the results, which indicate the toughnesses are slightly lower (5%) in air (at 31% relative humidity) than in the dry nitrogen, but the scatter is high and the results cannot be considered conclusive. (For example, the toughnesses computed from SEM microscopy for the lab ambient specimens at 0.5 mm/min and the dry-nitrogen specimens at the slower rate are nearly the same.) There appears to be a slight difference in toughness for the two different loading rates in dry nitrogen, but there is considerable scatter and overlap. The fracture surfaces of all these specimens were very carefully scrutinized with the SEM. No clear evidence of stable crack extension could be discerned. In a few (but only a few) specimens there were subtle features that hinted at stable crack extension.

Table 4
Environmental and loading rate influences on fracture toughness of Y-TZP.

K_{Ic} MPa·√m	Std. Dev. MPa·√m	# specimens	Conditions	Comments
4.49	0.21	8	lab ambient,* 0.5 mm/min	Optical
4.52	0.27	5	lab ambient,* 0.5 mm/min	SEM
4.84	0.29	3	dry nitrogen, 0.5 mm/min	SEM and Optical
4.60	0.62	3	dry nitrogen, 0.025 mm/min	SEM
4.72	0.45	6	dry nitrogen, avg. of both rates	SEM and Optical

* 31% relative humidity, 25°C

DISCUSSION

General
Overall, nearly all labs successfully applied the SCF method to the hot-pressed silicon nitride and the consistency in the results is reassuring. Reasonable success was also achieved with the more difficult hipped silicon nitride. The zirconia was rather challenging, but most of the labs that tried it obtained plausible results.

Fractographic analysis
The organizers sense that many participants had considerable anguish and uncertainty in finding and measuring the precracks, especially for the latter two materials. Many of the cracks were rather difficult to find or mark. In frustration, several participants complained that it was difficult or hopeless to mark precracks with any certainty. We can imagine many of the participants consulting with their colleagues and assistants and pondering what truly were the precracks.

Despite these problems, *one remarkable conclusion of this round robin is that the computed fracture toughness is not sensitive to the exact boundaries marked.* This is due in part to the square root dependence of fracture toughness on crack size. In addition, we observed that there is an *offsetting influence of Y upon errors or misjudgments in the crack size, a.* This is discussed in detail in Appendix 4. In contrast, the most sensitive input to fracture toughness in SCF method is the flexure strength measurement, which has no subjectivity and can be measured accurately and precisely!

Optical and SEM photo estimates of the precracks, while showing dramatically different views of the precracks, often gave similar results. The optical estimates might be a little higher or lower that the SEM precrack sizes, but as discussed in Appendix 4, the effect on fracture toughness is not strong. We recommend usage of whatever works best in showing the precracks for a given material. There was a sense, however, that optical readings might tend to give slightly smaller size estimates, and thus very slightly lower fracture toughness values. It was very clear that most precracks, even in the relatively easy NC-132 silicon nitride, do not show clearly on SEM television monitors. Pictures are essential. Instant developing photos are highly recommended, and should be viewed during the SEM session. We also noticed that there was a clear loss of clarity and resolution in the thermal prints or low resolution video image recording systems that some participants used in order to cut costs. Since clarity and resolution are critical, we do not recommend using these media.

Many precracks were discernable at low magnifications (<100X), but then were difficult to see at higher magnifications. The natural tendency is to make the feature being measured as large as possible in order to obtain a more precise reading. For the precracks in

this study, SEM magnifications in the 300-800X range were the best for size measurement, but sometimes photos as low at 50-100X were helpful. Optical microscopy was quite different. For the relatively flat cracks in the NC-132 silicon nitride and the zirconia, magnifications of 300-550X were possible. In contrast, the hipped silicon nitride precracks were best measured at much lower magnifications, sometimes as low as 100X. This was because the precracks were more three dimensional, and a greater depth of field was important. Best results for all three materials seemed to occur with combinations of low and high magnification photos.

The SEM photos of laboratory 20 were striking in their clarity and contrast. Precracks were easily seen for both the NC-132 and the Y-TZP. They reported that they used a very directional gold coating process during their preparation for the SEM. The fracture surface was located off to the side and parallel to the sputter source. This caused the deposition to be at a low, grazing angle which led to uneven coating thicknesses. There was slight charging on some surfaces which was very helpful.

Labs 12 and 24 suggested stereo SEM microscopy. NIST explored the use of this while the round robin was underway and can confirm that extraordinary clarity of the precrack topography can result. In many instances, especially with the hipped silicon nitride (which often had an undulating or segmented precrack), it was possible to discern subtle features that delineated the precrack boundary. These features were not visible or were missed on conventional SEM or optical photos. Stereo SEM is a valuable tool that we highly recommend for difficult materials.

Some of the more interesting photos from laboratory 11 had a different contrast and appearance that suggested the use of the backscattering mode in the SEM. NIST tried this on a hipped silicon nitride specimen with the results shown in Figure 21. Backscattering does appear to enhance precrack detectability in some instances.

During the final preparation phase of this report, Lab 21 reported that their difficulty in detecting the precracks in the Y-TZP was attributable to a too thick coating for the SEM examination. Once thinner coatings were tried, precracks were easily detected and calculated fracture toughness results were consistent with the other labs. It is not known if this problem was experienced by any of the other labs.

The round robin did reveal some important generalizations about precrack characterization. Success seemed to be dependent upon the following factors:

a. The quality of the microscopy (equipment and photos) both in electron or optical modes.

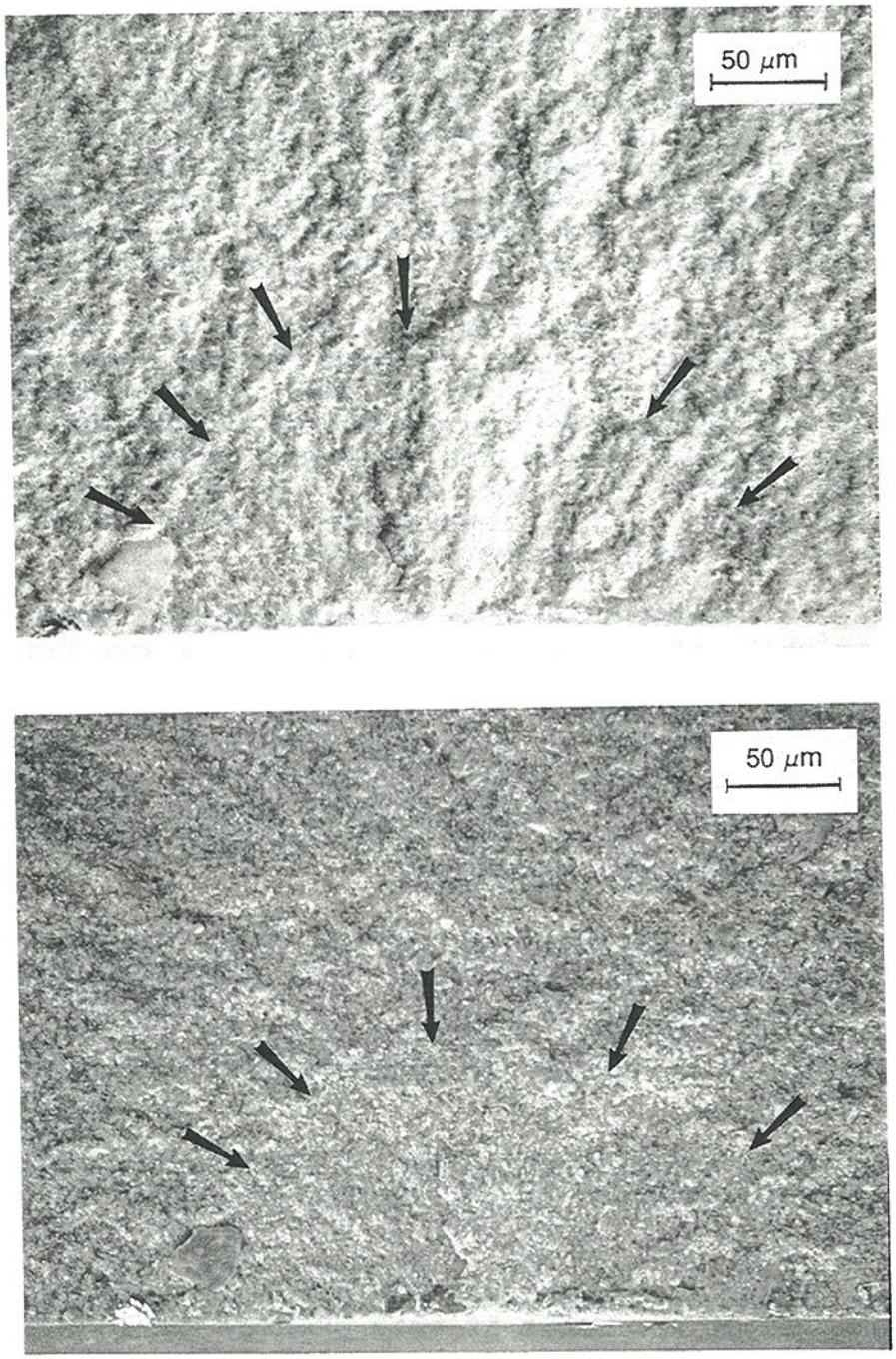

Figure 21. SEM photographs of precracks in the hipped silicon nitride, as photographed in the backscattering mode. Both photos are of the same specimen. The specimen was tilted 5° for the lower photo.

b. The general skill of the fractographer.
c. The experience of the fractographer with the material.
d. Luck.

These four factors played amazing roles in this round robin, which sometimes combined to help or hinder the participants. Sometimes the factors offset beneficially: an inexperienced fractographer was lucky and obtained photos of precracks that a novice could have marked correctly. Instances of this occurred for all three materials in this round robin. The labs somehow, by chance, had their equipment set up in favorable conditions. The fractographer did his analysis in just a few minutes or an hour or two. In other instances, skilled fractographers were severely handicapped because they were working from poor quality photographs taken by other persons. Some participants spent many hours scrutinizing photos which barely showed the necessary detail, or perhaps not at all.

One lab reported that their "experienced SEM operator" never found a precrack in the hipped silicon nitride. In this case the operator probably was a skilled microscopist, but may not have been familiar with ceramic fracture surfaces.

We therefore can conclude in general, *that a necessary prerequisite for the success of this project is that the analyst must have some ceramic fractographic experience*. In any case, the fractographer must work very closely with the SEM or optical microscope operator. It is not enough to ask that the latter person should take a few photos and present them to the analyst later.

This is not a method for fractographic novices (unless they are fortunate). The instructions to the round robin stated this clearly at the top of the first page: "This method requires interpretation of fracture surfaces. The microscopy (optical or SEM) and interpretation of the photos should be done by experienced personnel."

The five labs that began this round robin with experience in the method, in general did succeed. We venture to suggest that many of the participants, now that they are familiar with the procedure, have had a chance to read this report, and have seen the photos of the other participants, would be more confident and successful if they tried the method again.

We further add that there are many instances when it is pointless to try to mark a precrack in every specimen. Some photos just won't be clear. Some materials are more conducive ("fractographically friendly") to precrack characterization than others. One hundred percent success rates in characterization were sometimes achieved, but this is not essential. We recommend that for a new material, no fewer than ten, and preferably twenty specimens be obtained. A few (2-4) will be needed to assess a suitable indentation load and to determine whether the precracks

Table 5

Fracture toughness reported for NC-132, hot-pressed silicon nitride. Supplemental results by some of the laboratories participating in this round robin are also listed.

K_{Ic} MPa·√m	Std. dev. MPa·√m	Method	# specimens	Source
4.59	**0.37**	**SCF (csf)**	**107**	**This study**
4.58	0.10	IS	4	EMPA, This study
4.42	0.14	CN	2	ECN, This study
4.5-5.0	-	MD-Nat	6	Quinn and Quinn, [33]
4.5	0.4	SEPB	3	Salem et al., [50,70]
4.68	0.19	CN-SB	35	"
4.85	-	CN	4	"
4.64	~0.2	CN-SB	13	Bubsey, Shannon and Munz*, [71]
4.72	-	CN-SB	7	"
4.71	-	CN-SB	9	"
4.83	-	CN	2	"
4.85	-	CN	2	"
4.9	-	IS	-	Salem and Choi, [72]
5.2	-	DT	4	Annis and Cargill, [73]
4.1	0.21	DT	4	Govila, [74,75]
5.8	0.74	DT	3	Quinn, [76]
4.24	0.30	DT	-	Bansal and Duckworth, [77,78]
4.20	0.15	FM	-	"
4.0	-	DCB	-	Anstis et al., [79]
4.65	0.1	SCF (csf)	-	Petrovic et al. [10].**
4.64	0.25	SCF (csf)	4	Quinn and Quinn, [33]**
4.48	0.07	SCF (csf)	4	"
4.33	0.37	SCF (csf)	3	"
5.25	-	SCF (csf)	4	Gonczy and Johnson, [28]***

* Different chevron geometries and orientations.
** Different annealing conditions in air or inert atmospheres.
*** Annealed in air.
\- Not reported
SCF Surface Crack in Flexure (Controlled Surface Flaw)
IS Indentation Strength (Vickers)
MD-Nat Natural Flaws - Machining Damage in Flexure Bars
DT Double Torsion
CN Chevron Notch (Long Bar)
CN-SB Chevron Notch (Short Bar)
DCB Double Cantilever Beam
SENB Single-Edge Notched Beam
SEPB Single-Edge Precracked Beam
FM Fracture Mirror Analysis, Natural Flaws

can be seen at all. The indent and the residual stress need not be removed in these preliminary experiments. Only five to ten specimens more might have to be tested to obtain five useable results.

Polishing
The problems that some labs reported with the indentation removal were somewhat surprising. In general, any method that removes the necessary material is suitable provided that excessive damage or new residual stresses are not created. Some labs found the hand polishing to be easy and fast. Other labs preferred to use surface grinding and professional machining services. *We caution that in the latter case, it is very difficult to guarantee that the correct amount of material is removed in each specimen.* With a Vernier hand micrometer and a little patience, it is simple to polish the specimens by hand.

The zirconia was more sensitive to removal amounts, because many of the precracks were not much larger than some of the sintering defects. If too much material was removed, the specimens did not break from the precrack.

Comparison to other results: Hot-pressed Silicon Nitride, NC-132
Table 5 lists other results for fracture toughness of NC-132 silicon nitride. The results of this round robin with 107 specimens represents the largest sample set ever reported for this material. Listed immediately underneath the SCF results of this round robin are some additional results obtained in this project by ECN and EMPA using chevron notch and indentation strength methods, respectively.

The round robin SCF results are in excellent agreement with most of the other data, including the early SCF work of Petrovic and colleagues. We further note that the toughnesses all cluster in the 4.5 to 5.0 range, and seem to be independent of specimen type and size. This is a clear sign that the material exhibits flat R-curve behavior. Indeed, Bubsey et al. [71], and Salem and Shannon [50] reached this conclusion previously on the basis of chevron notch experiments with different specimen sizes. Salem and Choi [7] reached the same conclusions following indentation strength experiments. The SCF results are in excellent agreement with the large chevron notch data sets of Salem et al. [50,70] and Bubsey et al. [61], which all lie between 4.6 and 4.85 MPa$\cdot\sqrt{m}$.

Fracture toughness was not dependent on specimen orientation as illustrated in Figure 12. The crack for each was perpendicular to the original hot-pressed plate (155 x 155 x 25 mm) surface. Furthermore, Bubsey et al. [71] reported that there was no difference in fracture toughness for cracks running parallel or perpendicular to the plate surface. This is surprising, since there is a well-known **strength** anisotropy for the latter two orientations [53]. This is a consequence of the preferred orientation of the elongated β silicon nitride grains due to the uniaxial hot-pressing process.

Further results for comparison are given in Table 6 for the HS-130 grade of hot-pressed silicon nitride, the immediate predecessor to NC-132. These materials were made by the same company with similar starting powders, with the exception that greater care was taken for the NC-132 to control inclusion content [53]. The HS-130 results are also in good agreement with those of the present round robin. Petrovic noted the similarities of toughnesses for the two materials from SCF experiments [10].

Of special interest for both materials are the two cases where toughness was estimated from natural flaws. Such estimates are problematic due to the uncertainties in the stress intensity shape factors for real flaws, but the ranges shown are in excellent agreement with the fracture mechanics test results.

We therefore estimate that based upon the preponderance of data that NC-132 (and HS-130) hot-pressed silicon nitride has a flat R-curve and a fracture toughness of 4.6 MPa$\cdot\sqrt{m}$ ($\pm$0.2).

Table 6
Fracture toughness reported for
HS-130 grade hot-pressed silicon nitride.

K_{Ic} MPa$\cdot\sqrt{m}$	Std. Dev. MPa$\cdot\sqrt{m}$	Method	# Specimens	Source
4.45, 4.65	~0.6	SCF (csf) annealed	-	Petrovic et al., [10]
4.3, 4.5	~0.1	SCF (csf) air anneal	-	Petrovic et al., [11]
4.2	~0.2	SCF (csf) polish	8	Petrovic et al., [11]
3.9-4.4	-	NF	6	Lange, [80]
5.0	-	DT	5	Henschall et al., [81]
4.7	0.5	DT	-	Evans and Wiederhorn, [82]
5.1	0.3	DCB	10	Lange, [83]
4.5	0.3	SENB	-	Henschall et al., [84]

- not reported
NF natural flaws (inclusions) in flexure specimen

Comparison to other results: Hipped Silicon Nitride
Table 7 lists other lab results. There is less data available for this material.[19] The large crack specimen types (CN and SEPB) indicate a higher toughness which may result from R-curve behavior. The elongated grain structure illustrated in Figure 5, might support this interpretation. In any case, the SCF precracks did have undulations and more crack-microstructure interactions, unlike the flatter precracks in the hot-pressed silicon nitride and the Y-TZP. In contrast, the IS data from EMPA tends to indicate there is no R-curve behavior. Vickers indents were made at two loads: 49 and 249 N. The fracture strength decreased with the indentation load with a power law dependence with an exponent of -0.32 which is negligibly different from the minus one-third that is expected for a material with a flat R-curve.

Table 7
Fracture toughness reported for ESK hipped silicon nitride.

K_{Ic} MPa·$\sqrt{m}$	Std. Dev. MPa·$\sqrt{m}$	Method	# Specimens	Source
4.95	**0.55**	**SCF (csf)**	**105**	**This study**
5.39	0.19	IS	4	EMPA, this study
5.14	0.25	CN	3	ECN, Petten, this study
5.5	-	SEPB	10	Ref. 85*
5.3	-	SEPB	10	Ref. 85*

* (Hot-pressed Ekasin-D, not hipped)

Comparison to other results: Hipped Y-TZP
Table 8 gives the few results available for this material, a custom-made zirconia. Chevron notch (CN) data from ECN and indentation strength (IS) [86] data from EMPA did not concur with the SCF round robin data. The latter data is very suspect in any case, since it has been demonstrated that median cracks do not form under the Vickers indenter, thus violating one of the assumptions of the IS analysis.

The chevron notch results can not be dismissed as readily. Their higher values could be a sign of R-curve behavior. On the other hand, the very slow rate of loading, inert atmosphere SCF experiments conducted at NIST failed to exhibit any conclusive

---

[19] The manufacturer has also discontinued this particular vintage as well.

Table 8
Fracture Toughness reported for Y-TZP Zirconia.

K_{Ic} MPa·$\sqrt{m}$	Std. Dev. MPa·$\sqrt{m}$	Method	# Specimens	Source
4.36	**0.44**	**SCF (csf)**	**33**	**This study**
5.61	0.09	IS	4	EMPA, this study
5.27	0.27	CN	3	ECN, this study

signs of stable crack extension, either fractographically, or from the computed toughnesses. An x-ray diffraction analysis did reveal approximately 33% of monoclinic phase on the fracture surfaces of several SCF specimens. The estimate is based on comparing the integrated intensities of the ($\bar{1}11$) and (111) monoclinic to the (101) tetragonal peaks [87]. Little (~5%) or no monoclinic phase was detected on polished or machined surfaces as noted above. Thus, there may be some transformation toughening during crack growth in this Y-TZP.

The measured toughnesses (4.36 MPa·$\sqrt{m}$) for the Y-TZP is consistent with results from a number of other studies which obtained values in the 4.0 to 5.0 range [88-92]. Higher toughnesses (8-10) are possible with careful microstructural control. The grain size should be optimized just below a critical value (generally less than one micrometer), such that the grains will not spontaneously transform during cooldown to room temperature. The transformation will occur subsequently if a crack propagates through the material, the surface is ground, or if the material is indented. The critical grain size is a strong function of the yttria content in the 2-3 mole percent range [91-95]. For a yttria mole percent level of 3%, the critical grain size is of the order of 1 micrometer [93,94]. Thus, the 0.45 micrometer grain size of the zirconia in the present study probably has many stable tetragonal grains which are less apt to transform due to crack propagation or surface polishing or grinding. Higher toughnesses might have resulted had the grain size been increased or the mole percent yttria decreased. Several groups have reported that optimum toughnesses can be achieved in the 2 to 2.5 mole % concentrations (e.g. References 92,95).

Finally, we note that if there indeed is some transformation toughening, it is unclear how much effect it will have upon fracture from small flaws. Several recent studies have closely monitored the crack extension resistance in Y-TZP's [61,62,90]. Extraordinarily steep R-curves were noted in all three studies,

with baseline toughnesses starting at values as low as 1.0 [62], 2.0 [61], and 0.5 MPa·$\sqrt{m}$ [90]. The R-curves reached plateaus after remarkably short crack extensions: 5-10 micrometers, 3 micrometers, and 20-30 micrometers, respectively. Such small crack extensions might not have been noticed in this round robin. The artificial precracks in this study had depths of 20-40 micrometers. The strengths reported in Table 2 suggest that the natural flaws in the Y-TZP had a depth of 15-25 micrometers if they were semicircular surface flaws, or had a diameter of 30-50 micrometers if they were penny-shaped flaws in the specimen volume. Anderson and Braun [61] demonstrated that the initial precrack size will influence the apparent toughness. Fracture occurs at the instability point when the rate of toughening from the material's R-curve resistance is exceeded by the rate of stress intensity increase due to crack extension. The instability point, and thus the apparent toughness, will depend to some extent upon the initial crack size. This may have contributed to some of the scatter in the results of this round robin. Thus, a single value of toughness may not necessarily be appropriate. Nonetheless, it is useful to determine what the practical range of apparent fracture toughness results are from the surface crack in flexure method.[20]

It would appear that the surface crack in flexure method may measure toughnesses only at the low end of R-curves. We reiterate that the SCF precrack is most likely to give a fracture toughness that is relevant to real flaws in ceramic materials.

Results of the enclosed survey
A questionnaire was enclosed with the instructions and all labs were asked to give general comments and an appraisal of the project. Some of the questions and the answers are summarized below.

How long did the project require and what was the most time consuming step?
The times needed varied widely with the average being 2 weeks. It was not clear whether the respondents meant that two full man-weeks or two weeks part-time was needed. (The question was not clearly worded.) The shortest time reported was 3 days; the longest, 4 weeks. Six labs reported that the polishing to remove the indent was the most time consuming step; ten indicated that the fractography was most time consuming. Several labs indicated that preparation of the tilt or canting procedures for the indentation required some time.

---

[20] Since the R-curves are so steep and reach a plateau very quickly for Y-TZP's that do not exhibit extensive transformation toughening (3-4 mole % yttria), there may not be much variation of apparent toughnesses in any case. This might explain why most reported values of toughness have fallen in the 4-5 MPa·$\sqrt{m}$ range for materials with 3 mole % yttria.

Please identify the person performing each step of the project.
The answers varied considerably, but in most instances, two or more people were involved. Three labs reported that the principal contact was the sole participant. Students, technicians or engineers often did the precracking, polishing and testing, and in some instances, the fractography. In some cases, the most sensitive step, the fractographic interpretation, was left to inexperienced personnel or students. This was not necessarily bad. In one instance (lab 20), some of the best photos and fractography in the entire round robin were furnished by a student. In many cases, the fractography and the analysis were done by the principal scientist-engineer in cooperation with other staff members or students. In at least four instances, the final analyst did not include him or herself as participating in the fractography. In fifteen labs, the principal analyst performed some or all of the fractography.

Which way of orienting the specimen is preferred (3 x 4 mm; or 4 x 3 mm)?
Seven labs indicated that laying the specimen flat (4 mm face down) on the flexure fixtures was preferred; two preferred the 3 mm face down; and four said that it did not matter. The answers from two other labs were unclear. Most labs indicated that indenting a wide 4 mm face led to easier flexure testing since the wide face sat on the fixtures better, but most also said that indenting the narrow face had the advantage that less material had to be polished away, and it was easier to hold the specimen during polishing.

How was the removal of the indent done?
Nine labs followed the recommended procedure and used dry silicon carbide papers. Seven labs reported they used diamond paste or powder (wet). Two used a diamond impregnated disk or honing block. Three sent their specimens to machine shops for diamond grinding.

How were the precracks detected?
Two labs used optical microscopes without photographic equipment. Three used primarily or exclusively optical photomicrographs. Eight used only the SEM. Seven used combinations of SEM and optical microscopy. Lab 22 reported that precrack characterization was easier by optical microscopy than SEM examination. Other labs had mixed responses, depending upon the material.

Have you used this method in the past?
Only five responded yes, and fifteen said no.

Will you use the method in the future?
Seven said yes without qualification, seven said maybe, and four said no. (Two labs chose not to answer this question.) Two of the negative respondents were vociferous and strongly preferred chevron notch (lab 10) or single-edge notched beam, single-edged precracked beam, or chevron notch (lab 19). Lab 5 answered maybe and said that it depended on the round robin's results. Lab 23 said they

would use the method if it were improved.

The five labs that indicated they have used the method in the past reiterated their intent to use the method in the future. Only two new labs were willing to adopt the method without qualifications.

The general sense was that the method entails more work than most participants would like, especially in the polishing and fractographic steps. Improvements in detecting the precracks would help the acceptability of the method.

Please make suggestions for improvements or refinements to the method.
The most common suggestions were: tilting of the specimen in the SEM to improve crack detectability, stereo photography, and photographing the specimens at multiple magnifications, especially the use of low magnification views in which the cracks tend to stand out more clearly.

Other
NIST is continuing work on the SCF method to expand the data base to other materials and to better define and simplify the test procedures. It has been customary to empirically determine indentation precracking loads which are typically in the range of 10-100 N (1 to 10 kgf). Work is underway at NIST to devise a better means to choose a load, and to even estimate whether the method will work without the need for preliminary trial and error work.

CONCLUSIONS

1. Very consistent results were obtained from all labs for the NC-132 hot-pressed silicon nitride. The fracture toughness for 107 specimens was 4.59 ± 0.37 MPa·$\sqrt{m}$ (mean, standard deviation). The coefficient of variation is thus only 8%. The scatter in laboratory mean values is consistent with expectations based on normal sampling statistics. The mean is consistent with results from other credible test methods. Most participants had no problem measuring the precracks. All twenty labs had some measure of success. There was no dependence of toughness on specimen orientation.

2. Reasonably consistent results were obtained from sixteen of the eighteen labs that tried the ESK hot-isostatic pressed silicon nitride. The fracture toughness for 105 specimens was 4.95 ± 0.55 MPa·$\sqrt{m}$. The scatter of results from the individual sample sets was typically higher than obtained for the NC-132. The higher scatter reflects a greater difficulty in detecting the precracks, and possibly additional material variability.

3. Only eight of twelve labs that tried the zirconia sent acceptable results. Four lab data sets were not acceptable since the wrong features were marked as precracks. Two labs had acceptable results only after revision of their initial interpretations. The fracture toughness for 33 specimens was 4.36 ± 0.44 MPa·$\sqrt{m}$. This material was more difficult to test and interpret than the other two.

4. Material removal after indentation should not be difficult. The amount removed was not critical for the two silicon nitrides. 4.3 to 4.5X is recommended from Knoop indentation created precracks. This will ensure that the deepest part of the precrack has the highest stress intensity. Material removal amounts were more sensitive for the zirconia.

5. Fractographic interpretation of the exact precrack boundary varied from participant to participant, but the computation of fracture toughness is relatively *insensitive* to the exact crack size and shape. Fracture toughness is much more sensitive to the flexure strength, which can be measured very accurately and precisely with no subjectivity.

6. Not all the precracks had an ideal flat and semielliptical shape. Precracks in the NC-132 were the closest to ideal. The ESK cracks were less flat and more undulating. The zirconia cracks were flat, but were not simple semiellipses.

7. Ceramic fractographic skill is a necessary prerequisite for the surface crack in flexure method. High quality photos are essential.

8. The ability to accurately measure precracks depends upon the fractographer's skill, the skill of the microscopist, the quality of the pictures taken, and the fractographer's familiarity with the specific material. It is critical that the fractographer work closely with the microscopist.

9. New techniques for enhancing precrack detection were identified. These include tilting the specimen during indentation, illuminating from low angles with optical microscopy, using combinations of low and high magnification photos, sputter coating at a grazing angle, tilting the specimen in the SEM, using backscattering mode in the SEM, and using stereo SEM photography.

10. Consistent fracture toughness and precrack size measurements were obtained from SEM and optical microscopy.

11. A new procedure for precracking materials that are resistant to Knoop precracking has been devised. A Vickers indenter can be tilted and canted to create an oversized Palmqvist crack.

12. Participants who were unfamiliar with the method had much more difficulty. (Participants would probably have a much easier time and a higher success rate after reading this report and becoming more familiar with the procedures. This is especially true as regards finding and characterizing the precracks.)

13. Many participants felt that the method required too much work, and the fractographic work was too difficult for this method to be acceptable for routine, day-to-day screening or evaluation purposes.

14. The general perception of the labs was that the results give a good "scientific" result for fracture toughness. The fracture toughness result is pertinent to a small, naturally-occurring material flaw.

ACKNOWLEDGEMENTS

The organizers wish to thank all the participants for the many helpful comments and suggestions received, both during the testing and the review of this final report. The project was intended to require between one and one and one-half weeks of work per participant, but we realize now that this was optimistic. We thank the participants for their extra efforts to contribute to the success of the project.

Partial support for this program was furnished by the U.S. Department of Energy, Assistant Secretary for Conservation and Renewable Energy, Office of Transportation Technologies, as part of the Ceramic Technology Project of the Materials Development Program, under contract DE-AC05-84OR21400 with Martin Marietta Energy Systems, Inc.

REFERENCES

1. H. Awaji, J. Kon, and H. Okuda, "The VAMAS Fracture Toughness Test Round-Robin on Ceramics," VAMAS Report #9, Japan Fine Ceramics Center, Nagoya, Japan, (1990).
2. H. Awaji, T. Yamada, and H. Okuda, "Results of the Fracture Toughness Test Round-Robin on Ceramics," J. Jap. Cer. Soc., 99, [5], (1991) pp. 417-422.
3. H. Awaji, T. Yamada, and H. Okuda, "Results of the Fracture Toughness Test Round-Robin on Ceramics," J. Jap. Cer. Soc., Int. Ed., 99, (1991) pp. 403-408.
4. G. D. Quinn, J. Salem, I. Bar-on, K. Cho, M. Foley, and H. Fang, "Fracture Toughness of Advanced Ceramics at Room Temperature," J. Res. Natl. Inst. Stand. Technol., 97, (1992) pp. 579-607.
5. G. D. Quinn, "Fracture Toughness of Advanced Ceramics at Room Temperature, A VAMAS Round Robin," Cer. Eng. and Sci. Proc., Vol. 14, #7-8, (1993) pp. 92-100.
6. M. Mizuno and H. Okuda, "VAMAS Round Robin on Fracture Toughness of Silicon Nitride at High Temperature," VAMAS Technical Report No. 16, Japan Fine Ceramics Center, Nagoya, Japan, Dec. 1993.
7. M. Mizuno and H. Okuda, "VAMAS Round Robin on Fracture Toughness of Silicon Nitride at High Temperature," to be published, Cer. Eng. and Sci. Proc., 1994.
8. P. Kenny, "The Application of Fracture Mechanics to Cemented Tungsten Carbides," Powder Met. 14, [27] (1971), pp. 22-38.
9. K. R. Kinsman, R. K. Govila, and P. Beardmore, "The Varied Role of Plasticity in the Fracture of Inductile Ceramics," pp. 465-82 in Deformation of Ceramic Materials, eds. R. C. Bradt and R. E. Tressler, Plenum, NY, 1975.
10. J. J. Petrovic, L. A. Jacobson, P. K. Talty, and A. K. Vasudevan, "Controlled Surface Flaws in Hot-Pressed Si_3N_4," J. Am. Ceram. Soc., 58 [3-4] (1975) pp. 113-116.
11. J. J. Petrovic, R. A Dirks, L. A. Jacobson, and M. G. Mendiratta, "Effects of Residual Stresses on Fracture From Controlled Surface Flaws," J. Am. Ceram. Soc., 59 [3-4] (1976) pp. 177-178.
12. J. J. Petrovic and M. G. Mendiratta, "Fracture from Controlled Surface Flaws," in Fracture Mechanics Applied to Brittle Materials, ASTM STP 678, ed. S. W. Freiman, ASTM, Philadelphia, PA, 1979, pp. 83-102.
13. J. J. Petrovic, "Effect of Indenter Geometry on Controlled-Surface-Flaw Fracture Toughness," J. Am. Ceram. Soc., 66 [4] (1983) pp. 277-283.
14. D. B. Marshall, "Controlled Flaws in Ceramics: A Comparison of Knoop and Vickers Indentation," J. Am. Ceram. Soc., 66 [2] (1983) pp. 127-131.
15. C. A. Tracy, "Fracture Mechanics Analysis and Testing of Advanced Ceramics Using Controlled Flaws," Masters Thesis, Northeastern University, Boston, MA, 1988.
16. G. D. Quinn and C. A. Tracy, "Fracture Toughness by the

Controlled Flaw Method," to be publ. Ceram. Eng. and Sci. Proc., 1994.
17. R. Wills and J. M. Wimmer, "Controlled Surface Flaw-Initiated Fracture in Reaction-Densified Silicon Carbide," J. Am. Ceram. Soc., 59 [9-10] (1976) pp. 437-440.
18. J. J. Petrovic and L. A. Jacobson "Controlled Surface Flaws in Hot-Pressed SiC," J. Am. Ceram. Soc., 59 [1-2] (1976) pp. 34-37.
19. G. Ziegler and D. Munz, "Mechanical Properties of Precracked Si_3N_4 After Different Annealing Treatments," in Science of Ceramics, Vol. 9, ed. K. J. de Vries, Nederlandse Keramische Vereniging, 1977, pp. 502-509.
20. R. R. Wills, M. G. Mendiratta, and J. J. Petrovic, "Controlled Surface-Flaw-Initiated Fracture in Reaction-Bonded Si_3N_4," J. Mat. Sci., 11 (1976) pp. 1330-1334.
21. A. Ghosh, M. G. Jenkins, K. W. White, A. S. Kobayashi, and R. C. Bradt, "Elevated-Temperature Fracture Resistance of a Sintered α-Silicon Carbide," J. Am. Ceram. Soc., 72 [2] (1989) pp. 242-247.
22. R. L. Stewart and R. C. Bradt, "Fracture of Polycrystalline $MgAl_2O_4$," J. Am. Ceram. Soc., 63 [11-12] (1980) pp. 619-623.
23. A. Micski and B. Bergman, "High Temperature Strength of Silicon Nitride HIP-ed with Low Amounts of Yttria or Yttria/Alumina," J. Eur. Ceram. Soc., 6 (1990) pp. 291-301.
24. N. Shinkai, R. C. Bradt, and G. E. Rindone, "Fracture Toughness of Fused SiO_2," J. Am. Ceram. Soc., 64 [7] (1981) pp. 426-430.
25. Y. M. Mai, "Thermal-Shock Resistance and Fracture-Strength Behavior of Two Tool Carbides," J. Am. Ceram. Soc., 59 [11-12] (1976) pp. 491-494.
26. D. C. Larsen, "Property Screening and Evaluation of Ceramic Turbine Engine Materials," U. S. Air Force/IITRI Final Report AFML-TR-79-4188, Oct. 1979.
27. M. Srinivasan and S. G. Seshadri, "The Application of Single Edge Notched Beam and Indentation Techniques to Determine Fracture Toughness of Alpha Silicon Carbide," in Fracture Mechanics Methods for Ceramics, Rock, and Concrete, eds. S. W. Freiman and E. R. Fuller, Jr., American Society of Testing and Materials STP 745, ASTM, Philadelphia, PA, 1980, pp. 46-68.
28. S. T. Gonczy and D. L. Johnson, "Impact Fracture at High Temperature," in Fracture Mechanics of Ceramics, Vol. 3, eds. R. C. Bradt, D. P. H. Hasselman, and F. F. Lange, Plenum, NY, 1978, pp. 495-506.
29. D. Munz and T. Fett, Mechanisches Verhalten Keramischer Werkstoffe, Springer-Verlag, Berlin, 1989.
30. G. Ziegler and D. Munz, "Bruchwiderstandsmessungen an Al_2O_3 und Si_3N_4 mit der Knoop-Härteeindruck-Technik," Ber. Dt. Keram. Ges., 56 [6] (1979) pp. 128-131.
31. G. Mendiratta and J. J. Petrovic, "Slow Crack Growth from Controlled Surface Flaws in Hot-Pressed Si_3N_4," J. Am. Ceram. Soc., 61 [5-6] (1978) pp. 226-230.
32. T. Fett and D. Munz, "Knoop-Indentations as Surface Flaws for

Subcritical Crack Growth Measurements," in Fracture and Mechanical Properties of Ceramic Fuels and of Waste Ceramics and Glasses, ed. Hj. Matzke, Harwood Acad. Publ., London, 1987, pp. 1183-1197.

33. G. D. Quinn and J. B. Quinn, "Slow Crack Growth in Hot-Pressed Silicon Nitride," in Fracture Mechanics of Ceramics, Vol. 6, eds. R. C. Bradt, A. G. Evans, D. P. H. Hasselman, and F. F. Lange, Plenum, 1983, pp. 603-636.
34. G. D. Quinn, "Fracture Mechanism Maps for Advanced Structural Ceramics, Part 1, Methodology and Hot-Pressed Silicon Nitride Results, J. Mat. Sci., 25 (1990) pp. 4361-4376.
35. R. K. Govila, "Indentation-Precracking and Double-Torsion Methods for Measuring Fracture Mechanics Parameters in Hot-Pressed Si_3N_4," J. Am. Ceram. Soc., 63 [5-6] (1980) pp. 319-326.
36. T. Fett, K. Germerdonk, A. Grossmüller, K. Keller, and D. Munz, "Subcritical Crack Growth and Threshold in Borosilicate Glass," J. Mat. Sci., 26 (1991) pp. 253-257.
37. T. Fett, K. Keller, D. Munz, and J. Kübler, "Subcritical Surface Crack Growth in Borosilicate Glass Under Thermal Fatigue," Theo. Appl. Fract. Mech., 16 (1991) pp. 27-34.
38. M. Kawai, H. Abe, and J. Nakayama, "Indentation-Induced-Flaw Method for Measuring Crack Velocity in Sintered Si_3N_4," in Fracture Mechanics of Ceramics, Vol. 6, eds. R. C. Bradt, A. G. Evans, D. P. H. Hasselman, and F. F. Lange, Plenum, New York, 1983, pp. 587-601.
39. M. R. Foley and R. E. Tressler, "Threshold Stress Intensity for Crack Growth at Elevated Temperatures in a Silicon Nitride Ceramic," Adv. Cer. Mat., 3 [4] (1988) pp. 382-386.
40. E. J. Minford and R. E. Tressler, "Determination of Threshold Stress Intensity for Crack Growth at High Temperature in Silicon Carbide Ceramics," J. Am. Ceram. Soc., 66 [5] (1983) pp. 338-340.
41. G. Grathwohl, "Creep and Fracture of Hot-Pressed Silicon Nitride with Natural and Artificial Flaws," in Creep and Fracture of Engineering Materials and Structures, eds. B. Wilshire and D. Owen, Pineridge Press, Swansea, (1984), pp. 565-577.
42. A. Okada, M. Matsunaga, and Y. Akoh, "Crack Growth and Crack-Tip Blunting of Sintered Silicon Nitride at High Temperatures," Yogyo-Kyokai-Shi, 93 [8] (1985) pp. 426-432.
43. ASTM E-740-88, "Standard Practice for Fracture Testing with Surface-Crack Tension Specimens," Annual Book of ASTM Standards, Vol. 03-01, ASTM, Philadelphia, PA, 1993.
44. Japanese Industrial Standard, JIS R-1607, "Testing Method for Flexural Strength (Modulus of Rupture) of High Performance Ceramics," Japanese Standards Association, Tokyo, 1991.
45. T. Fujii and T. Nose, "Evaluation of Fracture Toughness for Ceramic materials", IJIS Int., 29 [9] (1989) pp. 717-725.
46. T. Nose, "Case Study-1: Testing Methods for Fracture Toughness of Fine Ceramics," in Proceedings of the International Conference on the Promotion of Standardization for Fine

Ceramics, Nagoya, Japan, pp. 54-59.
47. A. G. Evans, "Perspective on the Development of High-Toughness Ceramics," J. Am. Ceram. Soc., 73 [2] (1990) pp. 187-206.
48. DIN 51-110, Part 3, "Testing of Advanced Technical Ceramics, 4 Point Bending Test; Statistical Evaluation: Determination of Weibull Parameters," DIN, Berlin, 1992.
49. ASTM C 1239-93, "Standard Practice for Reporting Uniaxial Strength Data and Estimating Weibull Distribution Parameters for Advanced Ceramics," Annual Book of ASTM Standards, Vol. 15.01, ASTM, Philadelphia, PA, 1993.
50. J. A. Salem, and J. L. Shannon, Jr., "Fracture Toughness of Si_3N_4 Measured with Short Bar Chevron-Notched Specimens", J. Mat. Sci., 22 (1987) pp. 321-324.
51. G. D. Quinn, "Characterization of Turbine Ceramics After Long Term Environmental Exposure," U.S. Army Materials Technology Laboratory Technical Report, Watertown, MA., TR 80-15, April 1980.
52. J. J. Kübler, "Weibull Characterization of Four HIPPED/Post HIPPED Engineering Ceramics Between Room Temperature and 1500°C," presented at the American Ceramic Society Annual Meeting, Minneapolis, MN, April 1992.
53. M. L. Torti, "Processing Hot Pressed Silicon Nitride for Improved Reliability: HS-110 to NC-132," in Ceramics for High Performance Applications, III, Reliability, eds. E. M. Lenoe, R. N. Katz, and J. J. Burke, Plenum, NY, 1983, pp. 261-273.
54. F. I. Baratta, G. D. Quinn, and W. T. Matthews, "Errors Associated with Flexure Testing of Brittle Materials," U. S. Army Materials Technology Technical Report, TR 87-35, July, 1987.
55. European Standard, ENV 623-3, Advanced Technical Ceramics - Monolithic Ceramics - General and Textural Properties - Part 3; Determination of Grain Size," European Committee for Standardization, Brussels, March 1993.
56. European prenorm prEN 843-1, "Advanced Technical Ceramics: Mechanical Properties of Monolithic Ceramics at Room Temperature, Part 1: Determination of Flexural Strength," European Committee for Standardization, Brussels, May 1993.
57. ASTM C 1161-90, "Standard Test Method for Flexural Strength of Advanced Ceramics at Ambient Temperature," Annual Book of ASTM Standards, Vol. 15.01, ASTM, Philadelphia, PA, 1990.
58. MIL-STD-1942A "Flexural Strength of High Performance Ceramics at Ambient Temperature," U. S. Army Research Laboratory, Watertown, MA, 8 November 1990.
59. J. D. Sullivan and P. H. Lauzon, "Shape Profiles of Cracks Under a Vickers Pyramid Indenter," J. Mat. Sci. Let., 5 (1986) pp. 247-248.
60. S. L. Jones, C. J. Norman, and R. Shahani, "Crack-Profile Shapes Formed Under a Vickers Indent Pyramid," J. Mat. Sci. Let., 6 (1987) pp. 721-723.
61. R. M. Anderson and L. M. Braun, "Technique for the R-Curve Determination of Y-TZP Using Indentation-Produced Flaws," J. Am. Ceram. Soc., 73 [10] (1990) pp. 3059-3062.

62. A. P. Vicente, F. Guiberteau, A. Dominguez-Rodriguez, G. W. Dransmann, and R. W. Steinbrech, "Propagation of Short Surface Cracks in Y-TZP," in Euro-Ceramics II, Structural Ceramics and Composites, eds. G. Ziegler and H. Hausner, Deutsche Keramische Gesellschaft e.v., Berlin, 1992, pp. 1023-1030.
63. G. D. Quinn and R. Morrell, "Design Data for Engineering Ceramics: A Review of the Flexure Test," J. Am. Ceram. Soc., 74 [9] (1991) 2037-2066.
64. J. C. Newman, Jr. and I. S. Raju, "An Empirical Stress-Intensity Factor Equation for the Surface Crack," Eng. Fract. Mech., 15 [1-2] (1981) pp. 185-192.
65. T. Fett, "An Extension of the Newman-Raju Formula," Int. J. Fract., 33 (1987) pp. R47-R50.
66. G. C. Sih and Y. D. Lee, "Review of Triaxial Crack Border Stress and Energy Behavior," Theor. Appl. Fract. Mech., 12 (1989) pp. 1-17.
67. F. W. Smith and M. J. Alavi, "Stress-Intensity Factors for a Part-Circular Surface Crack," In Proc. 1st Intl. Conf. Pressure Vessel Tech., (1969) pp. 793-800.
68. M. L. Mecartney, "Influence of an Amorphous Second Phase on the Properties of Yttria-Stabilized Tetragonal Zirconia Polycrystals (Y-TZP)," J. Am. Ceram. Soc., 70 [1] (1987) pp. 54-58.
69. M. Ashizuka, H. Kiyohara, E. Ishida, M. Kuwabara, Y. Kubota, and T. Tsukidate, Yogyo-kyokai-shi, 94 [4] (1986) pp. 432-439.
70. J. A. Salem, J. L. Shannon, Jr., and M. Jenkins "Some Observations in Fracture Toughness and Fatigue Testing with Chevron-Notched Specimen", in Chevron-Notch Fracture Test Experience: Metals and Non-Metals, ASTM STP 1172 eds. K .R. Brown and F. I. Baratta, 1992, ASTM Philadelphia, PA., pp. 9-25.
71. R. T. Busbey, J. L. Shannon, Jr. and D. Munz, "Development of Plane Strain Fracture Toughness Test for Ceramics using Chevron Notched Specimens", in Ceramics for High Performance Applications III, Reliability, Plenum, NY, 1983, pp. 753-771.
72. J. A. Salem and S. R. Choi, "Toughened Ceramics Life Prediction" in Ceramics Technology Project Bimonthly Progress Report, Oct.-Nov. 1991, Oak Ridge National Laboratory, Oak Ridge, TN, 1991, pp. 220-234.
73. C. G. Annis and J. S. Cargill, "Impact Fracture of Ceramics at High Temperature", in Fracture Mechanics of Ceramics, Vol. 4, eds. R. C. Bradt, D. P. H. Hasselman and F. F. Lange, Plenum, NY, 1978 pp. 737-744.
74. R. K. Govila, "Material Parameters for Life Prediction in Ceramics", in Ceramics for High Performance Applications III, Reliability, Plenum, NY, 1983 pp. 535-567.
75. R. K. Govila, "Indentation Precracking and Double Torsion Methods for Measuring Fracture Mechanics Parameters in Hot-Pressed Si_3N_4," J. Am. Ceram. Soc., 63 [5-6] (1980) pp. 319-326.
76. G. D. Quinn, Unpublished results.
77. G. K. Bansal, W. H. Duckworth, "Effects of Specimen Size on

Ceramic Strength", in Fracture Mechanics of Ceramics III, eds. R. C. Bradt, D. P. H. Hasselman, and F. F. Lange, Plenum, NY, 1978, pp. 189-204.
78. G. K. Bansal, W. H. Duckworth, "Fracture Toughness of Hot-Pressed Si_3N_4", Am. Ceram. Soc. Bull., 14 (1981) p. 254.
79. G. R. Anstis, P. Chantikul. B. R. Lawn, D. B. Marshall, "A Critical Evaluation of Indentation Techniques for Measuring Fracture Toughness: I, Direct Crack Measurements", J. Am. Ceram. Soc., 64 [9] (1981) pp. 533-537.
80. F. F. Lange, "High-Temperature Strength Behavior of Hot Pressed Si_3N_4: Evidence for Subcritical Crack Growth," J. Am. Ceram. Soc., 57 [2] (1974) pp. 84-87.
81. J. L. Henschall, D. J. Rowcliffe, and J. W. Edington, "The Fracture Toughness and Delayed Fracture of Hot Pressed Silicon Nitride," in Special Ceramics 6, BCRA, Stoke-on-Trent, 1975, pp. 185-198.
82. A. G. Evans and S. M. Wiederhorn, "Crack Propagation and Failure Prediction in Silicon Nitride at Elevated Temperatures," J. Mat. Sci., 9 [2] (1974) pp. 270-278.
83. F. F. Lange, "Relation Between Strength, Fracture Energy, and Microstructure of Hot-Pressed Si_3N_4," J. Am. Ceram. Soc., 56 [10] (1973) pp. 518-522.
84. J. L. Henschall, D. W. Rowcliffe, and J. W. Edington, "The Measurement of K_{Ic} and Subcritical Crack Growth in Hot Pressed SiC and Si_3N_4," in Fracture 1977, Vol.3, ICF4, Waterloo, Canada, 1977, pp. 875-882.
85. P. Lange, Private Communication, ESK, Nov. 1993.
86. P. Chantikul, G. R. Anstis, B. R. Lawn, and D. B. Marshall, "A Critical Evaluation of Indentation Techniques for Measuring Fracture Toughness: II, Strength Method," J. Am. Ceram. Soc., 64 [9] (1981) pp. 539-543.
87. H. Toraya, M. Yoshimura, and S. Sōmiya, "Calibration Curve for Quantitative Analysis of Monoclinic-Tetragonal ZrO_2 System by X-ray Diffraction," Comm. Am. Ceram. Soc., June 1984, pp. C-119-121.
88. J. J. Swab, "Properties of Yttria-Tetragonal Zirconia Polycrystal (Y-TZP) Materials After Long-Term Exposure to Elevated Temperatures," U. S. Army Materials Technology Laboratory, Technical Report TR 89-21, March, 1989.
89. B. J. De Smet, P. W. Bach, P. P. A. C. Pex, "Fracture Toughness Testing of Ceramics," in Proceedings of the Second European Ceramic Society Conference, Augsburg, Sept. 1991, Deutsche Keramische Gesellschaft, Berlin, 1992.
90. S. Liu and I. Chen, "Fatigue of Yttria-Stabilized Zirconia: II, Crack Propagation, Fatigue Striations, and Short-Crack Behavior," J. Am. Ceram. Soc., 74 [6] (1991) pp. 1206-1216.
91. R. Stevens, "Engineering Properties of Zirconia," in Engineered Materials Handbook, Vol. 4, Ceramics and Glasses, ed. S. J. Schneider, Jr., ASM, Ohio, 1991, pp. 775-786.
92. M. V. Swain, "Limitation of Maximum Strength of Zirconia-Toughened Ceramics by Transformation Toughening Increment," Com. Am. Ceram. Soc., April 1985, pp. C-97 to C-99.

93. F. F. Lange, "Phase Retention and Fracture Toughness of Materials Containing Tetragonal ZrO_2," in Volume 3, ICM 3, Cambridge, England, August 1979, pp. 45-56.
94. F. F. Lange, "Transformation Toughening - Part 3, Experimental Observations in the ZrO_2-Y_2O_3 System," J. Mat. Sci., 17 (1982) pp. 240-246.
95. T. Masaki and K. Sinjo, "Mechanical Properties of Highly Toughened ZrO_2-Y_2O_3," Ceramics Int., 13 (1987) pp. 109-112.

APPENDIX 1

INSTRUCTIONS FOR THE ROUND ROBIN

Each participant received the following instructions in addition to the 10 specimens of each of the three materials. Supplemental information on the three materials and the test method in general was also included, as was company literature on the Norton NC-132 and hipped silicon nitrides. This was done to help the participants familiarize themselves with the materials.

In several instances, addenda have been made to these instructions in order to clarify certain points. These were not in the original instructions sent to the participants, but have been added in case these instructions are used for future work. These addenda are clearly labelled in this appendix.

A floppy computer disk was included which enabled the participants to save much time in entering the data into a standard format, and in computing the Newman-Raju shape factors. The spreadsheet calculated the stress at fracture, the Y factors at both the surface and depth, and then the correct fracture toughness for the specimen. Use of the spreadsheet eliminated many potential computational and data entry errors.

A survey questionnaire was also included to assess the general reaction of the participants to the round robin.

VAMAS
TECHNICAL WORKING AREA #3
SURFACE CRACK IN FLEXURE (SCF)
(CONTROLLED SURFACE FLAW)
FRACTURE TOUGHNESS ROUND ROBIN

SKILLS: This method requires interpretation of fracture surfaces. The microscopy (optical or SEM) and interpretation of the photos should be done by experienced personnel.

EQUIPMENT REQUIRED:

* Strength Testing Machine, Load capacity: 200 kg (2000 N)
* Four Point Flexure Fixtures, 20 X 40 mm spans
  (Three point or other spans permitted if above not available.)
* Hardness Indentation machine with Knoop and Vickers indenters, with a capacity of 2.5, 5 and 15 kg
* Optical microscope with magnification 100-400X. Camera attached
* Scanning Electron Microscope
* Conventional Metallographic Polishing Equipment
* Micrometer, with readout to 0.002 mm

ITEMS ENCLOSED:

1. Instructions
2. Three packs of 10 specimens:
   a. Hot-Pressed Silicon Nitride, Norton Grade **NC-132** (Black)
   b. Hot-Isostatic Pressed Silicon Nitride, ESK (Grey)
   c. Hot-Isostatic Pressed Zirconia, **Y-PSZ,** EMPA (White)
3. Report Sheets
4. 13.3 cm (5¼ ") Floppy Disk with a Lotus spreadsheet containing the report sheets and the Raju-Newman Formulas.
   (The spreadsheet is "CSFFORM.WK1", and a backup is labelled "CSFFORM.BAK".)
5. Background Information Sheets that are not necessary to read. These include Norton and ESK materials information literature.

SCHEDULE

1.	Specimen distribution:	Nov. 4, 1992
2.	Return of Report, and/or floppy disk:	Mar. 10, 1993
3.	Organizers contact participants for preliminary review of data:	Mar. 31, 1993
4.	Preliminary Report:	June 1993

Part 1. Hot-Pressed Silicon Nitride: NC-132 (Black)

1. Indent 5 specimens on the **wide** polished face that is **4 x 47.6 mm.**
(Ignore the black dots on the specimen end.)
(The extra five specimens are for practice or any other purpose that you wish. They can be used with different orientation, indentation size, rate of loading, or a different fracture toughness test method.)
The indentation must be close to perpendicular to the specimen long direction. The indentation should be approximately in the middle of the specimen length, and approximately in the middle of the specimen width. Put a pencil mark arrow on the specimen side which will help you remember where the indentation is located. The indentation conditions are:

Indenter:	Knoop
Tilt:	½° (see Figure attached)
Load:	**2.5** kgf (24.5 N)
Indent Time:	Any time from 5-45 seconds.

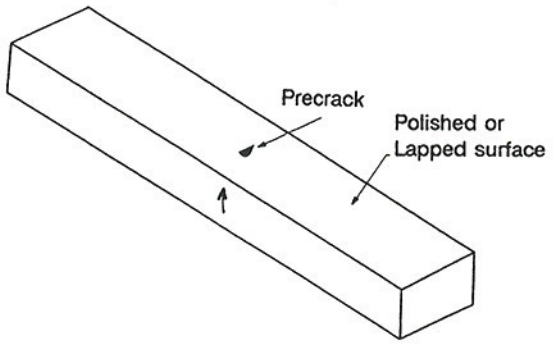

2. Measure the long diagonal size, **L**, for each impression, in the same manner that is done for a hardness measurement.
3. Compute the average approximate depth of the impression.
$$x = (1/30)\,L$$
4. Measure with a hand micrometer the specimen height, **h**, of each specimen in the middle, where the indentation is, to an accuracy of .002 mm.
5. Remove the indentation and the residual stress by polishing the indentation and additional material to a depth of **4 - 4.3x. ***** Use the hand micrometer to monitor the amount of material removal. The amount removed should be with a tolerance of +.002, -.000 mm. If too little is removed, the residual stress may not be completely eliminated, and the highest stress intensity shape factor, Y, may be at the surface.
Many methods can be used for this step. We have successfully used an ordinary 200 mm (8") polishing wheel with a disk of 70 micrometer (180 grit) silicon carbide paper. This is done dry to a depth close to the final size, then a final polish is performed with a 40-50 micrometer (240 grit) disk of silicon carbide, also dry. This can be done with the fingers with a medium pressure and will take 5-10 minutes per specimen. A diamond abrasive wheel (hone) also is satisfactory. Faster procedures are surely possible.
NOTE: do not use procedures that are too aggressive because they can cause surface damage that will interfere with the precrack.

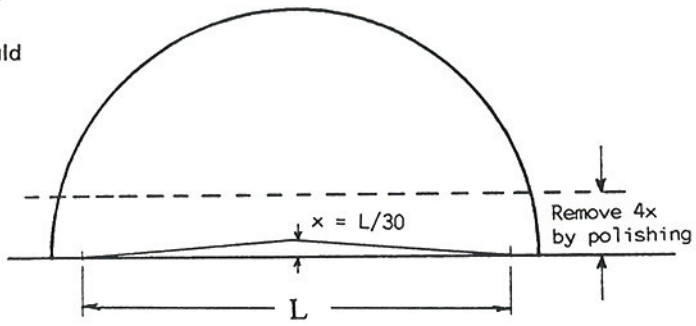

***** ADDENDA: Remove 4.3 to 4.5X. See text. *****

6. Measure and record the specimen height, **h**, and the width, **b**, for each specimen.
7. Fracture the specimen in four point flexure with the indented surface in tension, and with the indentation between the inner rollers. Thus, the specimen will be laid **flat** onto the fixture.
Put some soft material under the middle of the specimen so that the specimen does not impact the fixture bottom.
Test at a conventional rate such as 0.5 mm/ minute.

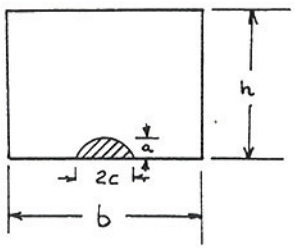

8. Compute the fracture strength from the conventional formula. Be careful to insert the correct values for **b** and **h** (and not get them mixed up.) Use the measured values of **b** and **h** for each specimen, and not the nominal size.

$$\sigma = (3\,F\,\ell)\,/\,(b\,h^2)$$

where
- σ is the fracture strength (MPa)
- F is the fracture load (Newtons)
- ℓ is the moment arm (outer span - inner span)/2 (mm)
- b is the specimen width (mm)
- h is the specimen height (mm)

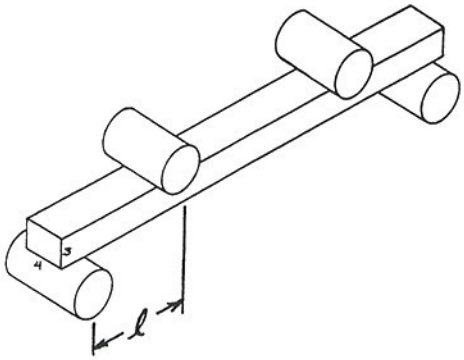

9. Examine the fracture surfaces to verify that the specimen broke from the artificial flaw, (and that the indentation was removed.) Find the artificial flaw by following the hackle lines back to the fracture mirror, and then back to the crack. Use an optical microscope first. A low power (100-200X stereo binocular microscope with low angle illumination can be helpful. **EITHER:**

   a. Use a conventional reflected light microscope with a magnification of 300 - 400X to photograph the artificial flaw.
   (Photograph a stage micrometer to verify the magnification.)

   b. Use a scanning electron microscope at 400 - 500X to photograph the artificial flaw. If you are not sure that you have found the precrack, then also photograph at 200X. In the report, you must state whether the SEM is calibrated or not. (Note: SEM magnifications may be 3-5% off).

(OPTIONAL: You may try both methods.)
Examples of optical and SEM photos are shown in an attached sheet.
Measure the crack depth, **a**, and the crack width, **2c**, for each specimen from the photos to the nearest 0.5 mm and then convert both the crack sizes to **millimeters** (not micrometers). Suggestions on how to interpret and measure the semiellipse are given later.

10. Fill in the data on the Lotus spreadsheet (CSFFORM.WK1) that is supplied on the floppy disk. Fracture toughness will be calculated automatically. The computer will calculate the shape factor Y for both the deepest point and the surface point of the crack. The toughness will be calculated with the higher Y factor.
(For the test conditions given for the hot pressed silicon nitride, the highest Y will be at the deepest point if the proper amount of material is polished away.)

ALTERNATE PROCEDURE (If floppy disk is not used.)
Compute the Newman-Raju stress intensity shape factors as follows:
(The term Y is dimensionless, but put all numbers in millimeters to be consistent.)
Note: These factors are only valid for $a/c \leq 1$.

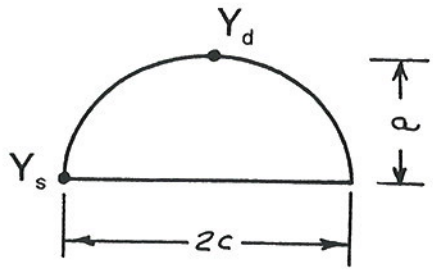

For the deepest point of the flaw:

$$Y_d = (\sqrt{\pi}\, M\, H_2) / \sqrt{Q}$$

where

$$Q = 1. + 1.464(a/c)^{1.65}$$

$$M = \{1.13 - 0.09(a/c)\} + \{-0.54 + 0.89\cdot[0.2 + (a/c)]^{-1}\}(a/h)^2 + \{0.5 - [0.65 + (a/c)]^{-1} + 14.\cdot(1-a/c)^{24}\}(a/h)^4$$

$$H_2 = 1. - [1.22 + 0.12(a/c)](a/h) + [0.55 - 1.05\,(a/c)^{.75} + 0.47(a/c)^{1.5}](a/h)^2$$

For the point at the surface:

$$Y_s = (\sqrt{\pi}\, M\, S\, H_1) / \sqrt{Q}$$

where

$$H_1 = 1. - [0.34 + 0.11(a/c)](a/h) \quad \text{and} \quad S = [1.1 + 0.35(a/h)^2]\sqrt{a/c}$$

Use the larger value of Y and then compute the fracture toughness:

$$K_{Ic} = Y\, \sigma \sqrt{a_m}$$

where K_{Ic} is the fracture toughness in $MPa\cdot\sqrt{m}$
Y is the dimensionless shape factor
σ is the stress in MPa
a_m is the crack depth in meters

11. Fill out the report sheet. (Alternatively, make a file on the floppy disk, and print out the file.) Add comments especially about how "good" or "bad" the crack appeared. Compute the average toughness and standard deviation. Mark one representative photo for a good crack, and one for a poor crack, with a pen or other marker with dashed line (so that it does not cover the whole boundary) to show the precrack. Send these photos with the report.

KNOOP INDENTATION - "TILT"

Use a ½° tilt on all specimens in this round robin. We recommend that a shim (a small strip of metal) be used to support a simple platform that the specimen rests flat on. If you put a shim directly under the specimen, be careful that the specimen does not rock or move during the indentation.

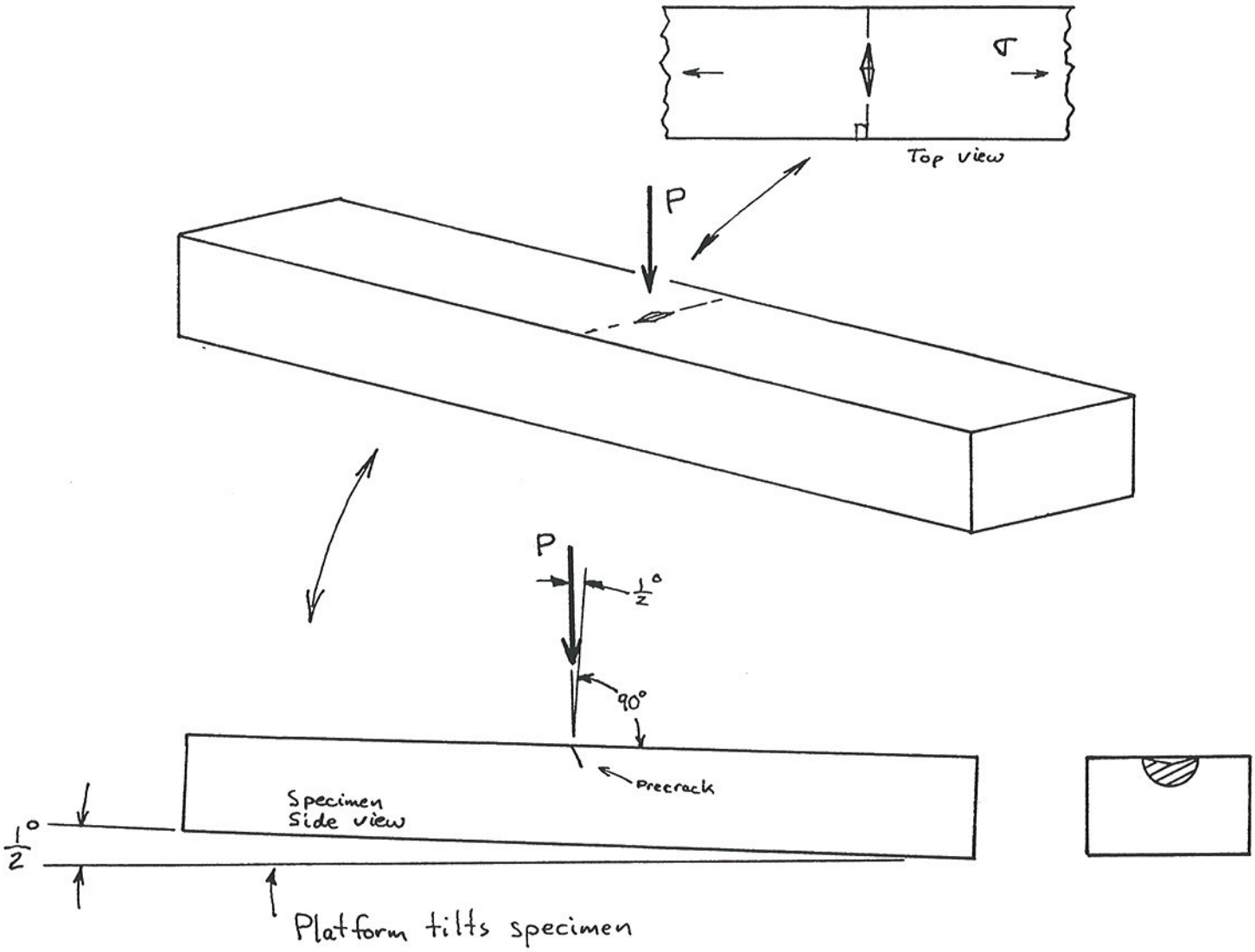

The ½° tilt will cause the precrack to go in at an angle from ½° - 5°. The stress intensity factor Y is not affected very much by such small tilt angles.

This technique is very useful since the precrack is at a slightly different angle than the final fracture surface. With low angle incident lighting, the difference in surfaces can be detected more easily. The different reflectivity can also help in ordinary microscopes or on an SEM. Note, even on specimens which are indented flat (without a tilt), sometimes the crack is a little off perpendicular which helps them to be detected.

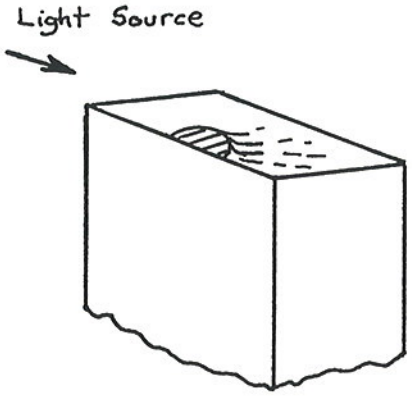

KNOOP PRECRACK - OBSERVATIONS AND TIPS

The Knoop precrack is detectable since:

1. It may be at a slightly different plane (angle) than the final fracture surface,
2. It may fracture in a different mode (transgranular) than the final fracture (mixed trans and intergranular).
3. It may leave an arrest line.
4. It may be dye penetrated. This is effective in only some cases, primarily "white" ceramics, and only if the dye is applied while the residual stress and damage zone are intact and hold the precrack open. Polishing must then be done dry.

ADDENDA 5. Either coarse or fine hackle lines change direction at the boundary.

Sometimes luck is a factor. It may be necessary to indent, polish, then break, 10 specimens in order to get 5 that are visible. (We hope that the hot-pressed silicon nitride will have a high success rate. The hipped silicon nitride an acceptable rate we hope.)

The best mode of viewing will vary from material to material. Sometimes simple optical measurements are satisfactory. In other cases, the SEM is necessary. We have measured precracks in the hot pressed silicon nitride with both the SEM and optical microscope and have obtained similar values.

Sometimes it is helpful to aim a light source at a low angle to create shadows. A precrack may have a "halo" either in optical or electron microscopy if the crack is tilted. This is due to the different reflectivity of the ridge as the crack realigns to the plane of maximum stress during fracture.

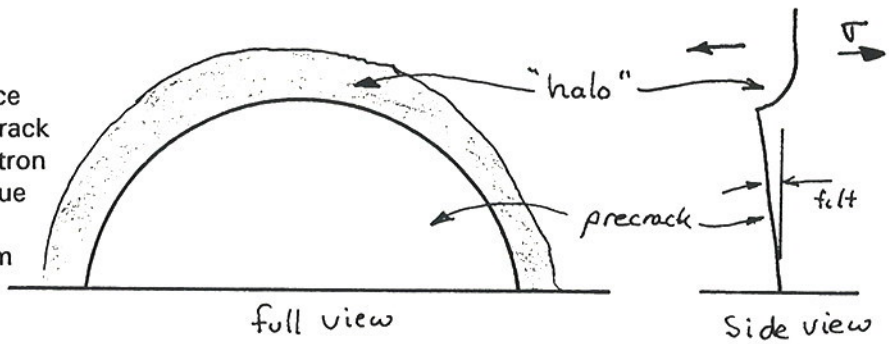

ADDENDA: Hackle lines change at the boundary.

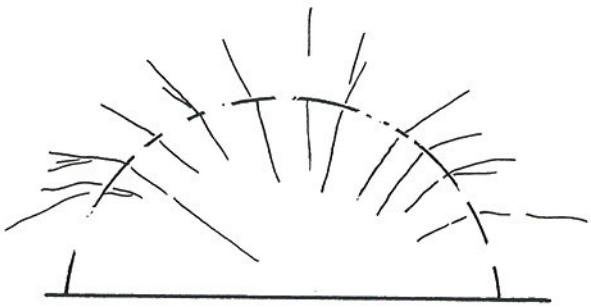

Sometimes a crack does not show itself clearly. Mark the edges that are clear, then estimate the remainder if necessary to give an "effective crack shape". If this is done, it must be stated in the report.

Generally, the best procedure with the SEM is to photograph the whole origin area at 100-200X, then make a closeup of the center of the fracture mirror with 300- 500X. Many times the precrack will be <u>easier to see on a good photo with good room lighting than on the video monitor.</u> As always, it is usually a good idea to

examine both halves of the fracture surface. Sometimes the precrack is much easier to see on one than the other! Another trick is to rotate the specimen 180° in the SEM.

Addenda: Alternatively, tilt the specimen 10-20° during the fractographic examination to help detect the precracks on the fracture surfaces. Photograph the fracture surface, then tilt the specimen back to a normal, perpendicular viewing angle. Photograph the fracture surface again and compare the two images.

A variation on this is to create stereo SEM paired photographs. A 10-15° tilt is usually satisfactory. When viewed with a stereo viewer, such paired photos reveal a wealth of detail.

Optical and SEM micrographs of NC132 Silicon Nitride

showing controlled surface flaw on fracture surface
made with Knoop indenter at a load of 2.5 kg, 1/2 degree tilt

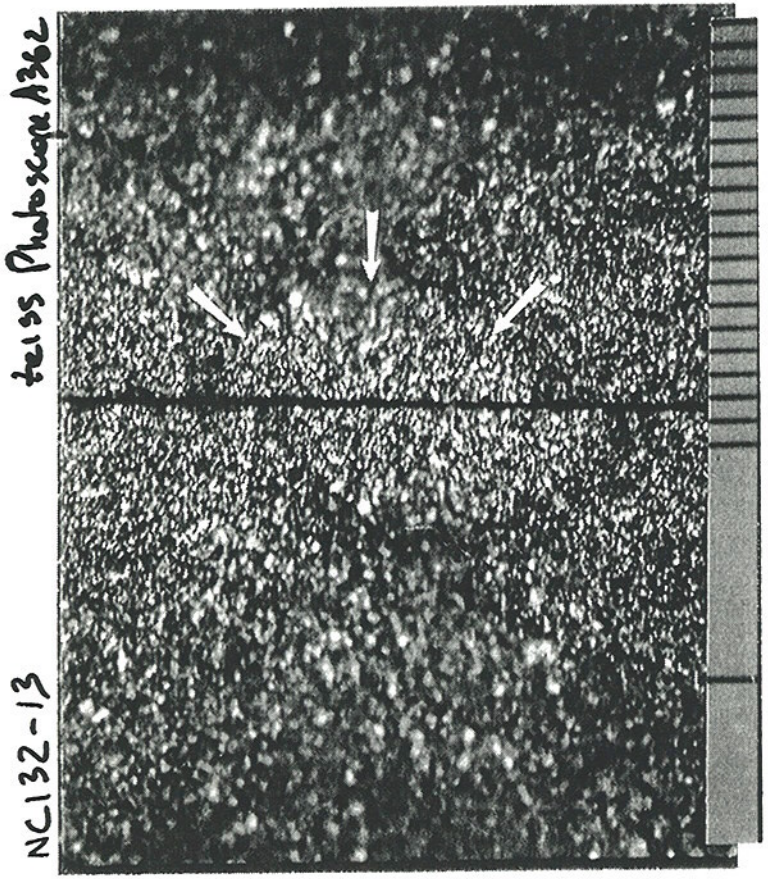

300X Optical micrograph

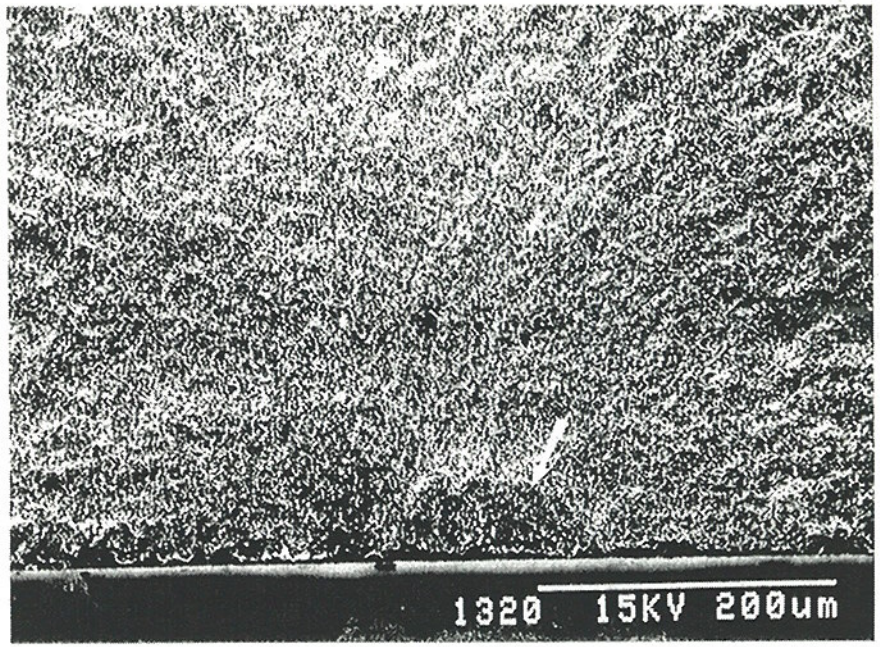

200X SEM micrograph

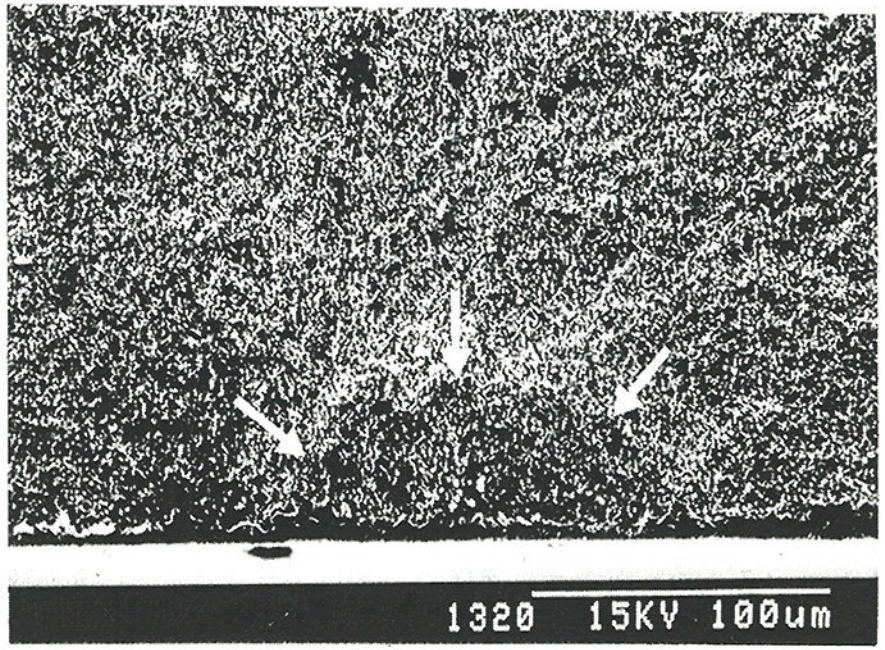

400X SEM micrograph

PRECRACK COMPLICATIONS

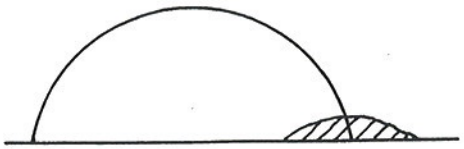

Polishing or Machining Damage
Do not be too aggressive in removing the last material when polishing the indentation off.
(For this round robin we recommend that:
if possible, the specimens be repolished with less severity,
or if necessary, approximate the ellipse shape as if the surface damage is not present.)

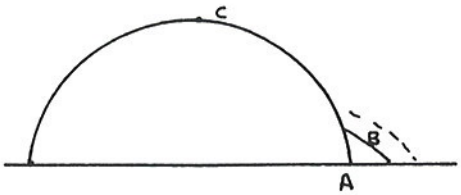

Corner Pop-in
During the fracture test, the precrack reaches critical fracture condition at Point A first. A small crack extends to B. Final fracture starts at Point C.
(For this round robin we recommend that:
you analyze the original ellipse, A-C.)

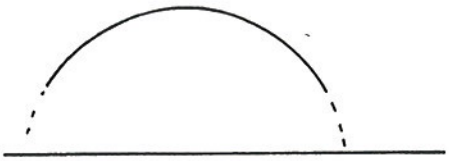

Poorly Defined Crack at the Surface
This often occurs on optical photos since the precrack and final crack are almost on the same plane.
(For this round robin we recommend that:
you estimate or approximate the ellipse shape.)

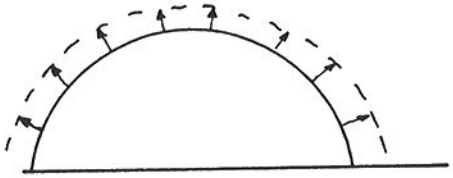

R-curve Crack Extension
Crack extends stably prior to fast fracture. This can either be an interference (which crack should be measured?) or a useful tool to study R-curve phenomena.
(For this round robin we recommend that:
you report the fracture toughness for both ellipses, using the maximum load at fracture, if you detect this for the zirconia, but not for Si_3N_4.)

Precrack Truncation
The final crack is on a different plane and only intersects a portion of the precrack.
(For this round robin we recommend that:
you do not analyze such a precrack.)

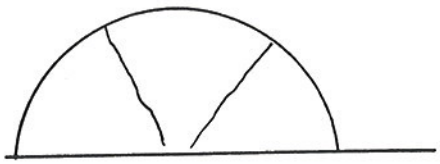

Precrack Segmentation
Precrack is actually made of three segments. There often is a 3-dimensional aspect to the precrack. It is "rippled" or "corrugated" as shown in the figure below. The interference may be from lateral or Hertzian cracks. This problem is common in some sintered ceramics. The organizers would like to hear suggestions or comments from the participants about this problem.

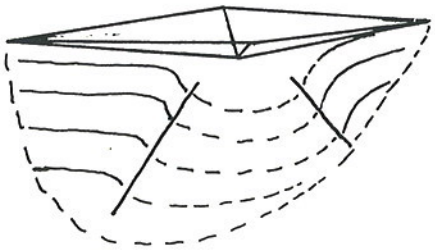

Part 2. Hipped Silicon Nitride: ESK (Dark Grey)

1. Indent all 10 specimens on the **narrow** (3 x 45 mm) polished face.
(All ten specimens should be used since it is harder to detect the semielliptical cracks in this material.)
The indentation must be perpendicular to the specimen long direction. The indentation should be approximately in the middle of the specimen length, and approximately in the middle of the specimen width. Put an arrow on the specimen side to help you remember where the indentation is located. The indentation conditions are:

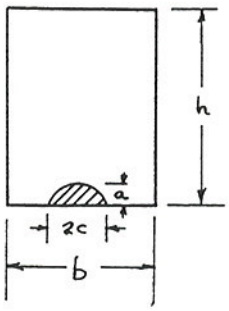

Indenter: Knoop
Tilt: ½°
(see attached Figure)
Load: 5 kgf (49 N)
(This load is different from that for the hot-pressed silicon nitride.)
Indent Time: Any time from 5-45 seconds.

2-11. Follow the same procedures as given for the hot pressed silicon nitride,

EXCEPT:

a. Insert the specimen into the flexure fixtures with the narrow polished face in tension as shown in the figure below. Be careful to use some shim or method to keep the specimen width (the 3 mm dimension) centered in the fixture.)

b. Be careful to use the correct values for b (about 3 mm) and h (about 4 mm) in the equations for stress and for Y.

c. The precracks will not be as easy to observe in this material, and they may not be regular. It may be that only a few out of the ten specimens may give acceptable cracks. Please see the notes on "Knoop Precracks, Observations and Tips" on how to mark an "effective precrack" size.

d. Use only the scanning electron microscope. See the notes in the appendix. Take photos at 200 and 500X.
(It may be possible to measure the precracks with a stereo microscope with 200X and low angle incident lighting, but we are not sure if this would be accurate.)

12. Keep a record of each specimen's identity (number and letter on the end of each specimen.)

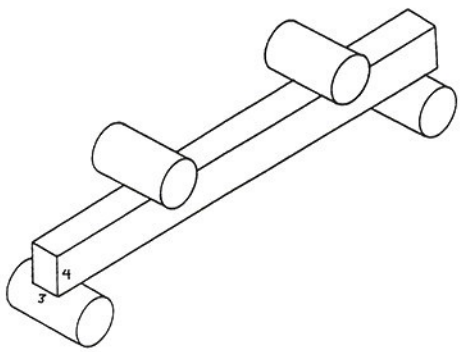

Part 3. Hipped Zirconia, Y-TZP (White)

1. **A special procedure is necessary to indent the Zirconia. See the attached figure sheet that is labelled: "MODIFIED CSF METHOD - Vickers".**
   Indent 5 specimens on the **narrow** polished face that is 3 x 45 mm wide.
   (The extra five specimens are for practice or any other purpose that you wish. They can be used with different orientation, indentation size, rate of loading, dye penetration, or another fracture toughness test method.)

   The specimen must have the ½° tilt, but must also be **canted** as shown in the attached figure. Note that since we are using a Palmqvist crack from the side of the indentation, the indent should be aimed about 0.3 - 0.4 mm to the side of the middle of the specimen as shown in the attached Figure.
   ***** ADDENDA: This may have been too much. 0.1 to 0.2 mm would be better. *****
   Put an arrow on the specimen side which to help you remember where the indentation is located. The indentation conditions are:

Indenter:	VICKERS	
Tilt:	½°	(see Figure attached)
Cant:	3°	(see Figure attached)
Load:	15 kgf (149 N)	(This load does not have to be exact.)

   Indent Time: Any time from **30-45** seconds but must be at least 30 seconds!

2. Measure the diagonal sizes, d_1 and d_2, for each Vickers impression and calculate the average **d**.
3. Compute the average approximate depth of the impression: **x** = (1/7) **d**
4. Measure with a hand micrometer the specimen height, **h**, of each specimen in the middle, where the indentation is, to an accuracy of .002 mm.
5. Remove the indentation and the residual stress by polishing the indentation and additional material to a depth of **2.5 x**. Be certain to record in the report how you removed the indentation.
   NOTE: Use care in polishing in order to minimize possible surface transformations to the monoclinic phase from polishing stresses. Polish as gently as possible.
   Optional for the spare 5 specimens: One procedure to eliminate the polishing residual stresses is, after polishing, to heat the specimen briefly to 1250°C in air in an ordinary laboratory heat treating furnace, and then cool down to ambient temperature.

6-8. Same as for hot pressed silicon nitride, **except** lay the specimen on the fixtures so that it rests on the polished 3 mm wide face as shown below. Be careful to center the specimen width (the 3 mm) in the fixtures. Measure the flexure strength at a rate of 0.5 mm/min.

9-11. Same as for hot pressed silicon nitride, **except** that the maximum Y may be at the surface for some of these cracks, and they may not be as semielliptical as the Knoop median cracks. It is possible the cracks will look more like a offset ellipse. Approximate the crack shape with an ellipse. Mark the precrack on the photos with dotted or dashed lines which do not completely cover the boundary. The Scanning Electron Microscope is recommended for this material.
   (Note: if a/c > 1.0, report the results, approximate the precrack by a semicircle.)
   ***** ADDENDA: The Newman-Raju factors are acceptable for a/c ratios a small amount over 1.0. See Text. *****

12. If you detect several crack sizes, report both the precrack size, and an apparent final crack size at instability, and compute the apparent fracture toughness values for both conditions using the maximum load at fracture.
13. Keep a record of each specimen's identity (number and letter on the end of each specimen.)

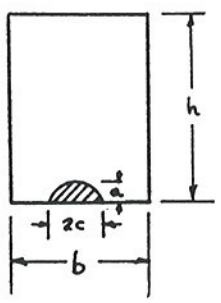

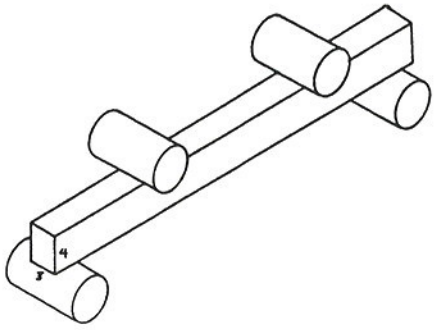

MODIFIED CSF METHOD (Vickers)

Indentation loads from 1-100 kgf (10-1000 N) are not effective in creating a Knoop precrack in the zirconia (Y-TZP). Cracks do form, but they are too shallow, presumably due to the higher toughness and greater ductility (?) of zirconia. When the indentation and the damage zone are removed, most of the precrack is also removed. Specimens then will fracture from natural flaws.

EMPA has devised a new method using the Palmqvist cracks that form from Vickers indentations. These are also shallow, but if the indenter is given a cant, then the crack on one side of the indentation will be deeper than the one on the other side. After the damage zone is removed, the remaining crack is an offset ellipse.

For the Y-TZP of this round robin, use both a 3° cant, and the standard ½° tilt. The cracks will be observable in optical microscopes or the SEM.

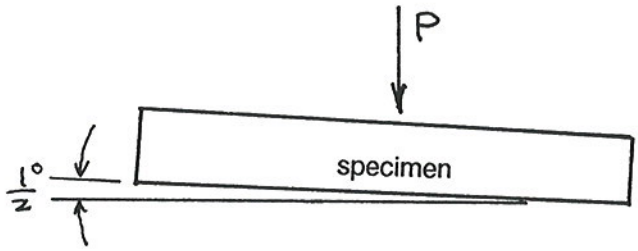

TILT ½°

and

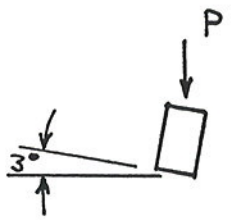

CANT 3°

Side View

End View

As shown below, it is necessary to indent the specimen about 0.3 - 0.4 off the middle. This will help to center the larger Palmqvist crack.

Normal Vickers Indentation

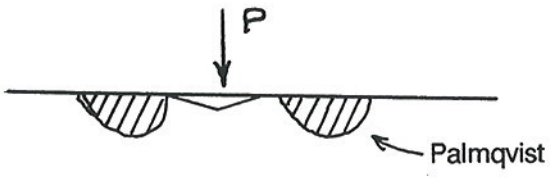

"Canted" Vickers indentation

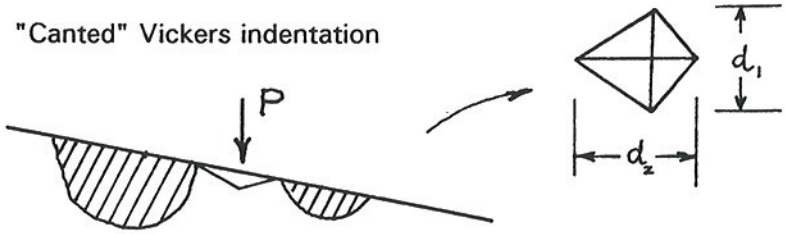

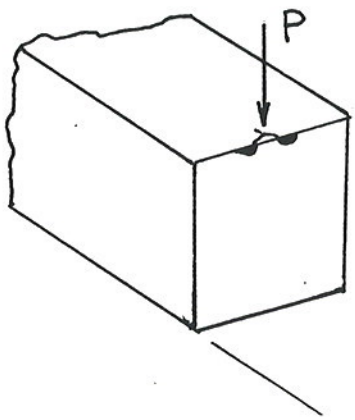

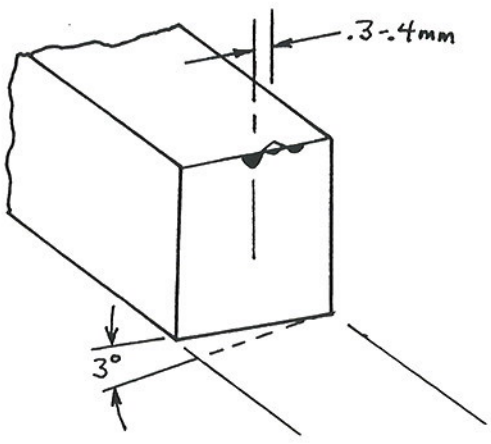

REPORT

1. Return the report sheet for each material. For the zirconia and the hipped silicon nitride, be sure to add the correct specimen identity. For the hot pressed silicon nitride, any number system is satisfactory (e.g. 1-5).
   Alternately: Fill out the floppy disk files. Make one file for each material. Make a printed copy of each file. Return the floppy disk.

2. Send at least two photos for each material with the precrack marked by dotted or dashed lines that do not cover the boundary completely. One photo will show a well defined precrack, the other, a poorly defined precrack.

3. Fill out and return the Survey sheet.

4. Return the specimens if you choose not to test the hipped silicon nitride or the hipped zirconia.

Return before March 10, 1993 to either:

Mr. George Quinn
Ceramics Division
NIST
Bldg. 223 A329
Gaithersburg, MD 20878
USA

Tel: (+001) 301 975-5865
FAX: (+001) 301 990-8729

Mr. Jakob Kübler
Metals and Ceramics Division
EMPA
Überlandstrasse 129
Dübendorf CH-8600
Switzerland

Tel: (+41) 1-823-5511
FAX: (+41) 1-821-6244

Controlled Surface Flaw (CSF) Round Robin Results

Testing Laboratory:

Material:

I. Indentation
Indent load P (kg):
Indent time (sec):

Machine:
Comments:

II. Material Removal (in millimeters)
Time between indentation and polishing (approximate):
Procedure used:

Knoop information
Avg. indent length (L):
Avg. indent depth (L/30):
Amount removed (4-4.3 x depth):

Vickers information
Avg. indent length (d):
Avg. indent depth (d/7):
Amount removed (2.5 x depth):

III. Flexure Test Procedure
Time between polish and fracture (approximate):
Average time to failure (approximate):
Temperature:
R. Humidity:

Crosshead Rate (mm/min):
Inner and outer spans (mm):
Moment span ℓ (mm):

IV. Crack Measurement
Procedure:

V. Results

Specimen Identity	Base (mm)	Height (mm)	Load F (N)	Stress (MPa)	Indent Break?	How Measured?	a (mm)	2c (mm)	Ysurf	Ydep	KIc MPa*m1/2	Comments

SURVEY SHEET

Laboratory and Investigator: _____

1. How long did this project require? What was the most time consuming step?

2. Who did the actual work (you, student, engineer, or technician)?
   Precracking:_____
   Polishing:_____
   Flexure Testing: _____
   Fractography: _____
   Analysis, Interpretation, Review
   _____

3. Which way of orienting the specimen (3 x 4 mm, or 4 x 3 mm cross section) did you prefer? (The orientation with the indentation in the 4 mm face allows easier 4 point flexure test articulation, but there is more material to remove by polishing.)

4. Can you suggest some improvements to the technique?

5. Have you used this method in the past?

6. Will you use this method in the future?

Thank you for your assistance! We do not think we have all the answers on this method. We are eager to learn and benefit from your experiences. Any help or suggestions would be greatly appreciated!

VAMAS
TECHNICAL WORKING AREA #3
CONTROLLED SURFACE FLAW (CSF) FRACTURE TOUGHNESS
ROUND ROBIN

MATERIALS:

Part 1. Hot Pressed Silicon Nitride, Grade NC-132

Black. Specimen size: 3 x 4 x 47.6 mm.

The chamfers are not within specifications. Some are too large. This will cause a reduction of the "moment of inertia" of the cross section, and thus the formula for stress (which assumes a rectangle shape) will be in error by a few percent. Since the chamfers are not uniform, no attempt will be made to correct the stress.

Source: Norton Company, Grade NC-132

Fabricated by uniaxial hot pressing in 1974 to a shape of 155 x 155 x 25 mm. All specimens in this round robin were cut from a single plate of material. All 240 specimens for this round robin were cut with the same orientation, with the 3 x 50 mm faces parallel to the billet top and bottom flat surfaces.

This material is pressed with a sintering aid of about 1 weight percent MgO which combines with residual SiO_2 on the starting powder surfaces. The material is fully dense and has a uniform, fine β silicon nitride grain structure. Additional details are in the company product sheets enclosed. This material was used for many years in many mechanical property studies due to its good properties and uniformity.

Part 2. Hot Isostatic Pressed Silicon Nitride

Dark Grey. Specimen size: 3 x 4 x 45 mm.

Source: ESK, Kempten, Germany

Fabricated in the form of four 50 mm diameter cylinders, 100 mm long. Cold isopressed, then hot-isostatic pressed. All specimens cut with the same orientation, along the axis of the cylinders. Note: Records have been made of the billet and location of every specimen prepared. Therefore participants should note the specimen identity in the report.

ESK product literature and figures from a presentation: "Weibull Characterization of Four HIPPED/ Post HIPPED Engineering Ceramics Between Room Temperature and 1500°C," by J. Kübler, presented at the American Ceramic Society Annual Meeting, Minneapolis, MN, April 1992, are included with these notes. The characteristic strength of the specimens was 859 Mpa with a Weibull modulus of 14. Computed tomography profiles show that the material is very uniform.

Part 3. Hot Isostatic Pressed Zirconia, Y-PSZ

White. Specimen size: 3 x 4 x 45 mm.

Source: EMPA, Switzerland.

Fabricated in the form of a single 50 mm diameter cylinder, 200 mm long. Yttria stabilized. Cold isopressed, then sintered, then post-Hipped. All specimens were cut with the same orientation along the axis of the cylinder. Note: Records have been made of the billet and location of every specimen prepared. Participants should note the specimen identity in the report.

This is a yttria stabilized zirconia using TOSOH powder.

Additional details on this material are in the same paper as listed in #2 above. Copies of some slides are included with these instructions.

Appendix 2

FRACTOGRAPHIC PROCEDURES USED BY THE PARTICIPANTS

In the following table, the following are listed in order for each lab:

a. The procedure used to make the actual precrack measurements.
b. Calibration procedure.
c. The fractographer. If more than one, the primary observer is listed first.
d. Additional comments and observations.
e. Improvements or recommendations.

* An evaluation of the laboratory's analysis, made by the organizers of the round robin is then listed in *italics*.

Representative photos are enclosed for some of the labs. The markings on these photos were made only by the individual labs. Many labs sent contact prints, thermal prints, or photocopier prints which, although they showed the precracks reasonably well, will not duplicate well. They are not included in this appendix.

LAB **PROCEDURE**

Lab 1

a. NC-132 and hipped silicon nitride specimens measured by low power (~200X) optical microscope.
No photos were furnished, contrary to instructions.
b. Unknown.
c. Fractography by a student and experienced materials scientist.
d. There was no success in finding the precracks on the SEM, either with the monitor or on photos. Only a few very low power (25-50X) optical photos were taken.
e. No comment.

* *This laboratory furnished incomplete fractographic information.*

Lab 2

a. NC-132 specimens measured on SEM photos at 156X magnification. Hipped silicon nitride measured on SEM photos at 213X.

b. Calibrated lattice, SEM settings identical to specimen photo conditions.

c. Fractography by a principal scientist, with alternate readings from engineer, scientist and technician.

d. Extensive additional measurements were taken on several optical microscopes, including stereo and optical measuring models, at different magnifications, and with different viewers. These indicate there is considerable variability in interpretation and sizes measured by the different inspections.
Lab 2 reports that the hipped silicon nitride and zirconia materials were <u>easier</u> to interpret than the NC-132, unlike most other labs!
Measurements on SEM <u>display</u> were felt to be unreliable, and while reported, they are not used in the analysis.

e. Tilting in the SEM is preferred.

* *This laboratory did a lot of work in trying different methods of viewing the precracks.*
Some zirconia precracks were actually kidney shaped and may have been misinterpreted at first.
Higher magnifications (about 2X more) would enable more accurate readings of the sizes, and possibly a closer view of the precrack boundaries.

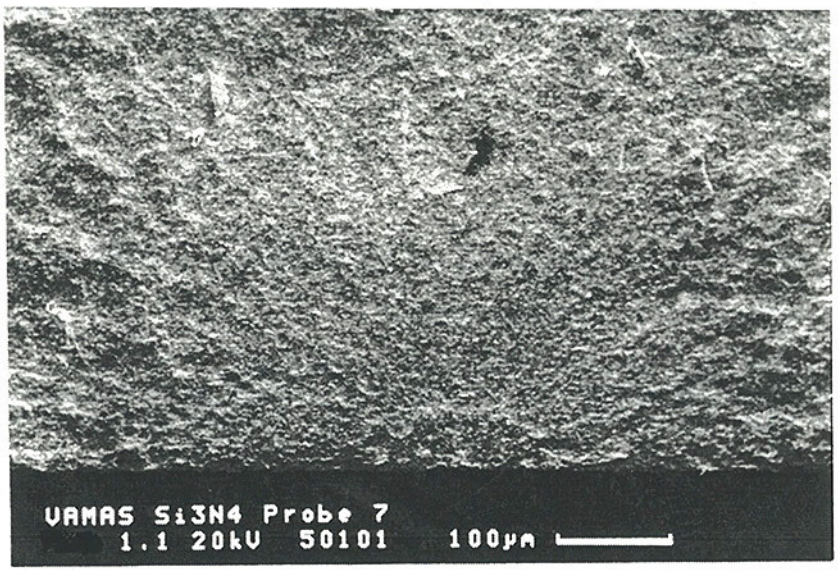

SEM micrograph of NC-132 silicon nitride at 150x.

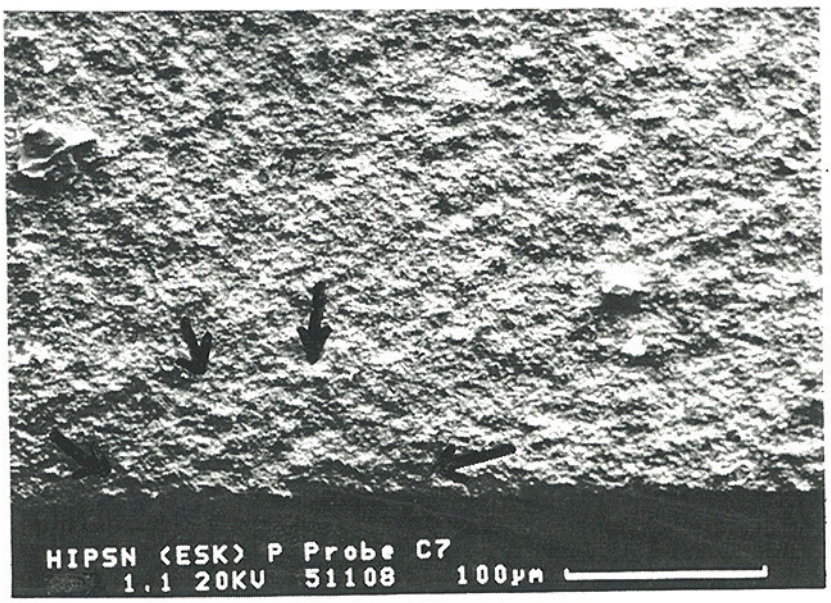

SEM micrograph of hipped silicon nitride at 200x.

Lab 2 continued

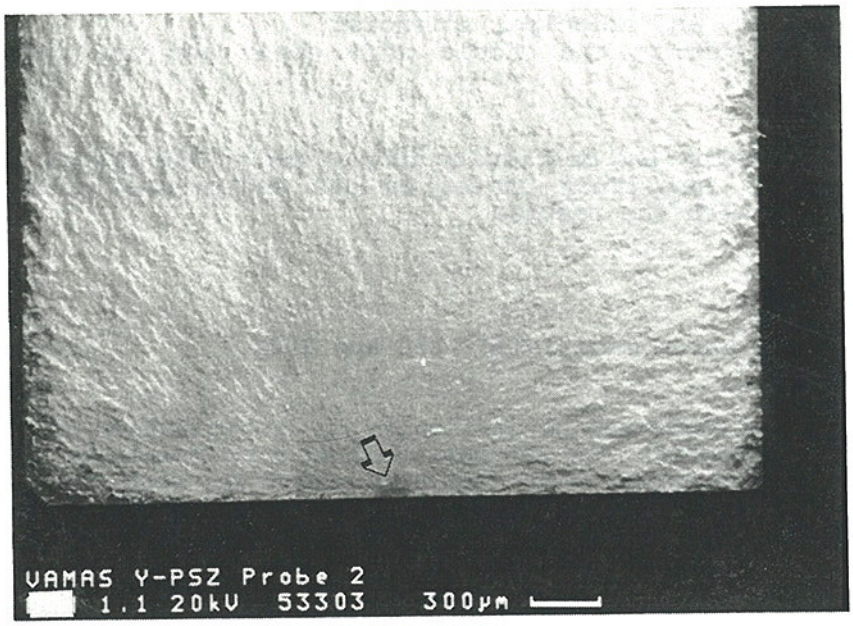

SEM micrograph of zirconia at 30x.

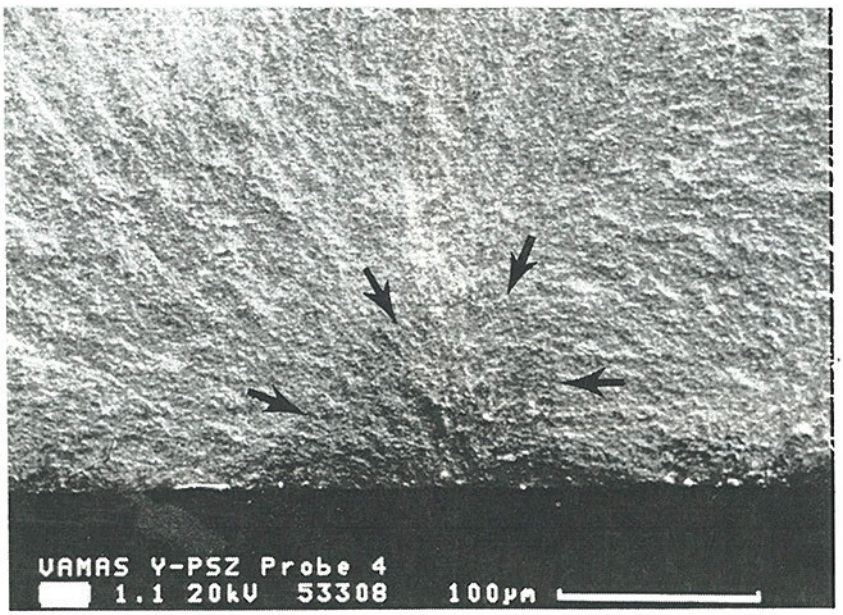

SEM micrograph of zirconia at 200x.

Lab 3

a. An optical microscope was used to measure the precracks at unspecified magnification. Only a few low power photos were taken of the hipped silicon nitride. Magnification not reported.
b. Unknown.
c. Student, engineer, and principal scientist.
d. This laboratory was in the middle of a move, and the photo equipment was unavailable.
e. None.

* *This laboratory had difficulty in performing the fractography. Only a few low power, indistinct photos of the hot-pressed silicon nitride were furnished with the results.*

Lab 4

a. SEM used for all three materials. 250 and 500X.
b. Not reported.
c. Not reported.
d. This lab reported there was no difficulty in determination of crack size for the NC-132 and the zirconia. The had considerable problems in determining the hipped silicon nitride precracks. Only one measurement was reported. Precracks in four other specimens were not detectable, although they did fracture from the surface crack. Four zirconia specimens fractured from material defects.
e. None.

* *Good photos were furnished showing the precracks reasonably well, but the precracks were not marked.*

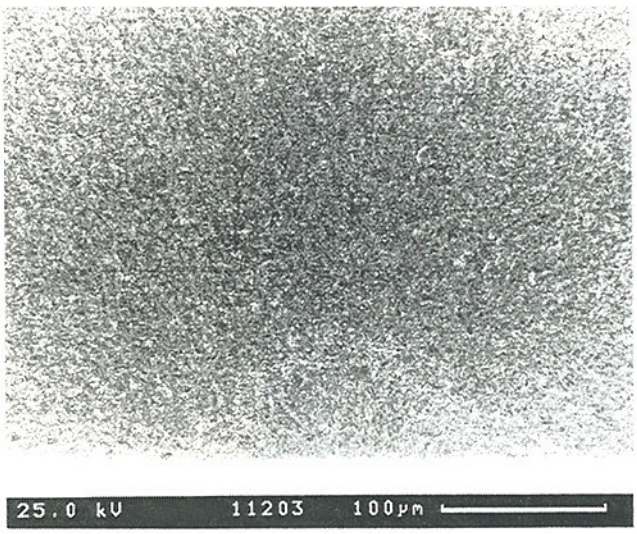

SEM micrograph of NC-132 silicon nitride at 200x.

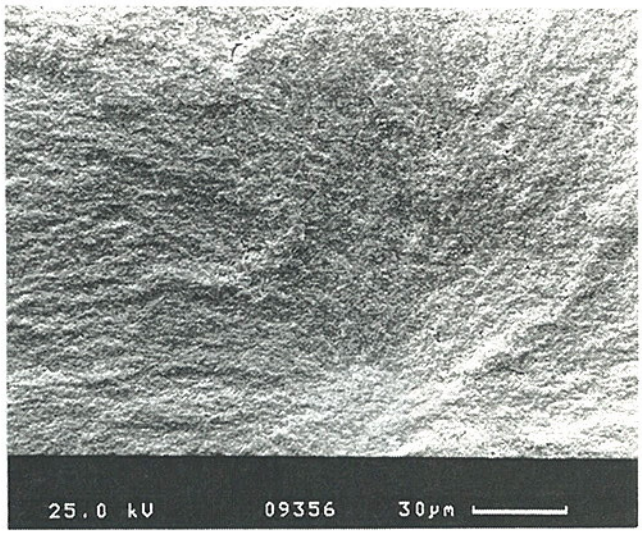

SEM micrograph of zirconia at 400x.

Lab 5

a. SEM photos measurement at 400X were used for the NC-132 and the hipped silicon nitride. SEM at 200X was used for the zirconia.
b. Not reported.
c. Materials scientist.
d. This lab reported that the precrack measurements are subjective. They are very dependent on the skillfulness of the investigator who has to identify the crack size.
e. None.

* *The NC-132 and hipped silicon nitride precracks were well-marked on the furnished photos. Hackle lines were marked on the zirconia specimens and not the precracks.*

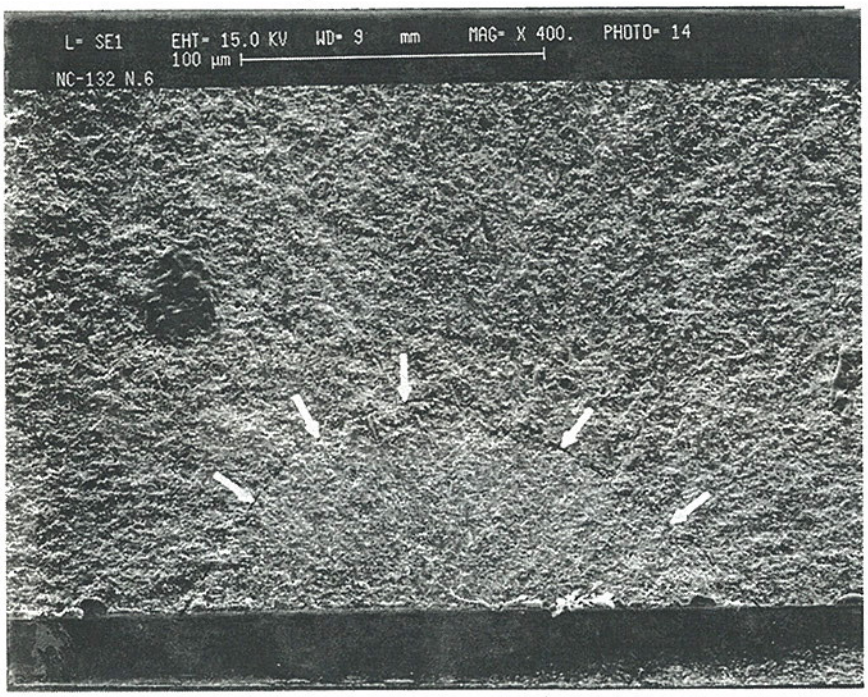

SEM micrograph of NC-132 silicon nitride at 400x.

Lab 5 continued

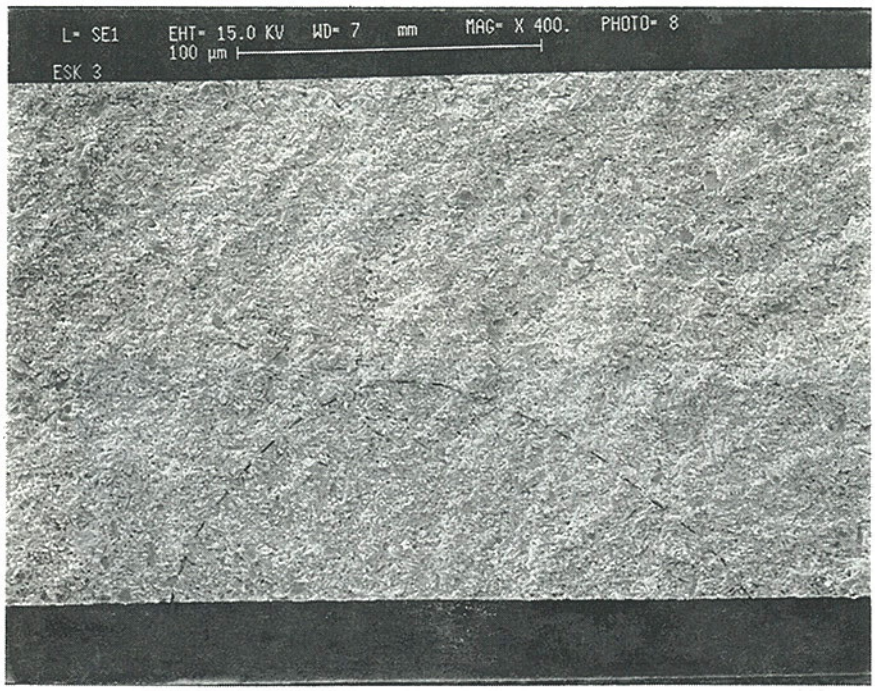

SEM micrograph of hipped silicon nitride at 400x.

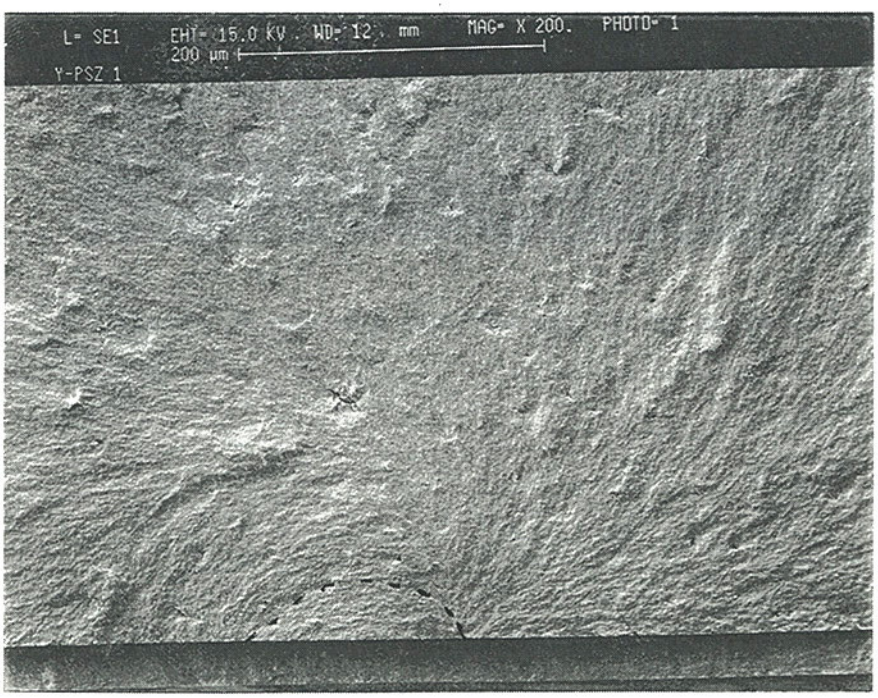

SEM micrograph of zirconia at 200x. Participant erroneously marked hackle.

Lab 8

a. SEM photos at 500X was used for the NC-132 and hipped silicon nitride, and at 350X for the zirconia.
b. Calibration was by an optical stage micrometer.
c. Chemist and technician.
d. Optical microscopy did not give good results.
e. None.

* *Copies of NC-132 photos were furnished and were well-marked. The hipped silicon nitride photos (also copies) were less clear. The magnifications were good for both the hipped silicon nitride and NC-132. The zirconia photo copies had hackle lines marked as the precracks, and not the precracks themselves.*

Lab 9

a. Measurements for all three materials were by optical microscopy photographs at 200 and 400X. All specimens gold coated.
b. Not reported.
c. Not reported.
d. Precrack detection was not difficult for the NC-132, very difficult for the hipped silicon nitride material. An experienced SEM operator could not find the precracks. Two low power (120-150X) SEM photos furnished.
e. None.

* *The NC-132 precrack were quite distinct and well marked on the furnished optical photos. The hipped silicon nitride precracks were much less clear. The zirconia photos suggested that hackle lines had been marked rather than the precracks.*

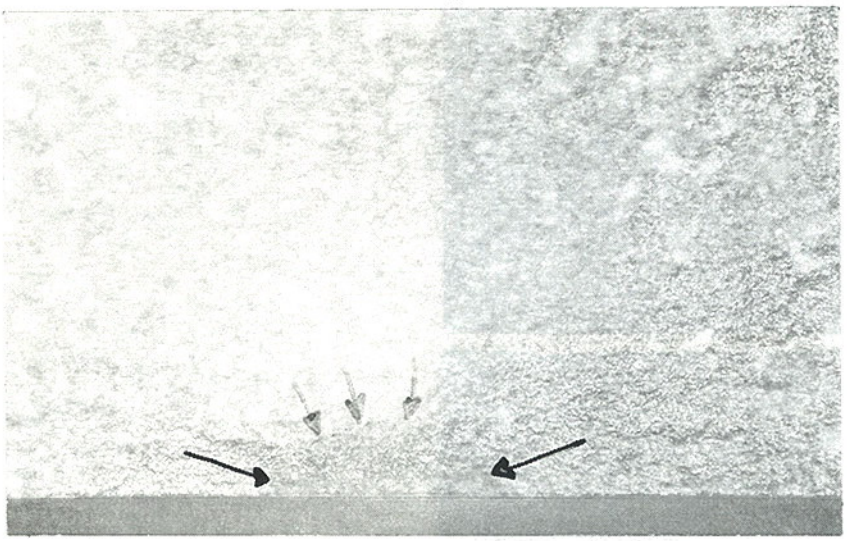

Optical micrograph of NC-132 silicon nitride at 200x.

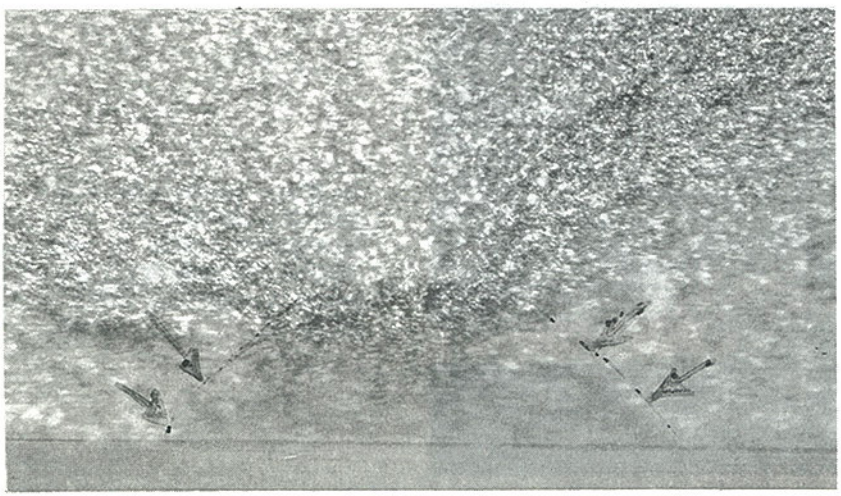

Optical micrograph of NC-132 silicon nitride at 400x. Same sample as above.

Lab 10

a. SEM was used for all three materials. Tilting was helpful. 500X photos with a specimen tilt of 16 degress were sufficient for the NC-132. The hipped silicon nitride specimens were more difficult, and low (50 - 100X) magnification photos matched with higher (400 - 500 X) magnification photos with 16-41 degree tilts were used. Zirconia precracks were photographed from 400 - 600 X.

b. Not reported.

c. Principal engineer.

d. None.

e. None.

* *Photos of every specimen were returned, but only during the final review of this report. Good pairs of low and high magnifiaction photos were helpful. The hipped silicon nitride precracks were very vague, whereas the NC-132 and Y-TZP cracks were well-defined.*

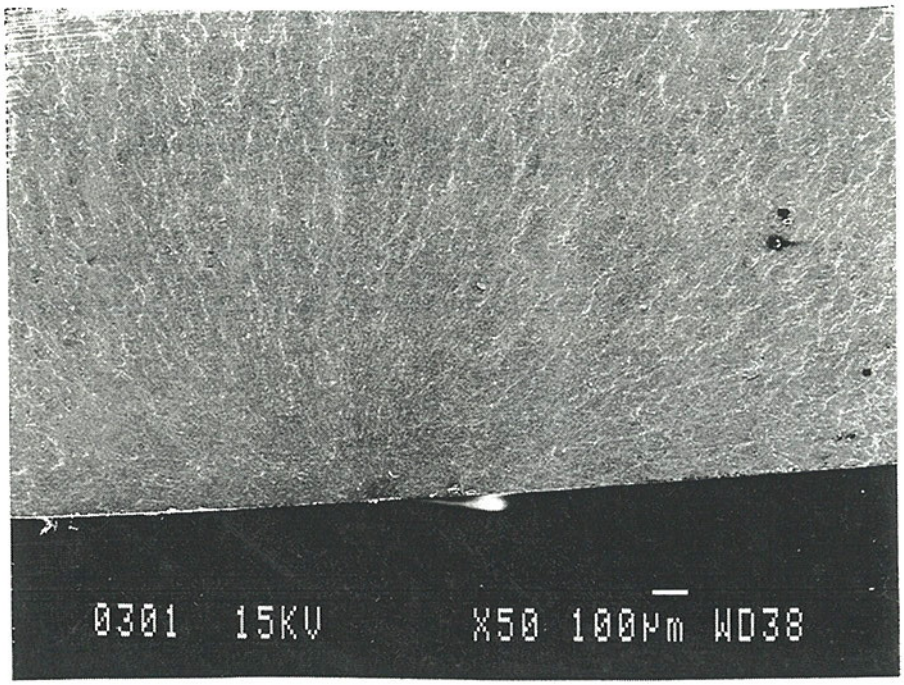

SEM photo of a Y-TZP precrack at 50X. The precrack is the small dark zone in the middle of the bottom edge.

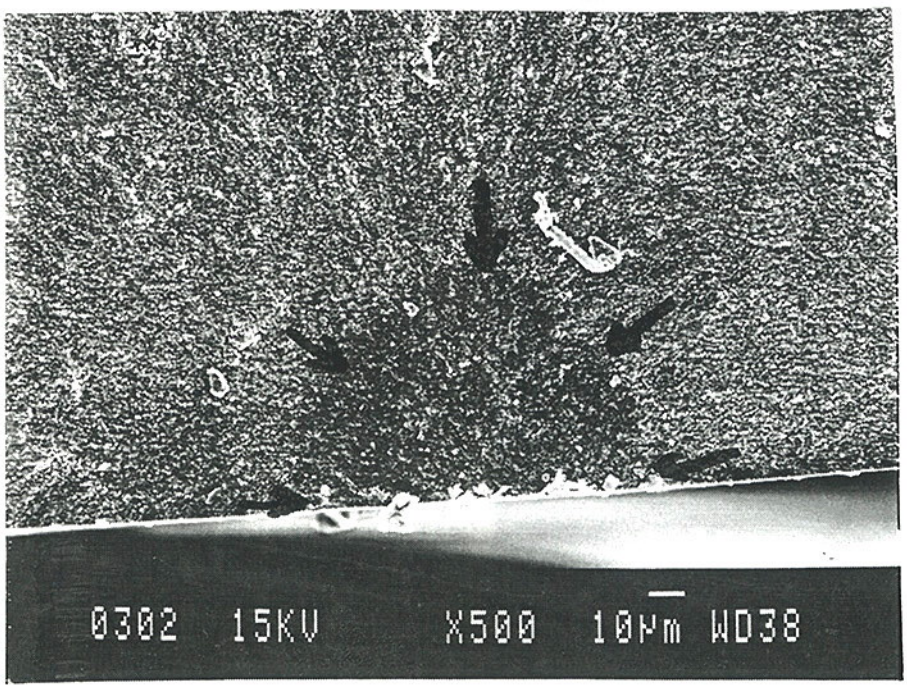

Higher maginifaction photo (500X) of the same specimen. The arrows were transcribed from a transparent overlay sent by lab 10.

Lab 11

a. SEM photos were used for both silicon nitrides at 100 and 200X.
b. Not reported.
c. Doctoral student and Principal scientist.
d. Specimens were first examined by a stereo optical microscope, and the best fracture half used for SEM inspection. The CSF method has been used by this lab previously. Backscattering mode is sometimes very helpful in detecting surface topography.
e. Precautions should be taken during testing so that the fractured specimens do not impact into the test machine. Several fracture surfaces were damaged.

* *Low magnification (contact print) photos were sent and they show as well the precracks very well.*

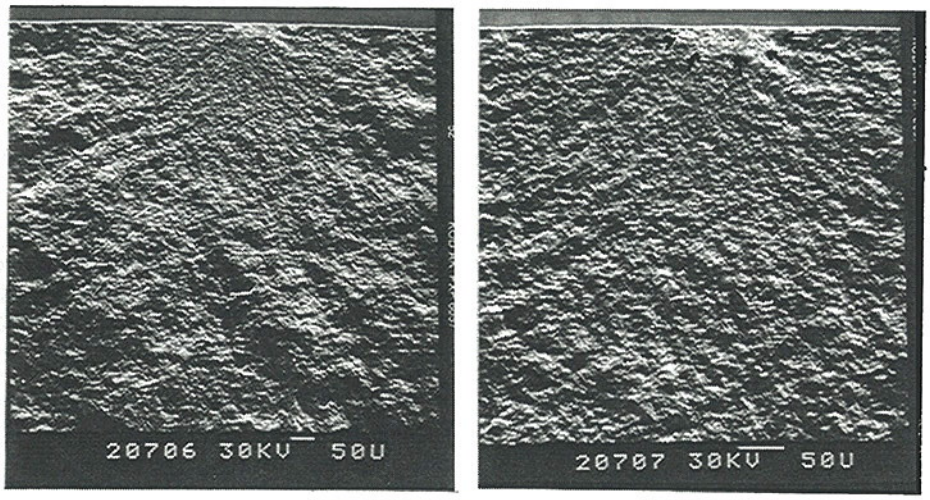

SEM micrographs of hipped silicon nitride. At left, 60x, at right, 120x.

Lab 12

a. SEM examination with an image storage system was used. Thermal prints were produced from the stored images. Print magnifications were 154 and 385X.
b. A grid with 100 lines per one inch was used on the SEM, at a magnification intermediate between the two listed above.
c. Principal scientist (expert fractographer) and technician.
d. None.
e. Stereo pair SEM photos could be a valuable aid.

* *SEM photos were good and well-marked for both silicon nitrides. Five NC-132 and nine hipped silicon nitride specimens were measured, indicating no serious problems. Three hipped silicon nitride specimens labelled as difficult.*

Lab 13

a. SEM photos at 465 or 500X for the NC-132.
SEM photos at 260 or 350X for the hipped silicon nitride material.
b. Optical stage micrometer, photographed on the SEM at the same magnifications as used for the precrack photos.
c. Principal engineer.
d. For the NC-132, most photos at 500X. In a few instances, lower magnification photos taken to aid in precrack identification. In half the cases, the specimen was tilted up to 20° at 500X to make the precrack appear more clearly, then a second 500X photo was taken with the specimen fracture surface normal to the detector. Sizes were measured from the latter photos. The same tilting procedures was used on all ten hipped silicon nitride specimens with excellent results. This lab reported that delineation of the precrack from the fracture mirror and other microstructural features was difficult. Thermal prints of digitized images were furnished. Multiple magnifications were used for the photography.
e. Two matching photos, one perpendicular and one tilted 10-20 degrees relative to the detector, are an excellent method to make precrack detection easier.

* *The NC-132 precracks were very well-defined and marked very well. The hipped silicon nitride precracks were less clear, but the thermal print photos furnished were excellent, and were well-marked. Pictures would have been better if by Polaroid photography with larger print size. Photos of every specimen were returned to the organizers. This lab did an excellent job.*

Lab 15

a. Measurements for the NC-132 were made with SEM photos at 200 and 500X, as well as optical photos at 305X.
Measurements for the hipped silicon nitride material were made with SEM photos at 150 and 300X.
Measurements for the zirconia were made with SEM photos at 624X, as well as optical photos at 536X.
b. SEM calibration was made by a high precision SEM calibration standard.
Optical calibration was by a conventional stage micrometer.
c. Engineer and Principal scientist (expert fractographer).
d. All specimens, both fracture halves were first examined by a stereo optical microscope up to 128X. A conventional lab metallographic microscope was used for all optical measurements. SEM was used for nearly all specimens, usually on the best half. Optical and SEM precrack sizes were very self-consistent for some specimens. Overall, the optical and SEM average fracture toughness values were in excellent agreement. Stereo SEM microscopy, tilting, and photos at various magnifications often helped.
e. Tilting specimens in the SEM can help. Stereo SEM microscopy helps reveal much more detail as well as the topography of the precrack.

* *This lab was experienced with the surface crack method and was familiar with the materials.*

Lab 17

a. Measurements on all three materials were made on an optical microscope with a precision (1 micron) traversing stage. Magnifications were up to 450X.
b. Calibration checked with stage micrometer.
c. Principal engineer.
d. Low-angle incident light was very helpful. No success with one particular SEM machine. A sputtered gold coating was helpful on the zirconia.
e. For optical work, it is better to use very low angle incident illumination.

* *This lab was experienced with the testing method and was familiar with the materials.*

Lab 18

a. NC-132 was measured with the SEM at 300 and 600X for two specimens. Optical photos at 200X were used for measurements also.
b. Not reported.
c. Principal engineer.
d. SEM and optical photos were made of the same specimen in three instances. Precrack measurements varied somewhat between the two methods. Optical magnifications higher than 200X not successful due to small depth of field. No success in measuring precracks for the hipped silicon nitride material, either with optical or SEM microscope. Some precrack features were found, but in no case could a precrack be seen with certainty. Two zirconia specimens attempted without success.
e. Dye penetrant may be helpful.

* *One optical and one SEM photo were furnished for the NC-132 which were quite clear and well marked. Optical photos were unclear. Five hipped silicon nitride optical photos at 200X were not clear.*

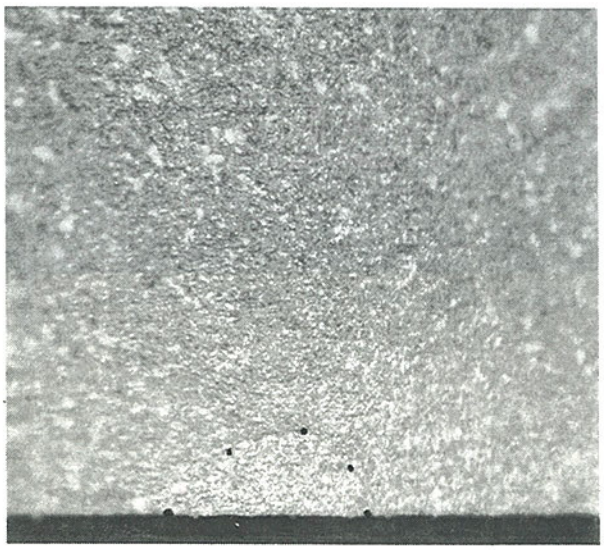

Optical micrograph of NC-132 silicon nitride at 200x.

SEM micrograph of NC-132 silicon nitride at 450x.

Lab 19

a. NC-132 measured by SEM photos at 200-350X. Optical photos at 100 and 400X also used.
b. Stage micrometer for the SEM measurements.
c. Engineer and student.
d. Optical and SEM photos of every NC-132 HPSN specimen were furnished. Optical and SEM precrack sizes were in excellent agreement. Measurements were made at several different magnifications for comparison, and these measurements were also very consistent. 9 of 10 NC-132 specimens analyzed. No success on hipped silicon nitride specimens. either with SEM or optical microscope.
e. Dye penetration would be possibly useful for white ceramics.

* *The precracks were visible on most SEM photos which were mostly at 200X. Better accuracy might have been obtained at 300 or higher magnification. Optical photos at 100X showed the precracks clearly, but were rather small to measure. Higher magnification (400X) photos showed the precracks, but were more difficult to interpret.*

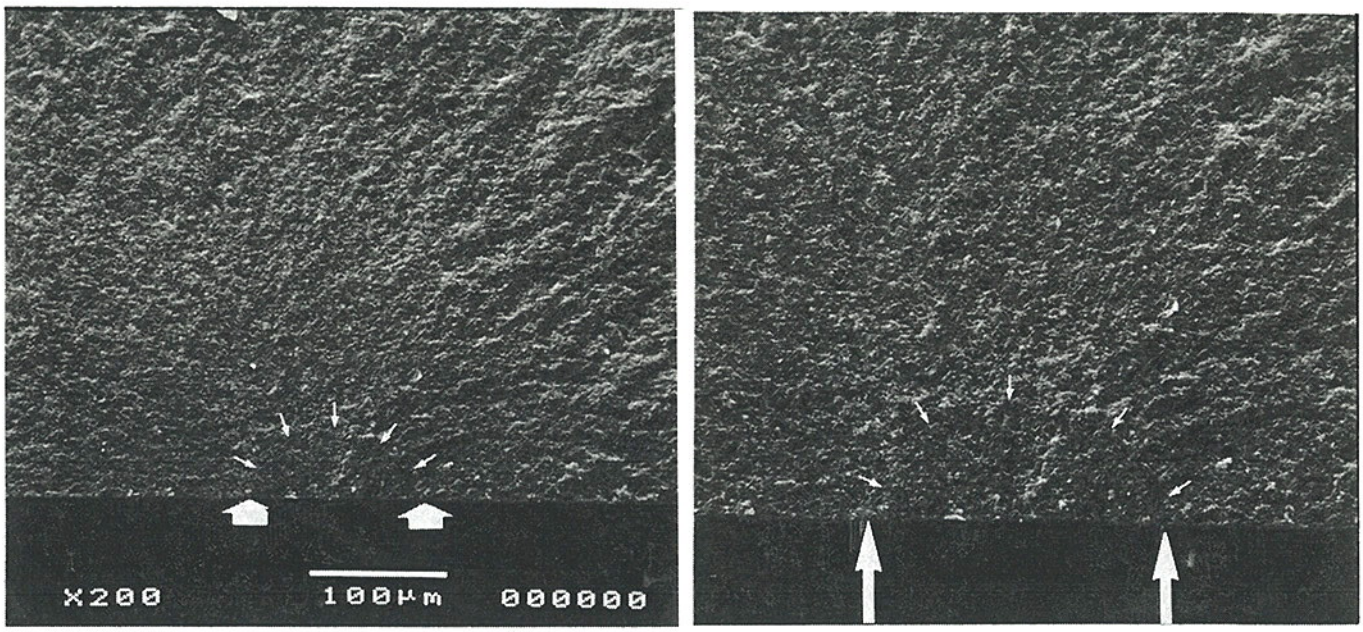

SEM micrographs of NC-132 silicon nitride. At left, 200x and at right, 350x.

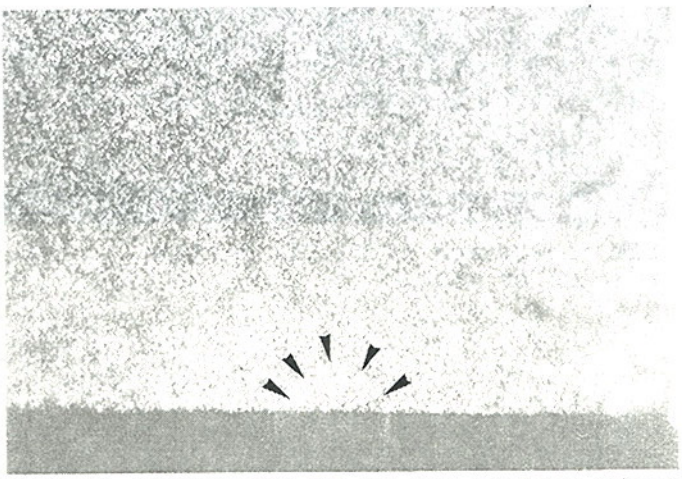

Optical micrograph of NC-132 silicon nitride at 100x.

Lab 20

a. NC-132 was measured from optical (324X) and SEM photos at 250 and 500X. hipped silicon nitride and zirconia precracks were measured on SEM photographs at 250 and 500X.

b. Yes, but method used not reported.

c. Assistant.

d. Generally, two SEM photos were taken: one at 250X to locate the precrack, and one at 500X for an accurate measurement. NC-132 was relatively easy, whereas the hipped silicon nitride silicon nitride and zirconia were difficult. Sputtering the gold-paladium coating onto the specimens at a high angle helps create shadows on the fracture surface.

e. Dye penetration would be helpful.

* *Superb optical and SEM photos were furnished. Precracks were clear and well-marked for the NC-132. The photos for the hipped silicon nitride were also excellent, but the precracks are more difficult to precisely mark. These photos and the interpretation are among the best in the round robin. The shadow gold coating trick is very helpful!*

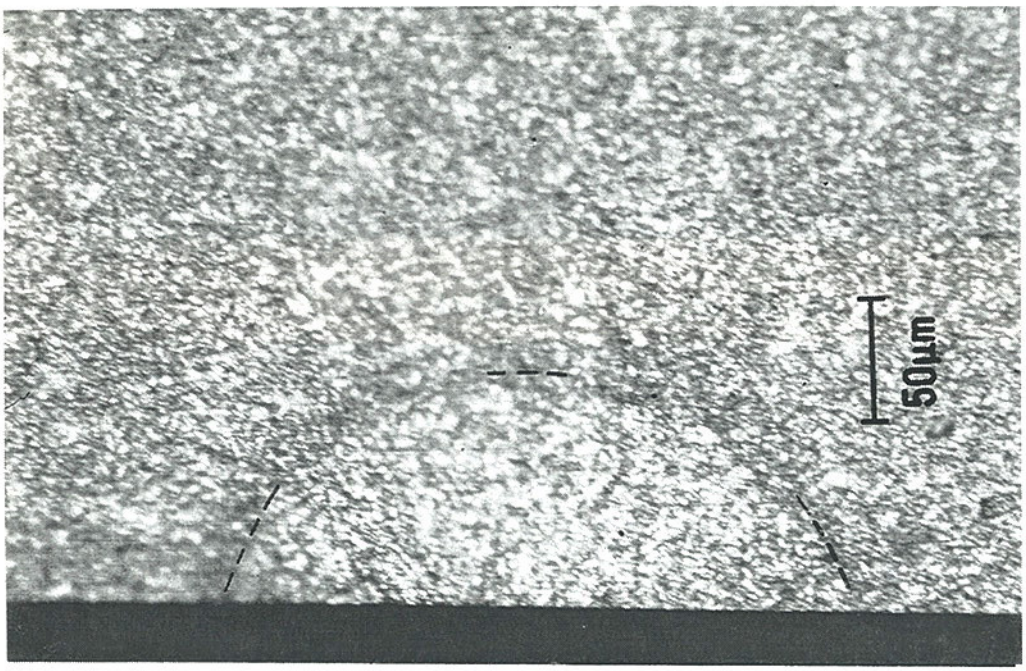

Optical micrograph of NC-132 silicon nitride at 320x.

Lab 20 continued

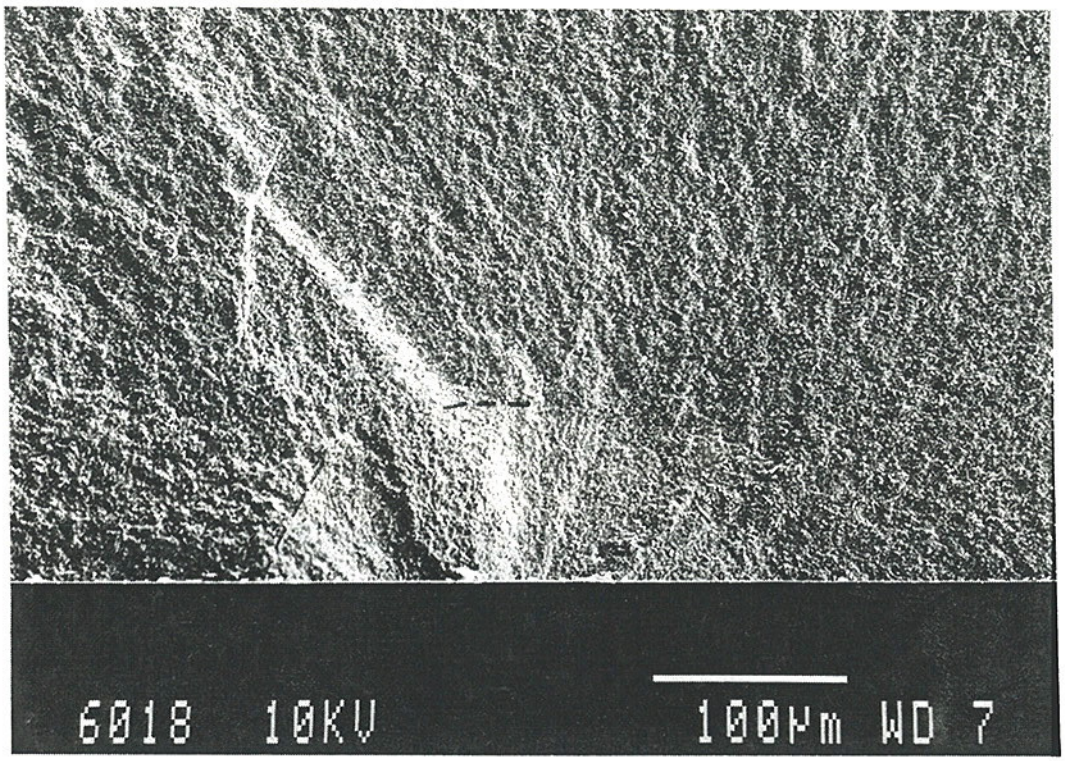

SEM micrograph of NC-132 silicon nitride at 250x.

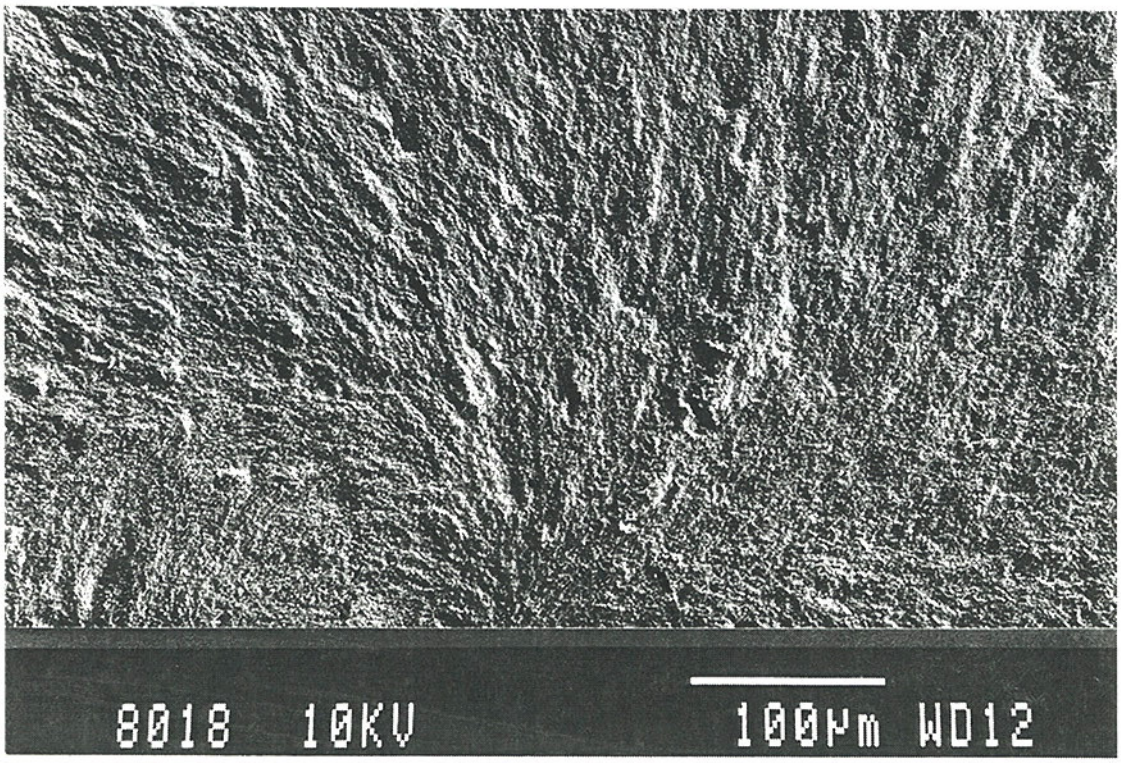

SEM micrograph of zirconia at 250x.

Lab 21

a. NC-132 was measured by SEM photos at 400X. Optical photo measurements were also taken at 64X.
Hipped silicon nitride precracks were measured from SEM photos at 250 and 500X; and from optical photos at 64, 100, and 250X.

b. Stage micrometer was used for the optical photos. SEM calibration procedure not reported.

c. Technician and principal engineer.

d. Very difficult to unequivocally mark the precrack. Reasonable consistency in the precrack sizes between optical and SEM measurements was reported.

e. Dye penetrants, possibly under fluorescent light.

* *Color photocopy prints of every specimen were furnished, but these are not as clear as Polaroid photos. SEM photos were not optimal. Very low contrast in the SEM photos inhibited the detection of the precracks. Hackle lines, and not the precrack were marked in at least two of five specimens. The NC-132 optical photos at 64X were at too low a magnification to allow the precracks to be clearly seen. Data was reanalyzed and two specimens corrected and two discarded.*

The hipped silicon nitride SEM photos were reasonably clear and the precracks marked satisfactorily. The hipped silicon nitride optical photos at 100X and 250X were from a different microscope than used (for the NC-132) with better clarity and depth of field. Machining damage at the surface interfered with the interpretation of two photos.

It was subsequently reported by lab 21 to the organizers that the use of too thick an anticharging coating caused difficulty in discerning precracks in the Y-TZP. Thin coatings dramatically improved the precrack visibility.

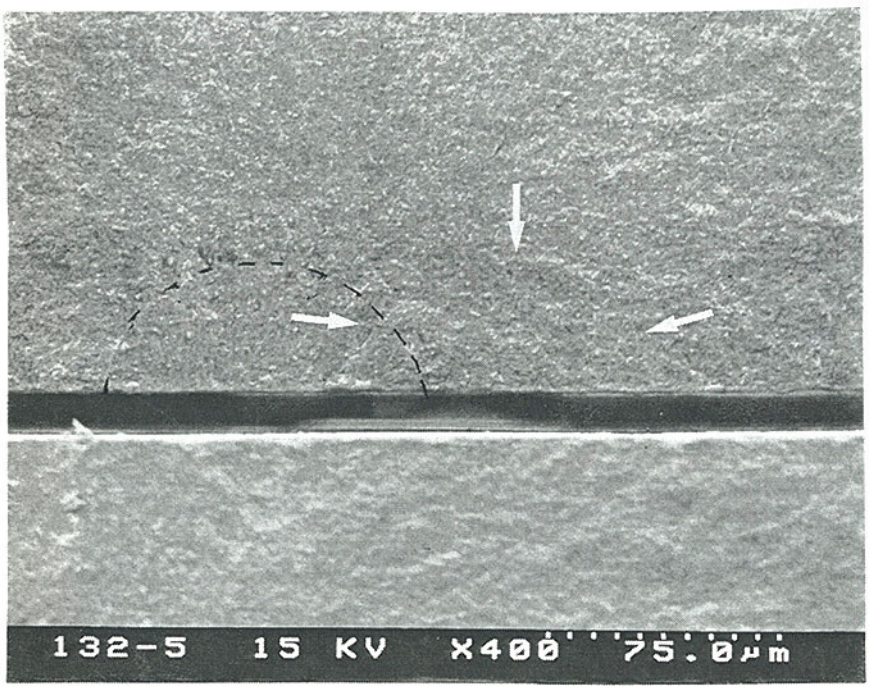

SEM micrograph of NC-132 silicon nitride at 400x.

Lab 21 continued

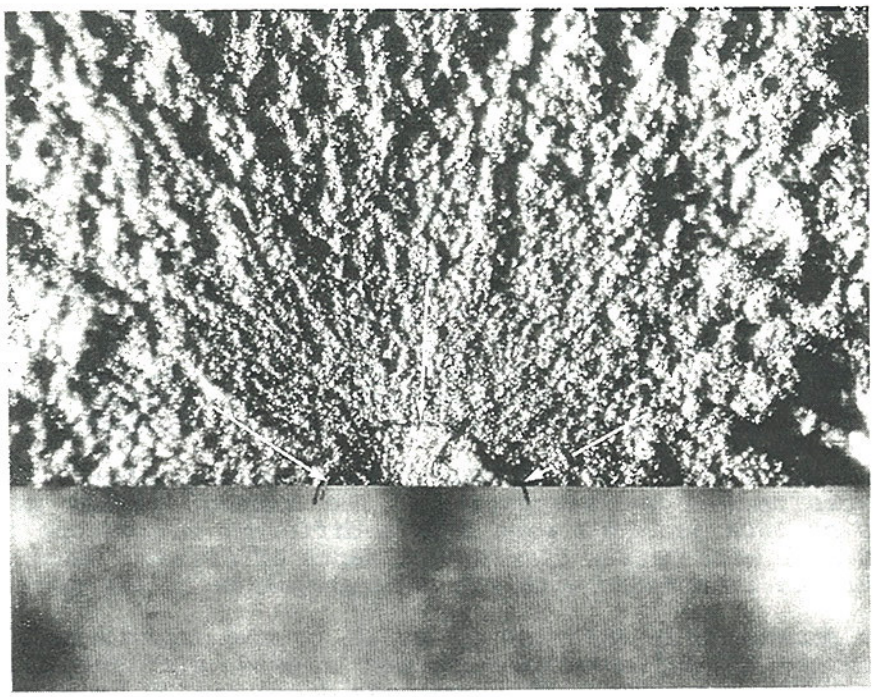

Optical micrograph of hipped silicon nitride at 100x.

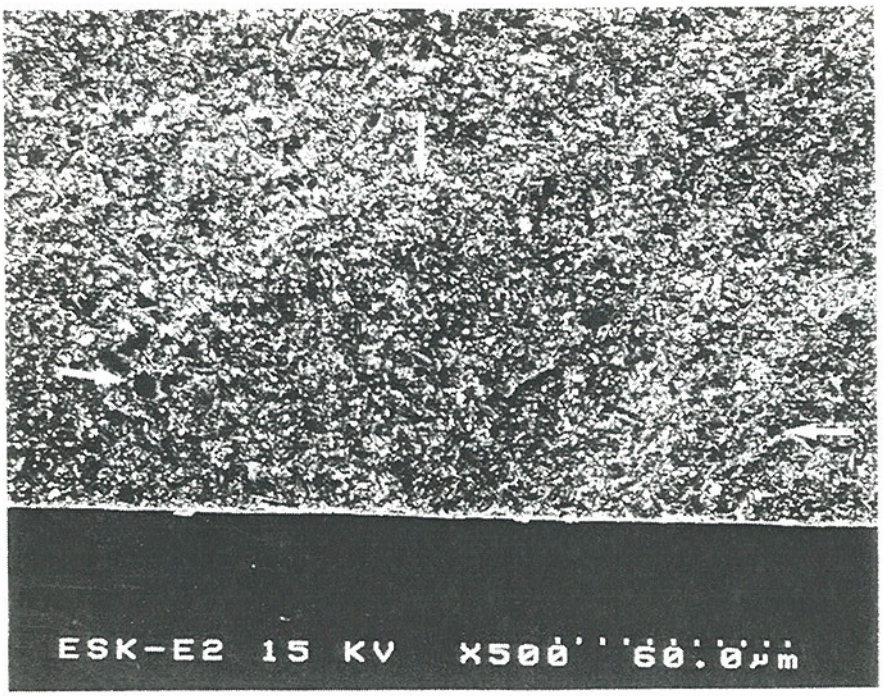

SEM micrograph of hipped silicon nitride at 500x.

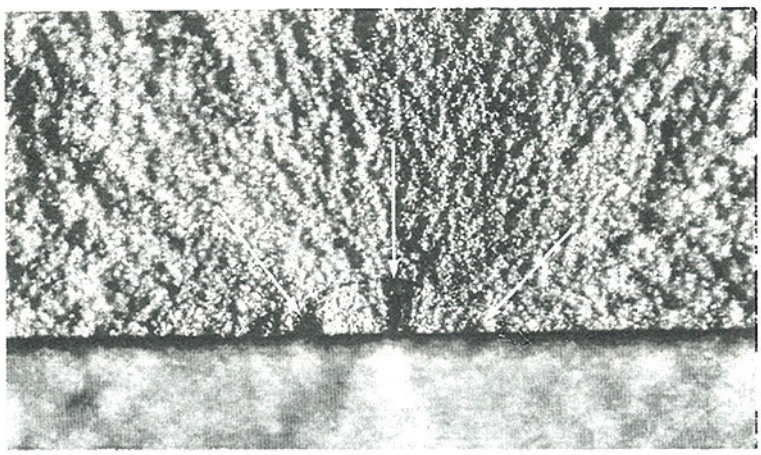

Optical micrograph of hipped silicon nitride at 100x.

Lab 22

a. NC-132 was measured by SEM photos at 400X. Optical measurements were also taken at 200X.
hipped silicon nitride specimens were measured by SEM photos at 500X. Optical measurements at 200X also taken.
zirconia measurements by SEM photos at 500X and optical photos at 200X.

b. Calibrated, but procedure not reported.

c. Principal engineer.

d. Identification of precracks was difficult in the SEM, but easier on optical micrographs. Optical microscopy limits the magnification, due to depth of field, and therefore measurements may not be so accurate. hipped silicon nitride measurements were very difficult. Similar results were obtained for optical and SEM measurements, but optical is preferred since detection was easier.

e. None.

* *This lab was not experienced in the technique and initially marked fracture mirrors as possible precracks. All results were reanalyzed. NC-132 optical and SEM photos were good and well-marked. hipped silicon nitride photos were quite sharp but the precracks did not stand out well. They were not marked on photos. Precracks were not clear on the optical photos and hackle might have been the marked feature.*

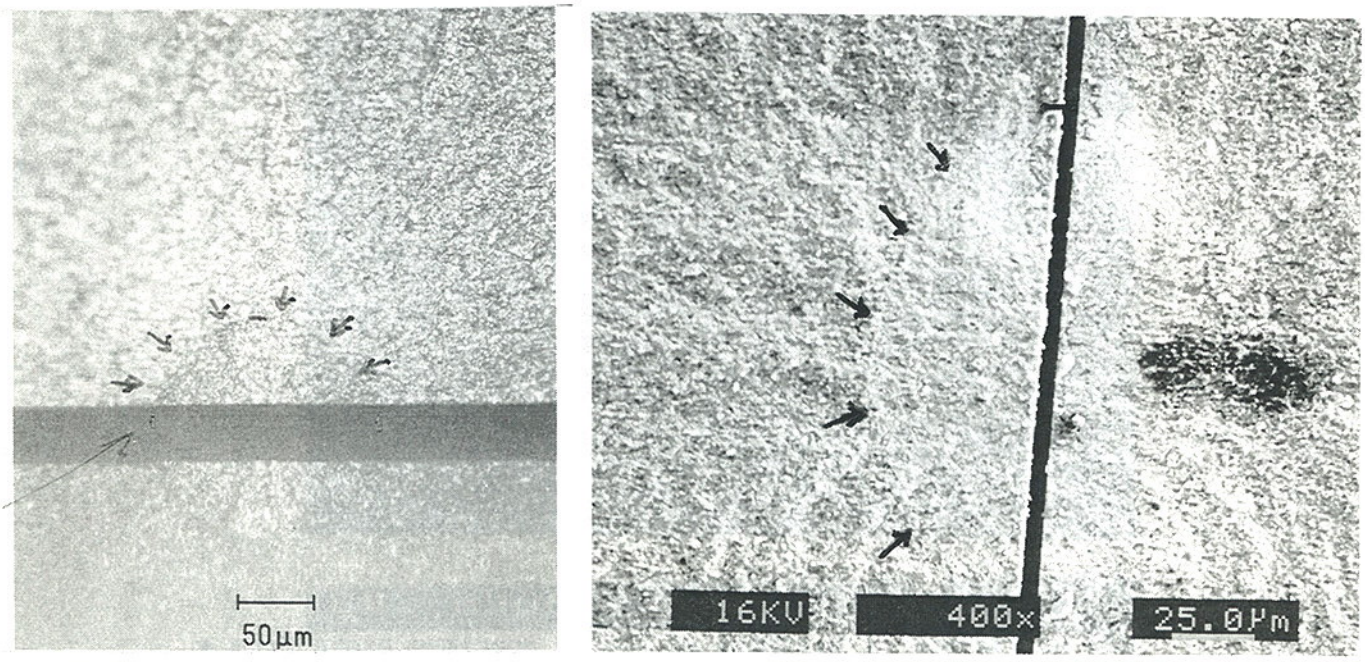

Micrographs of NC-132 silicon nitride. At left, 200x optical, at right, 400x SEM

Lab 23

a. Precracks for NC-132 and zirconia materials measured from 200 and 400X SEM photos. (This laboratory did not receive hipped silicon nitride specimens.)
b. SEM machine reported to have been calibrated in 1993.
c. SEM operator.
d. None.
e. None.

* *Excellent SEM photos furnished for one NC-132 and one zirconia specimen. Most specimens broke from natural flaws due to excess material removal, both for NC-132 and zirconia.*

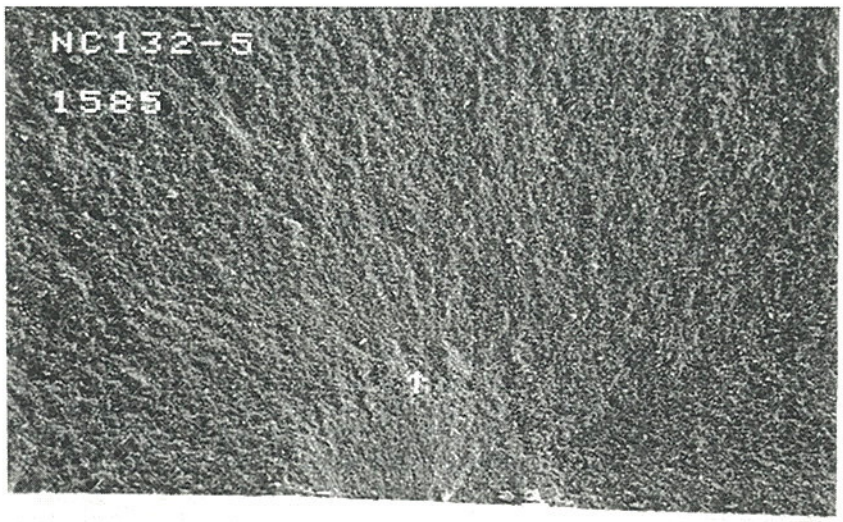

SEM micrograph of NC-132 silicon nitride at 200x.

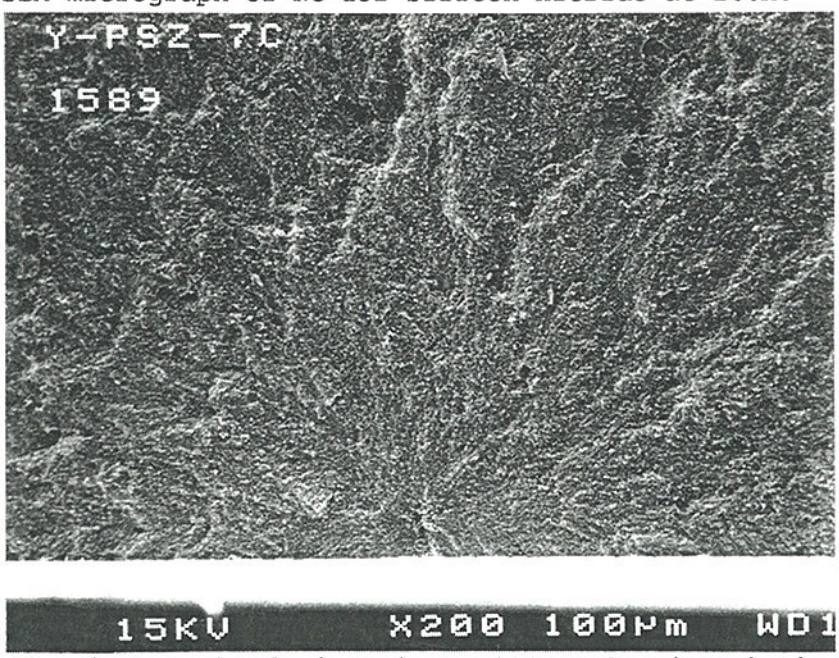

SEM micrograph of zirconia at 200x. Specimen broke from a volume distributed sintering defect near the tensile surface.

Lab 24

a. NC-132 and zirconia measurements by SEM stereo microscopy. 30 - 150X was used for the NC-132, and 30 - 300X for the Y-TZP.
(This laboratory did not receive hipped silicon nitride specimens.)
b. Calibrated, but procedure not reported.
c. Principal scientist.
d. Zirconia precracks were difficult to identify, even with stereo SEM microscopy.
e. No comment.

* *Precracks were found for all ten NC-132 specimens tested. Photos of evry specimen were sent, but only during the final review of this report. This lab had an excellent success rate for the NC-132. Hackle lines and some contamination problems caused most Y-TZP precracks to be misidentified. This lab made a nice report form to be used for each specimen.*

APPENDIX 3

INDIVIDUAL FRACTURE TOUGHNESS OUTCOMES

The following table lists the fracture toughness values from the individual labs that were accepted and used to compute a "grand average" and standard deviation.

Either a whole lab data set was included, or it was excluded for a given material. Data from sets which were correct for some specimens, but incorrect for other specimens, were not used to compute the grand average. The criterion which was used to include or exclude data from this "grand average" was as follows: All data from a lab was used *unless* there was a *serious* mistake in precrack interpretation. This usually occurred when a lab marked hackle lines or the fracture mirror as the precrack. In instances where no photos were sent in with the results, the data was retained (since it could not be demonstrated that the wrong features had been measured.) The summary Table 3 and Figures 13 and 16 show the excluded data, marked with an "x", but the data was not used to compute the average toughness.

In several instances, laboratories did both optical and scanning electron microscopy evaluation of their precracks. The fracture toughness values computed by these two different methods are shown *separately* in the summary figures in the main body of the report. In the following table, however, if a specimen is measured by both scanning electron and optical microscopy, then only *one fracture toughness* value is listed. It is the average of the values computed from scanning electron and optical microscopy.

Figure A3.1 - A3.3 show frequency histograms for all acceptable results. The same horizontal axis is used and the interval size is 0.1 MPa$\cdot\sqrt{m}$.

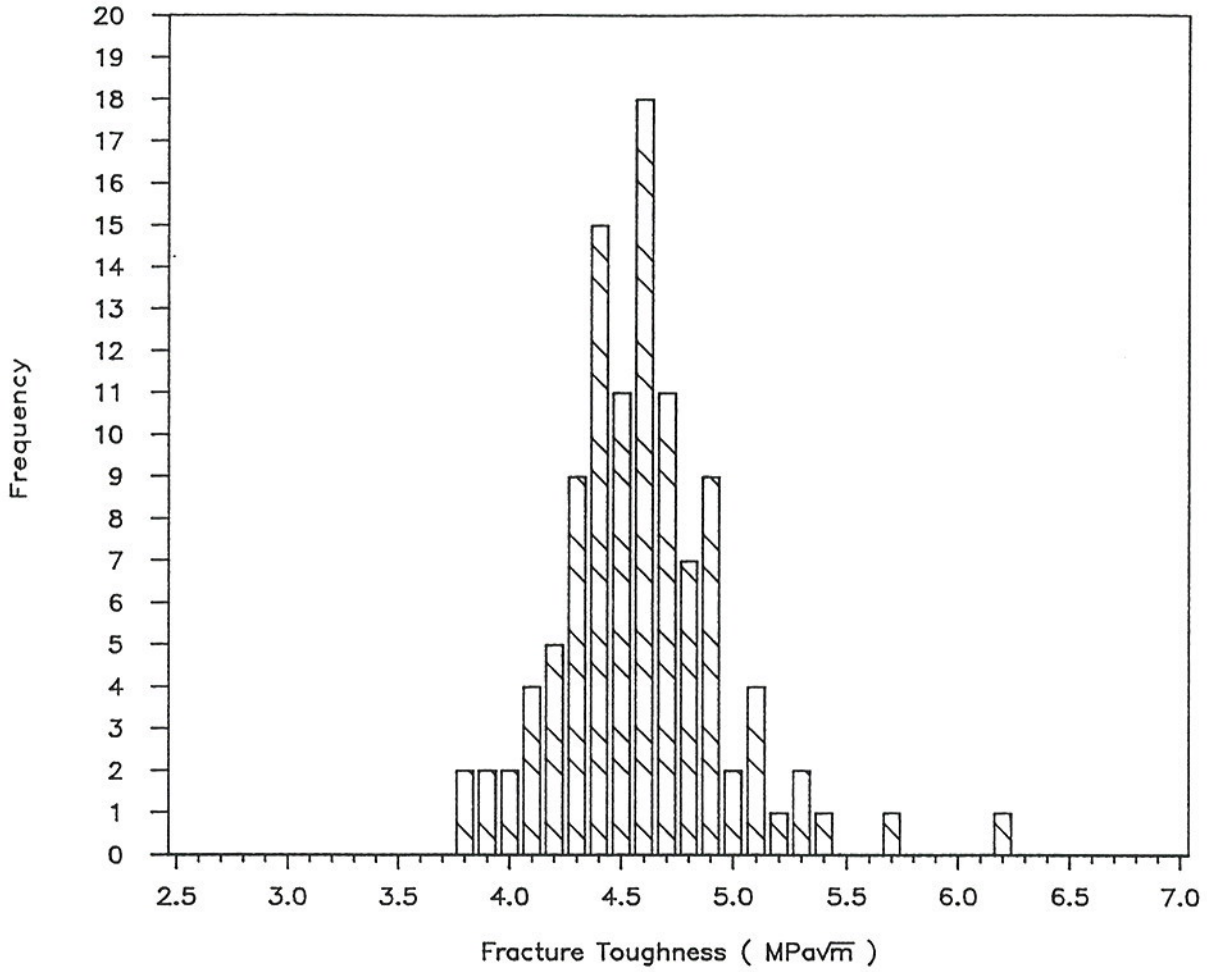

Figure A3.1 Frequency distribution graph for the hot-pressed silicon nitride, NC-132.

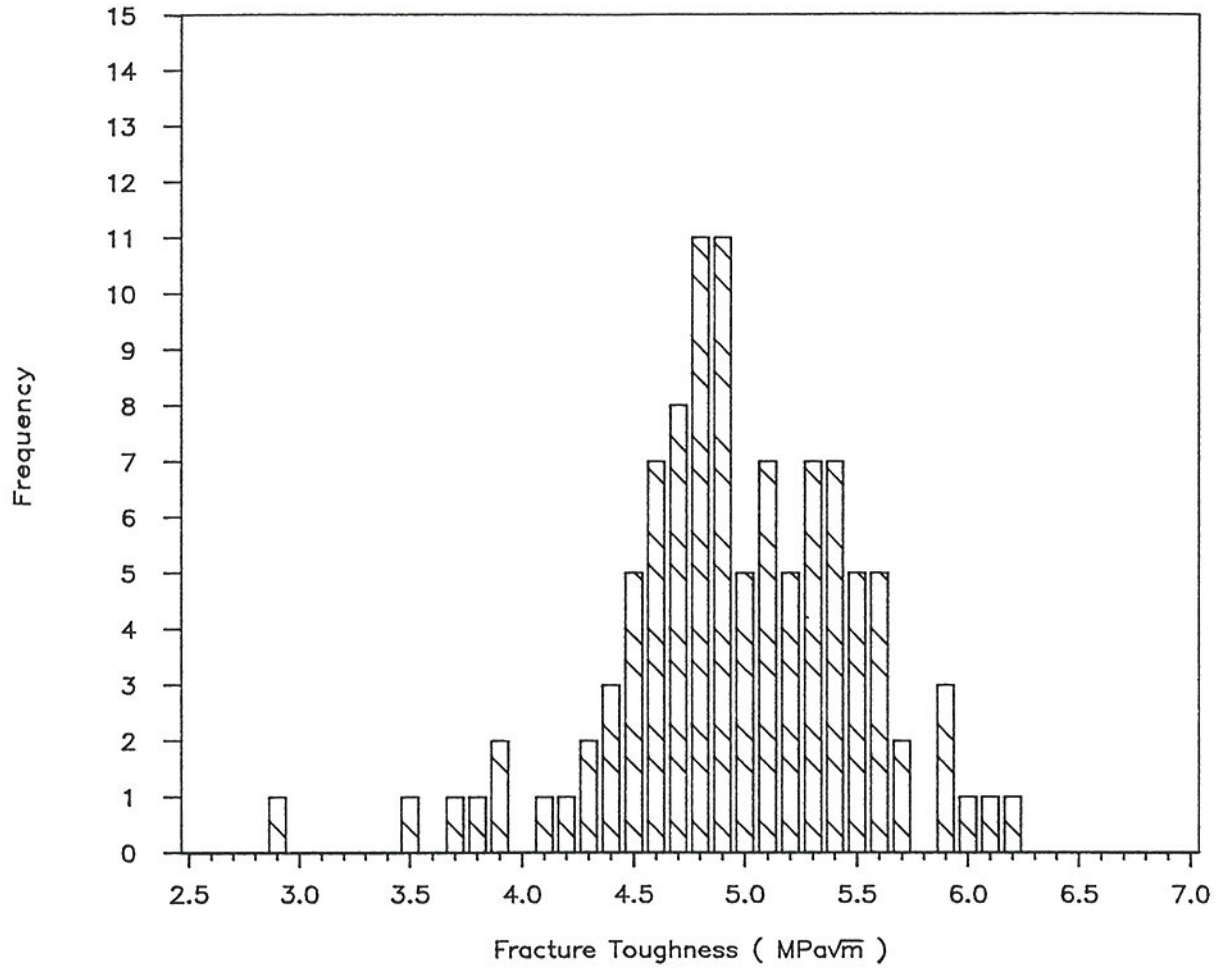

Figure A3.2 Frequency distribution graph for the hipped silicon nitride.

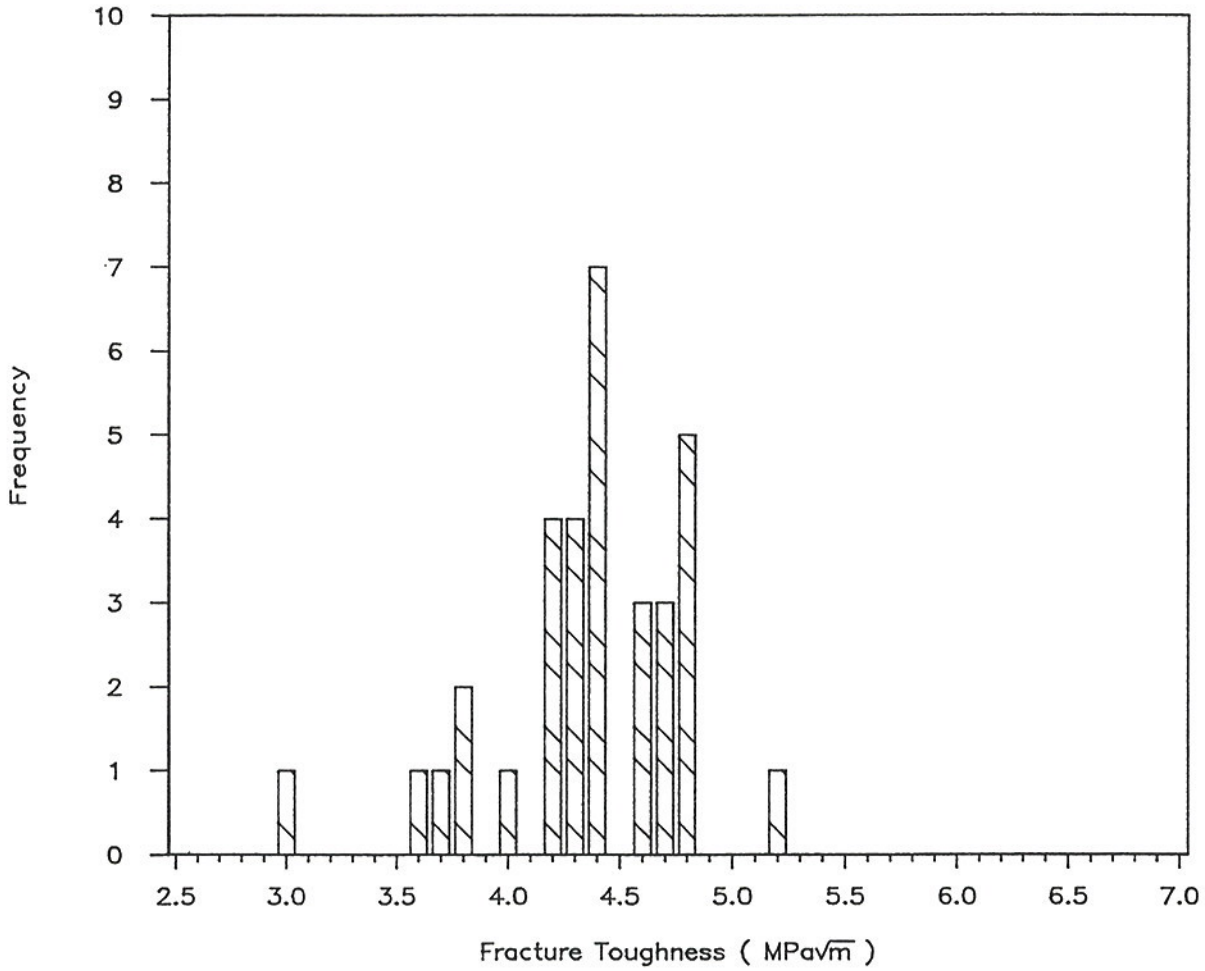

Figure A3.3 Frequency distribution graph for the yttria-stabilized, tetragonal zirconia polycrystal (Y-TZP).

Table A3.1
Fracture toughness outcomes. ID is the specimen identity number.

	NC-132 Si_3N_4		Hipped Si_3N_4		Y-TZP ZrO_2	
lab	ID	K_{Ic} MPa·√m	ID	K_{Ic} MPa·√m	ID	K_{Ic} MPa·√m
1	2	4.35	1	4.37		
	3	4.31	2	5.21		
	4	4.39	3	4.81		
	5	4.44	4	4.84		
	6	4.13				
2	4	4.52	C1	5.60	C6	4.80
	6	4.62	C2	4.87	C7	4.24
	7	4.52	C3	5.37	B7	4.43
	8	3.89	C4	5.48	B8	4.21
	9	4.70	C5	4.82		
			C6	5.39		
			C7	4.92		
			B6	5.33		
			B7	5.55		
			B8	5.52		
3	1	5.32	1	4.75		
	2	5.44	2	4.72		
	3	5.10	4	5.61		
	5	4.76	5	5.04		
	6	4.65	6	5.47		
	8	5.27	7	4.90		
	10	4.82	8	4.46		
			9	5.67		
			10	4.77		
4	3	4.73	1E	5.17	7	4.23
	4	4.60			3	4.43
	5	4.83				
	7	4.88				
	8	4.92				
	9	4.38				

	10	4.11				
5	1	4.62	1	5.07		
	2	4.51	2	5.94		
	3	4.64	3	4.85		
	4	5.05	4	4.63		
	5	4.73	6	5.09		
	6	4.54	7	5.31		
	7	4.40	8	5.09		
			9	4.95		
			10	4.78		
8	1	4.20	1C	5.43		
	2	4.28	2C	4.18		
	3	4.81	3C	4.30		
	4	3.79	4C	5.01		
	5	4.53	6C	4.70		
			7C	4.59		
			8B	4.88		
9	1	4.58	1	4.74		
	2	4.92	2	4.81		
	4	4.89	3	4.62		
	6	4.73	4	4.45		
	7	4.59	5	4.44		
	8	4.45	6	4.87		
			7	4.79		
			9	4.13		
			10	3.69		
10	1	4.71	II-1	3.93	III-1	3.58
	3	4.72	II-3	3.87	III-3	3.65
	5	4.31	II-4	2.92	III-4	2.98
			II-6	3.47	III-5	4.00
			II-8	5.29		
11	8	4.50	6	4.37		
	10	4.37	7	4.73		
	7	4.40	8	4.49		
			9	4.59		

			10	4.77		
12	1	4.37	1	5.71		
	2	4.40	2	5.29		
	3	4.61	3	5.07		
	4	4.60	4	5.22		
	5	5.16	5	4.53		
			6	4.61		
			7	5.53		
			8	3.75		
			9	4.85		
13	T1	4.56	2	4.48		
	T2	4.31	3	5.12		
	T4	4.79	4	4.64		
	T5	4.47	5	4.80		
	T3	4.69	6	4.60		
			8	4.66		
			9	4.91		
15	11	4.56	1E	4.86	2C	4.40
	12	4.47	2E	5.56	3C	4.82
	13	4.30	3D	4.79	4C	4.67
	14	4.01	7D	5.12	8B	4.35
	15	4.35	9D	4.72	3B	4.17
			10D	5.01	4B	4.44
					7B	4.62
					6B	4.63
17	1	4.32	SG-1	5.23	E-1	4.68
	2	4.42	SG-2	5.22	E-2	4.82
	3	4.36	SG-3	5.25	E-3	4.78
	4	4.32			D-5	4.77
					D-6	4.34
18	6	4.55				
	7	4.10				
	8	4.35				
	9	4.60				
	10	4.21				

19	1	4.63				
	2	4.15				
	3	4.62				
	4	4.17				
	5	4.37				
	7	3.93				
	8	3.81				
	9	4.28				
	10	4.16				
20	1	4.69	3A	5.38	1H	4.71
	2	4.65	4A	5.39	3G	3.80
	3	4.58	5A	4.91	4G	3.79
	4	4.87	6A	4.72	5G	4.43
	5	4.63	6C	5.12	6G	4.25
	6	4.88	7C	5.34		
			9C	5.28		
				5.08		
21	1	5.66	F1	4.96		
	2	6.17	F2	5.93		
	3	5.12	E1	4.93		
	4	5.14	E2	5.89		
	5	4.83	E3	5.45		
			E4	5.43		
			D8	5.37		
			D9	6.13		
			D10	6.03		
			D11	6.19		
22	1	4.64	3F	4.31	1C	4.29
	2	4.46	4F	5.60	2C	4.31
	4	4.75	5F	4.73	3C	5.19
	5	4.92			6B	4.35
23	5	4.10			5C	4.64
24	sn1	4.44				
	sn2	4.65				
	sn3	4.04				

	sn4	4.99				
	sn5	4.70				
	sn6	4.88				
	sn7	4.42				
	sn8	4.48				
	sn9	5.04				
	sn10	4.94				

# Samples	107	105	33
Average	4.59	4.95	4.36
Standard Deviation	0.37	0.55	0.44

APPENDIX 4

INFLUENCE OF THE UNCERATINTY OF THE PRECRACK SIZE MEASUREMENTS UPON THE CALCULATED FRACTURE TOUGHNESS

Fracture toughness is calculated from the formula:

$$K_{Ic} = Y \sigma \sqrt{a}$$

where: Y is the stress intensity shape factor (dimensionless)
σ is the flexure strength of the specimen (MPa)
a is the crack depth (m)

The shape of the ellipse (the a/c ratio) has an effect on the stress intensity shape factor, Y, which has values that range from 1.28 to 1.99 for shallow semicircular and semielliptical surface cracks in bending. The factors were taken from the empirical equation developed by Newman and Raju [A5.1]. To a first order, an uncertainty in K_{Ic} is half the uncertainty in "a" because of the square-root dependence of the former upon the latter. Thus, a 10% uncertainty (or error) in "a" is diminished to a 5% uncertainty in fracture toughness.

In many instances the uncertainty or error diminishment *is even greater!* That is due to a moderating influence of the Y factor. For example, if "a" is underestimated, the corresponding Y factor is overestimated, and vice versa. The following Figures illustrate how the error in K_{Ic} varies with errors in "a" (alone), "c" (alone), and both "a" and "c" simultaneously.

In all instances, the specimen was assumed to be 4 mm wide and 3 mm high. The initial ("correct") crack depth, a, was set at 50 micrometers. The initial ("correct") crack widths were set accordingly. For example, for an a/c = 1.0, c was set at 50 micrometers. Similarly, for an a/c = 1/1.25, c was set to 62.5 micrometers.

The correct crack geometry is listed in bold letters in the middle of each figure. The underestimate or overestimate of the crack size parameter is shown as the abscissa (horizontal axis).. The resultant error in K_{Ic} is shown as ($K_{Ic\ erroneous}/K_{Ic\ correct}$) on the vertical axis. No error in K_{Ic} is represented by a horizontal line at 1.0 on the vertical axis. The maximum Y value is used, whether it occurs at the surface or at the deepest point of the precrack. The curves change slope when the maximum Y factor shifts from one location to the other.

<u>In every instance, the maximum error is bounded by the error locus for the both "a": and "c" error.</u> In this case, both "a" and "c" are underestimates or overestimates by the same amount, and therefore the shape factor Y is nearly constant. The resulting error in K_{Ic} is thus from "a" alone, and is half the uncertainty in "a".

This leads to a remarkable conclusion: the uncertainty in fracture

K_{Ic} is thus from "a" alone, and is half the uncertainty in "a" due to the square root dependence of fracture toughness on crack size.

This leads to a remarkable conclusion: the uncertainty in fracture toughness is always one half (and often is much less) than the uncertainties in either "a" or "c", or both simultaneously.[1,2,3]

1. The Newman-Raju formula is used and is limited to cases of $a/c \leq 1.0$. For the case of the semicircular precrack, some of the erroneous precracks shapes have a/c ratios greater than 1, but the error in using the Newman-Raju formula a little outside its' recommended range is not expected to be significant.

2. The error for the instance of when a is overestimated and c is underestimated, and vice versa has not been calculated.

3. We suspect that this fortuitous insensitivity of fracture toughness upon precrack size has not been appreciated previously since most users of the Newman-Raju stress intensity factors have used an average Y factor for their precracks, and have not calulated the maximum Y factors for each and every precrack. This may be due to the cumbersome form of the graphs and equations in Ref. A5.1.

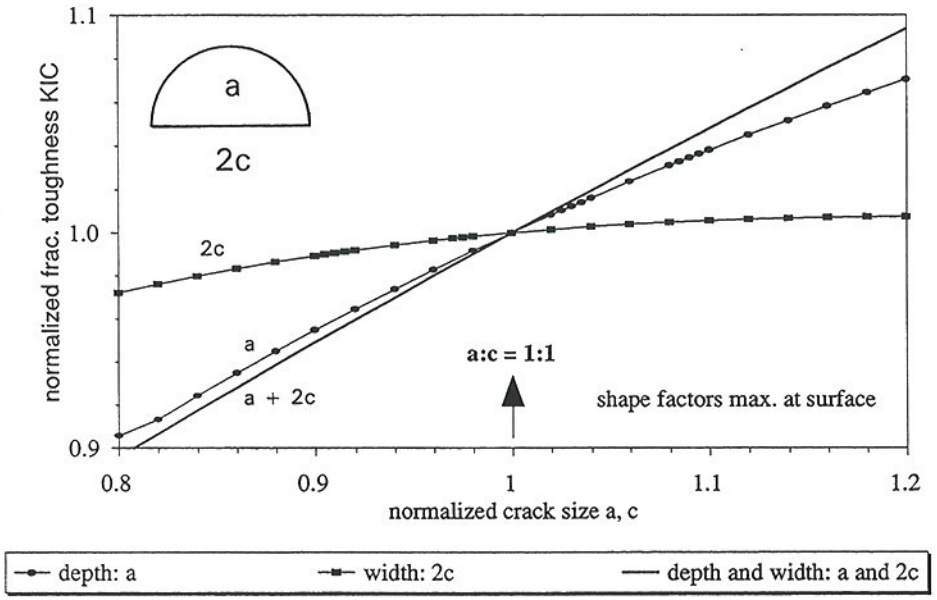

Figure A4.1 Uncertainty or error in fracture toughness as a function of uncertainty or error in crack size estimates: "a", "c", and simultaneously "a and 2c". The maximum Y factor (and thus stress intensity) is at the surface for all conditions for this initially semicircular shaped precrack.

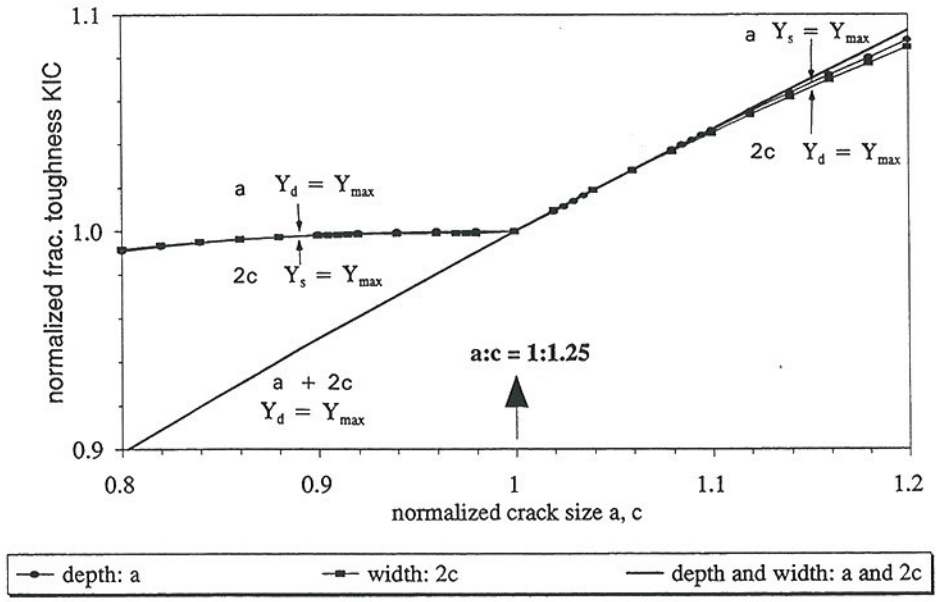

Figure A4.2 Uncertainty in fracture toughness as a function of uncertainty in "a", "c", and simultaneously "a and 2c". For this semielliptical precrack shape, the maximum Y factor is about the same at the surface and the deepest point.

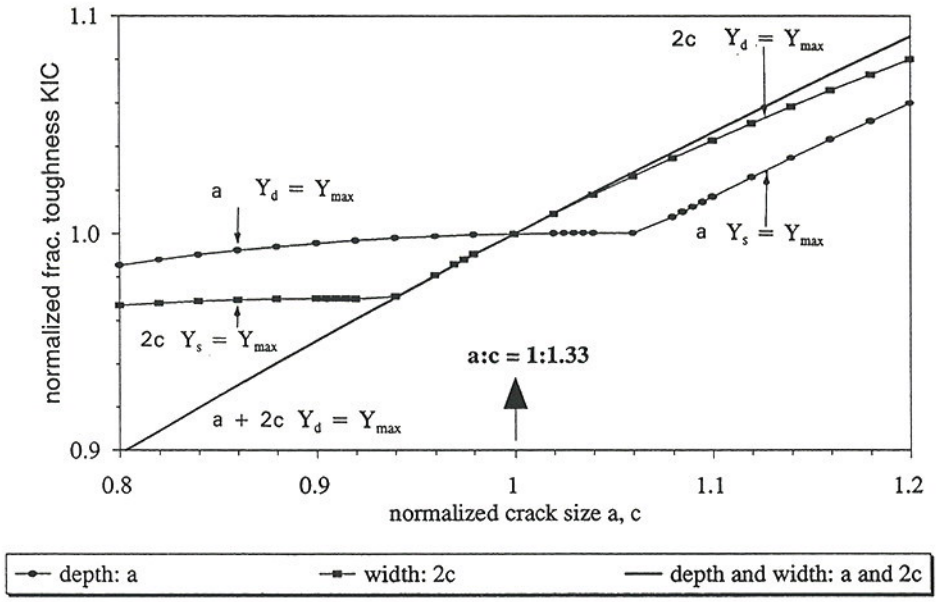

Figure A4.3 Uncertainty in fracture toughness as a function of uncertainty in "a", "c" and simultaneously "a and 2c". For this semielliptical precrack shape, Y is a maximum at the deepest point of the precrack initially, but can shift to the surface if the "a" or "2c" estimate is sufficiently in error.

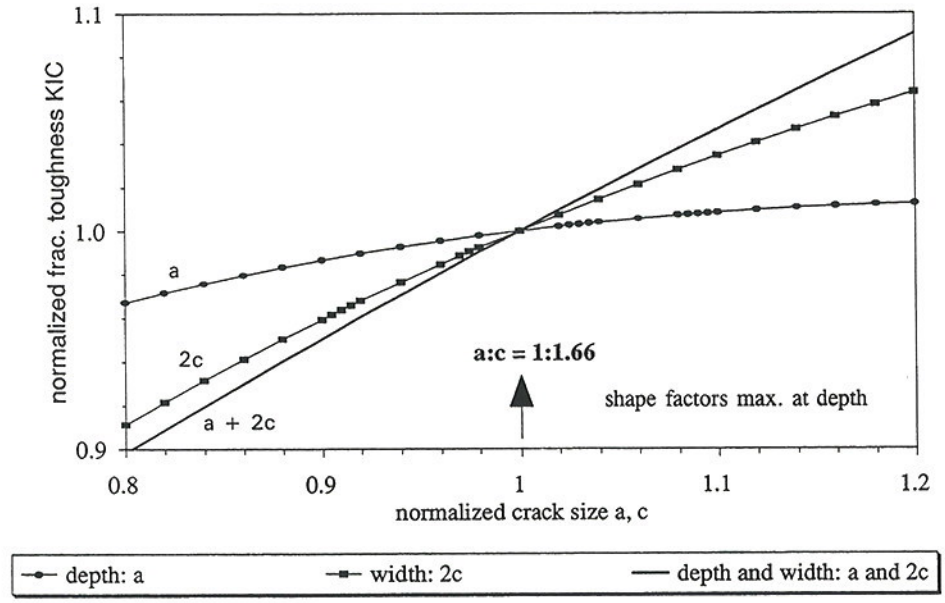

Figure A4.4 Uncertainty in fracture toughness as a function of uncertainty in "a", "c" and both "a" and "c". For this semielliptical precrack shape, Y is a maximum at the deepest point of the precrack for all conditions shown. This is the norm for shallow-long ellipses.

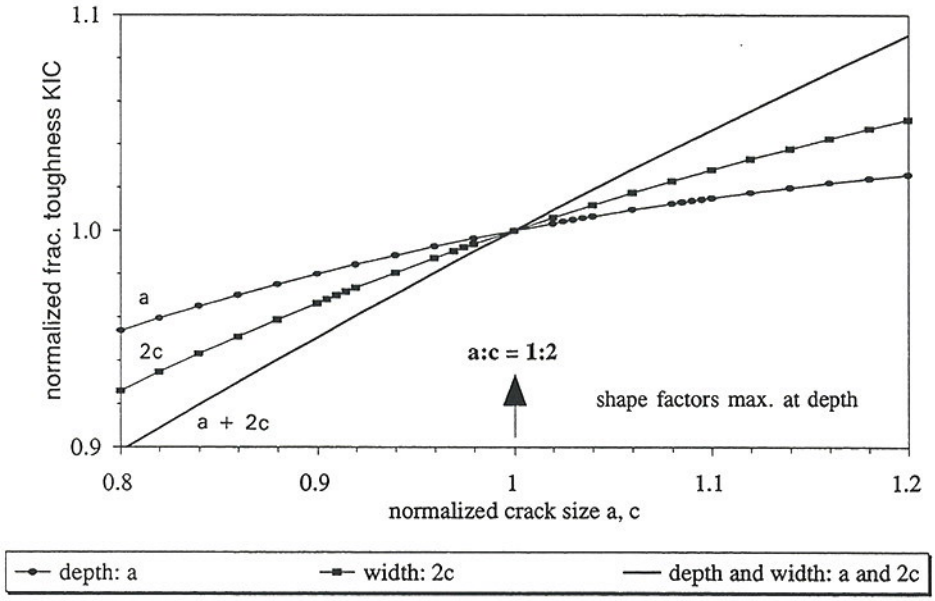

Figure A4.5 Uncertainty in fracture toughness as a function of uncertainty in "a", "c", and simultaneously "a and 2c". For this semielliptical precrack shape, Y is a maximum at the deepest point for all conditions shown. This is the norm for shallow-long ellipses.

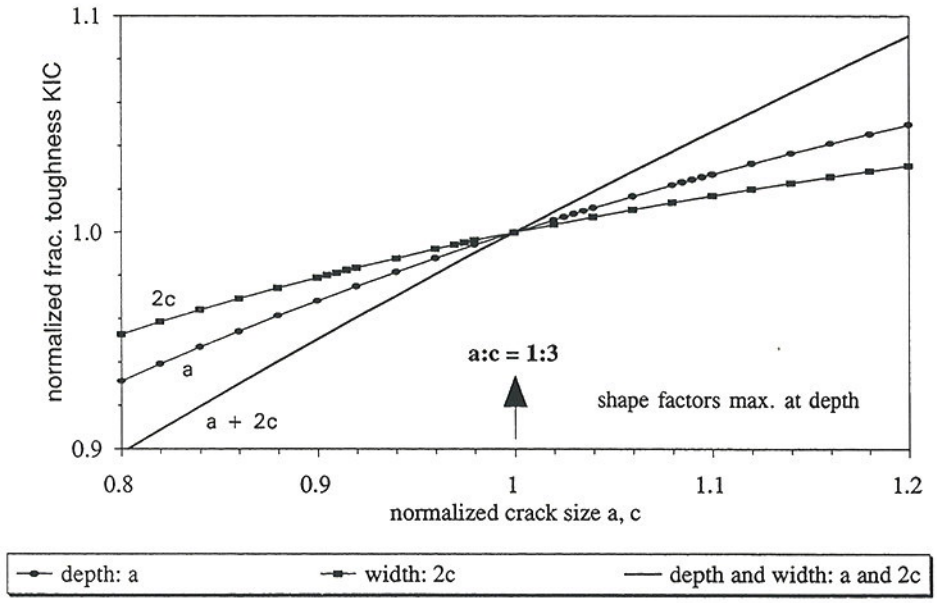

Figure A4.6 Uncertainty in fracture toughness as a function of uncertainty in "a", "c", and simultaneously "a and 2c". For this semielliptical precrack shape, Y is a maximum at the deepest point for all conditions shown. This is the norm for shallow-long ellipses.

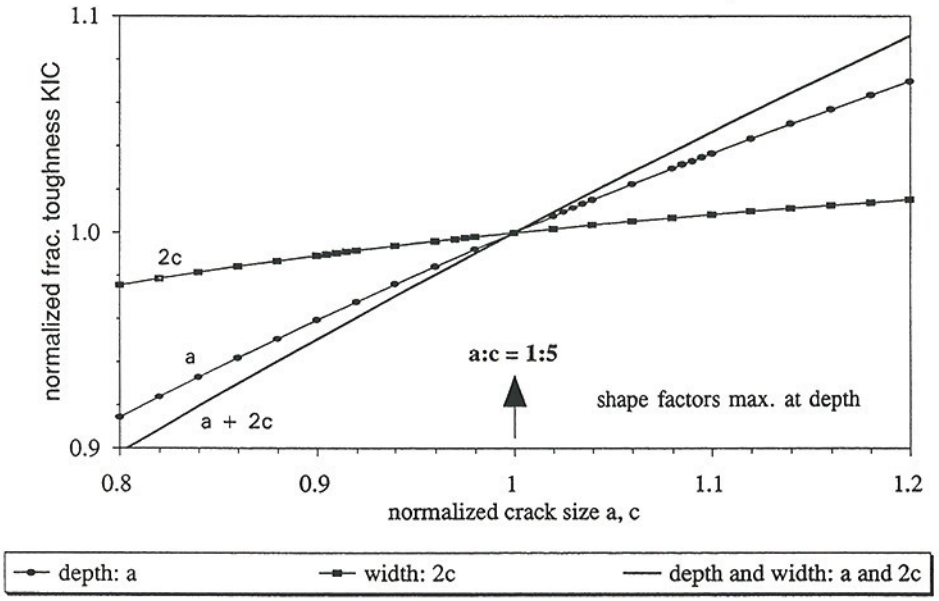

Figure A4.7 Uncertainty in fracture toughness as a function of uncertainty in "a", "c" and both "a" and "c". For this semielliptical precrack shape, the maximum Y factor is a maximum at the deepest point for all conditions shown. This is the norm for shallow-long ellipses.

APPENDIX 5

NOTES ON THE STRESS INTENSITY SHAPE FACTOR Y

A. Newman-Raju Equation

The stress intensity shape factors for semicircular or semielliptical surface flaws in bending were calculated from the empirical formulas of Newman and Raju [A5.1]. These factors take into account the finite thickness and widths of a specimen. They reported that the empirical equation was within 5% of their finite element solutions for all instances of relatively shallow cracks (crack depth/specimen thickness < 0.8). Additional computation analyses have verified their estimates [A5.2-A5.4]. Fett estimates the accuracy is within 3% for the tensile results. The bending results agree within 2% for shallow cracks in bending to results by Isida et al. [A5.2].

B. Approximation of a Part-Circular Crack by a Semiellipse

The approximation of a precrack shape by a semiellipse needs further explanation. Most as-indented precracks in brittle ceramics are nearly semicircular in shape. They have aspect ratios, a/c, between 0.85 and 1.0 [A5.6-A5.9]. If 4X is polished or lapped away then the precrack shape changes to a part-circular or part-elliptical shape. Figure A5.1 shows a semicircular precrack with 4X removed so that the precrack becomes a part circle. The semiellipse has been chosen such that its minor and major axes match the part-circle dimensions, a and 2c.

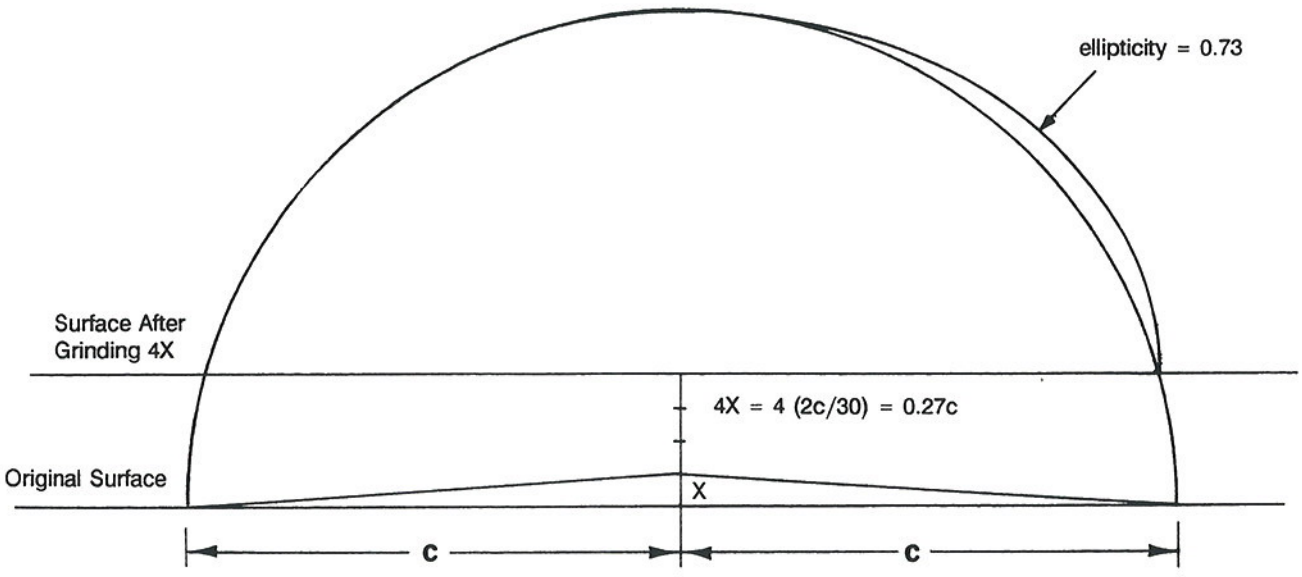

Figure A5.1 Schematic of a Knoop impression with a semicircular precrack. If 4X is removed by polishing, then the resultant precrack is a part circle. The semiellipse with matched major and minor axes is a good geometrical match. The Y factor will not be significantly altered at the deepest part of the precrack.

Numerous solutions and analyses exist for the semielliptical or semicircular shapes, both in tension and bending (e.g., see reviews by Newman [A5.4] and McGowan [A5.3]) but the part-circular shape has been treated much less frequently, and only in tension by Smith et al. [A5.10-A5.14].

The earliest solutions, by Smith and Alavi [A5.10], were listed in the Compilation of Rooke and Cartwright [A5.15]. These were subsequently refined by Smith [A5.11], Thresher and Smith [A5.12] and experimentally checked by Smith and Jolles [A5.13]. The experimental work which used photoelastic stress freezing experiments with epoxy, tended to verify the numerical results. Uncertainties about the use of a material with such a high Poisson's ratio (~.5) interfered with comparisons to theoretical results [A5.3, A5.14]. Differences in the effective stress intensity factors between part-circular and matching ellipses have been discussed by Smith [A5.11], McGowan [A5.3], and briefly, by Newman [A5.4]. The part-circle precrack can be matched by different possible semiellipses as shown by Smith and Alavi [A5.10]. Assuming that the part-circle and semiellipse have the same depth, the latter can then be chosen such that they have: a, the same area as the part-circle; or, b, the same curvature (at the deepest point); or c, the same width, 2c. For shallow flaws such that the maximum stress intensity, Y, is at the depth ($a/c < 0.8$), the agreement in Y for the latter two matches is within 2%. This shouldn't be surprising, since Figure A5.1 shows the geometries to be very similar.

The general consensus of all these studies is that the part-circular and semielliptical Y factors agree within a few percent at the deepest point of the crack for cracks where the maximum stress intensity is at this point, provided that the crack is not too deep relative to the plate thickness [A5.4, A5.11].

These conclusions are <u>not</u> true for instances where the maximum stress intensity is at the surface, in which case, the semiellipse may be a poor simulation of the part circle or part ellipse.

Tada and Paris, in a written comment at the end of Newman's review [A5.4], argue further that stress intensities of many surface cracks are quite similar and can be approximated by a simple formula, provided that Y is maximum at the depth. These conclusions are not too surprising in light of the geometric similarity of the semielliptical and part-circular cracks for the geometries of concern to us here.

Thus, we conclude that approximating the precracks by a semiellipse is reasonable, providing that the maximum stress intensity is at the deepest point. The error in the shape factor is estimated to be less than 5%.

C. Precrack Tilt Limitations

Fractographic examinations reveal that cracks that were tilted slightly off-axis as shown in Figure A5.2 were more easily detected whether by SEM or optical microscopy. The greater visibility was presumably due to

different optical or SEM scattering. A tilted crack will experience some Mode II loading as well as the primary Mode I stress intensity, but Jayatilaka [A5.13] showed that, in general, for a straight through crack in a plate in tension, the mixed Mode I and II effect is negligible, irrespective of the failure criterion (maximum stress, Griffith maximum stress, maximum strain energy density) for angles up to 5° for fully embedded cracks. Similarly, new stress intensity solutions by Murikami [A5.17] for tilted semielliptical cracks in tension fields show small (<5%) influences on stress intensity Mode I factors for angles up to 15°. Interpolation of Murikami's results of 0, 15, 30, and 45° indicates the effect on Y is of the order of less than 1% at 5° as shown in Figure A5.2.

Use of too large a tilt angle (>5°) can cause difficulties, especially if fracture commences from a point on the precrack periphery, and then truncates the precrack. The precrack will thereby not be revealed on the fracture surface. It was empirically determined in the preliminary work for the present round robin that the angle of the precrack was generally larger than the tilt of the indenter. Thus, for this study, a ½° tilt of the specimen to the indenter produced precracks with 2-3° tilt off perpendicular to the surface. Indenter tilts of 2° could produce precrack tilts of 10° or more. These would be excessive.

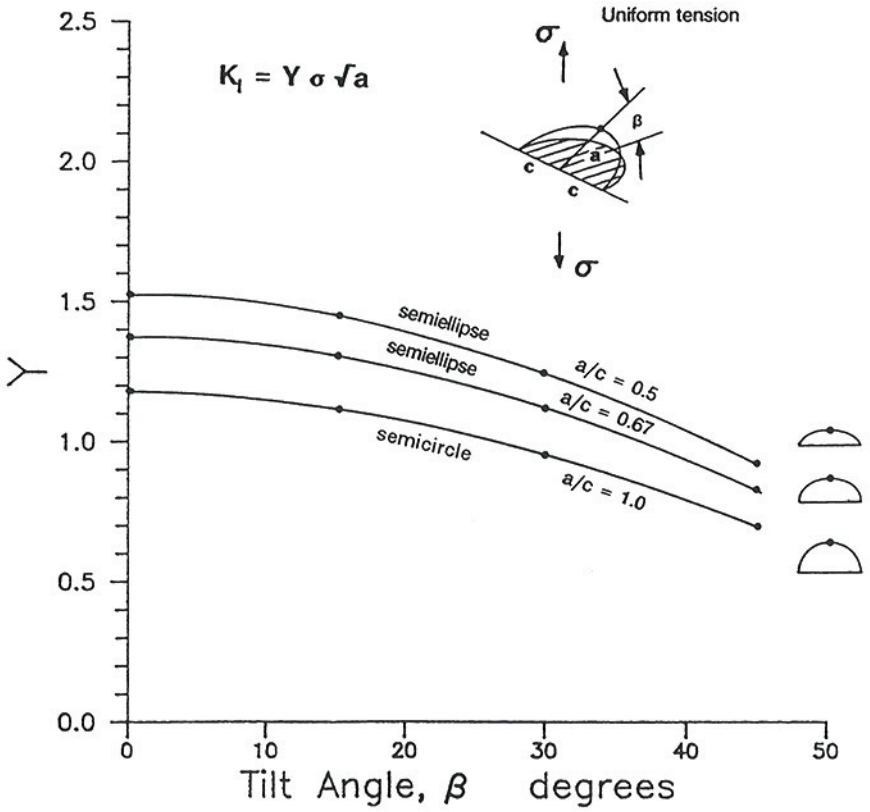

Figure A5.2 Influence of precrack "tilt" upon the stress intensity factor Y at the deepest point of the precrack. After Murakami [A5.17].

References for Appendix 5

A5.1 J. C. Newman, Jr. and I. S. Newman, "An Empirical Stress-Intensity Factor Equation for the Surface Crack," Eng. Fract. Mech., 15, [1-2] (1981), pp. 185-192.

A5.2 M. Isida, H. Noguchi, and T. Yoshida, "Tension and Bending of Finite Thickness Plates with a Semielliptical Surface Crack," Int. J. Fract., 26 (1984), pp. 157-188.

A5.3 J. J. McGowan, "A Critical Evaluation of Numerical Solutions to the Benchmark Surface Flaw Problem," Society for Experimental Stress Analysis, Westport, Conn., 1980.

A5.4 J. C. Newman, Jr., "A Review and Assessment of the Stress-Intensity Factors for Surface Cracks," in Part-Through Crack Fatigue Life Prediction, ASTM STP 687, J. B. Chang, ed. ASTM, 1979, pp. 16-42.

A5.5 T. Fett, "Stress Intensity factors for Semi-elliptical Surface Cracks in a Plate Under Tension Based in the Isida's Solution," Int. J. Fract., 48 (1991), pp. 139-151.

A5.6 J. J. Petrovic, Jr., L. A. Jacobson, P. K. Talty, and A. K. Vasudevan, "Controlled Surface Flaws in Hot-Pressed Si_3N_4," J. Am. Ceram. Soc., 58 [3-4] (1975) pp. 113-116.

A5.7 J. J. Petrovic, "Effect of Indenter Geometry on Controlled-Surface-Flaw Fracture Toughness," J. Am. Ceram. Soc., 66 [4] (1983) pp. 277-283.

A5.8 G. D. Quinn, and J. B. Quinn, "Slow Crack Growth in Hot-Pressed Si_3N_4," in Fracture Mechanics of Ceramics, Vol.6, eds. R. C. Bradt, A. G. Evans, D. P. H. Hasselman, and F. F. Lange, Plenum, NY, 1983, pp. 603-635.

A5.9 C. A. Tracy, "Fracture Mechanics Analysis and Testing of Advanced Ceramics Using Controlled Flaws," Masters Thesis, Northeastern University, May, 1988, Boston, MA.

A5.10 F. W. Smith and M. J. Alavi, "Stress Intensity Factors for a Part-Circular Surface Flaw," Proc. 1st Int. Pressure Vessel Conf., Delft, Holland, Oct. 1969, pp. 793-800.

A5.11 F. W. Smith, "The Elastic Analysis of the Part-Circular Surface Flaw Problem by the Alternating Method," in The Surface Crack: Physical Problems and Computational Solutions, Am. Soc. of Mech. Eng., N.Y., 1972, pp. 125-152.

A5.12 R. W. Thrasher, and F. W. Smith, "Stress Intensity Factors for a Surface Crack in Finite Solid," J. Appl. Mech., 39 Series E [1] (1972), pp. 195-206.

A5.13 C. W. Smith and M. Jolles, "Stress Intensities in Deep Surface Flaws in Plates Under Mode I Loading," in Developments in Theoretical and Applied Mechanics, ed. R. McNitt, Virginia Polytechnic Institute, Blacksburg, VA, 1976, pp. 151-160.

A5.14 C. W. Smith, W. H. Peters, G. C. Kirby, and A. Andovian, "Stress Intensity Distribution for Natural Flaw Shapes Approximating 'Benchmark' Geometries," in Fracture Mechanics: Thirteenth Conference, ASTM STP 743, ed. R. Roberts, ASTM, Philadelphia, PA, 1981, pp. 427-437.

A5.15 D. P. Rooke and D. J. Cartwright, Compendium of Stress Intensity Factors, Her Majesty's Stationary Office, London,

1976.

A5.16 A deS Jayatilaka, Fracture of Engineering Brittle Materials, Applied Sciences, Ltd, 1979, pp. 80-115.

A5.17 Y. Murakami, Stress Intensity Factors Handbook, Vol. 1, Pergamon Press, Oxford, 1990, (section 9.50), pp. 827-830.